NEW FLUORESCENT CHEMOSENSORS FOR DETECTING LIPIDS

A Dissertation

presented to

the Faculty of the Graduate School

at the University of Missouri-Columbia

In Partial Fulfillment

of the Requirements for the Degree

Doctor of Philosophy

---

by

JAE SEUNG LEE

Dr. TIMOTHY E. GLASS, Dissertation Supervisor

December 2011

The undersigned, appointed by the dean of the Graduate School, have examined the thesis entitled

NEW FLUORESCENT CHEMOSENSORS FOR DETECTING LIPIDS

Presented by Jae Seung Lee,

A candidate for the degree of doctor of philosophy,

and hereby certify that, in their opinion, it is worthy of acceptance.

Professor Timothy E. Glass (Thesis Advisor)

Professor Paul R. Sharp (Committee member)

Professor Susan Z. Lever (Committee member)

Professor Peter A. Tipton (Outside member)

ACKNOWLEDGEMENTS

I would like to thank all people who have helped an inspired me during my doctoral study.

First of all, I appreciate to my mother, Myung Sun Hwang, and my brother, Jae Kyung Lee. They have supported me to continue study without any concerns in the United States.

I especially want to thank my advisor, Dr. Timothy E. Glass, for his guidance during my study and research at University of Missouri-Columbia. His enthusiasm in research had motivated me. In addition, he was always accessible and willing to help his students with their study and research.

Also, I thank to thesis committee members, Dr. Susan Lever, Dr. Paul Sharp, and Dr. Peter Tipton, who teach me how to keep research and to write thesis.

I thank to all my friends in the lab and the Department of Chemistry for their friendship; Alan Yuksel, Chad Cooley, Chun Ren, Jess Klockow, Ken Hettie, Nick Cooley, Patrick Cavins, Shaohui Zhang, Xiaole Shao, Wanjun (Selina) Zhu, Morgan Moody, Jamison Arends, and all others in the Department of Chemistry.

In addition, I want give special thanks to all my best friends in Korea; Elli Kim, Dong Hoon Lee, Yong Hyuk Lee, Suk Hoon Kim, Jin Suk Lee, Sang Woon Nam, Byung Nam Kim, Hyung Dong Park. They have given me excellent friendship for long time.

Dedicated to my father, Tae Hee Lee, who is in the heaven.

TABLE OF CONTENTS

LIST OF SCHEMES

LIST OF FIGURES

LIST OF TABLES

NEW FLUORESCENT CHEMOSENSORS FOR DETECTING LIPIDS

JAE SEUNG LEE

Dr. TIMOTHY E. GLASS, Dissertation Supervisor

Abstract

Lipids represent an important class of biomolecules which have received little attention in the area of fluorescent sensing. Chemosensors for certain bioactive lipids would have a number of potential biochemical and biomedical applications. We have been using macrocyclic sensors to selectively detect lipids based on shape-selective hydrophobic interactions. The next generation sensors are based on open-tube shape structures, used mainly for ease of synthesis and ready functionalization with head group binding units. A series of receptors for the recognition of various lipids has been synthesized. The open-tube **102** and **103** were easily synthesized and purified compared to molecular tubes which are the previous hosts for the recognition of lipids. The open-tube sensors **102** and **103** were used in fluorescence titrations with a variety of lipids. Changes in the fluorescence emission were observed for most guests. The longer straight chain lipids were bound with higher affinity than shorter lipids. The greater hydrophobic surface of longer chain lipids renders them less soluble in water. The straight chain alcohols have been shown much higher association constant because they have less repulsion with carboxylates of sensors. The binding of open-tubes and lipids are less selective than those of the molecular tubes.

Chapter 1. Moelcular Recognition

1.1 Overview

The field of molecular recognition[1-3] covers the association of molecules by selective non-covalent interactions through hydrogen bonding, metal coordination, hydrophobic interactions, pi-pi interactions, or electrostatic effects in biological systems and chemical research.[1] Molecular recognition has various applications[3] including drug design, biosensors, and chemosensors.

Chemical sensors (chemosensors)[4-6] are organic molecules that provide detectable signal in the presence of a specific compound, which is called an analyte. Chemosensors often detect biological analytes; anions, cations, or small organic molecules.

Chemical sensing requires the continuous monitoring of the presence of analytes. Chemical sensing uses molecular recognition methods; however, it is different from molecular recognition. Chemical sensing does not cover covalent interactions and molecular recognition does not include a signal change. The work reported here will include molecular recognition, host-guest chemistry, and chemical sensing.

1.2 Host-Guest Chemistry

Host-guest chemistry is molecular recognition involving two or more molecules, a host and a guest, involved in non-bonding interactions to form a supramolecular complex.[7] A host is defined as a chemical species that has binding sites which bind a guest

and is also called a receptor. Some examples of host and guest are shown in Table 1.

Table 1 The list of common host and guest and their interaction

Host	Guest	Interaction
Crown ether	Metal ion	Ion-dipole
Cyclrodextrin	Organic molecule	Hydrophobic
Calixarene	Organic molecule	Van der Waals
Spherand	Alkyl ammonium cation	Hydrogen bonding
ion	ion	Ion-ion

The formation of a host-guest complex is reversible. The association constant K_a , which is known as a binding constant between host and guest, for the equilibrium is defined by equation 1:

$$K_a = \frac{[H_m \bullet G_n]}{[H]^m [G]^n} \qquad \text{(eq. 1)}$$

Where m is the number of host molecules and n is the number of guest molecules.

The host-guest chemistry began with research on crown ethers which are receptors for metal ions. Crown ethers were discovered[8,9] by Charles Pedersen who, working at the American du Pont, synthesized dibenzo-18-crown-6(**4**) accidently. Crown ethers are excellent receptors for metal ions. Compound **1**,**2**, and **3** are effective receptors for alkaline metal ions, Na^+, K^+, and Cs^+, respectably. The coordination between crown ethers and metal ions depend upon their size that was called “the hole-size-selectivity” principle.[10,11]

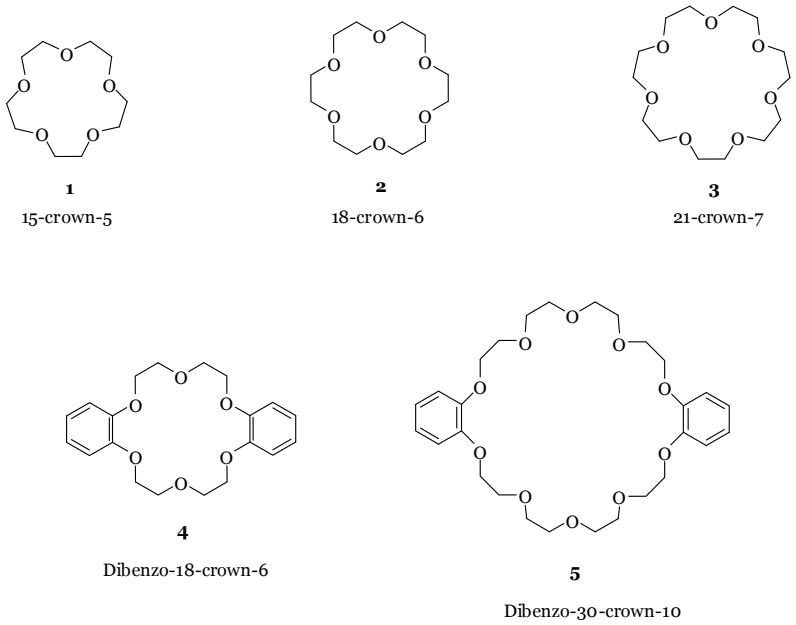

Figure 1 Common crown ethers

The association constant, log K_a, for a variety of crown ethers and cations are shown in Table 2. This research shows that 18-crown-6 has higher association constants for Na^+, K^+, NH_4^+, and Ca^{2+} than other crown ethers. This means that 18-crown-6 has an appropriate size for coordination with those metal ions particularly K^+. Their coordination is shown in Scheme 1. A host has a binding site, which interacts with a guest, and forms a binding conformation. This effect is called *complementarity*.[12]

Scheme 1 Complexation of metal ions by crown ether

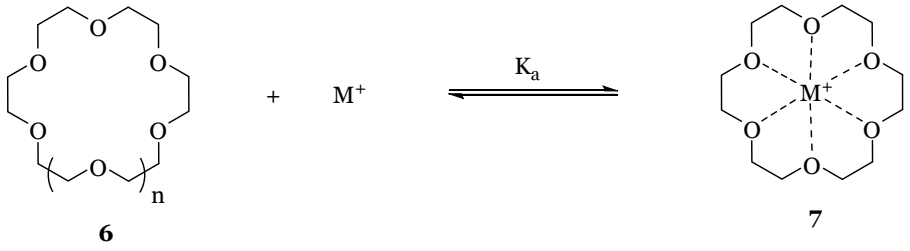

n = -1, 0, 1, 2, 3
M = Na^+, K^+, Ca^{2+}, Cs^+, NH_4^+

Table 2 Association constant (log K_a) for crown ethers and cations at 25°C in anhydrous methanol[13]

	Log K_a			
Crown ether	Na^+	K^+	NH_4^+	Ca^{2+}
12-crown-4	1.70	1.74	1.30	ND
15-crown-5	3.24	3.43	3.03	2.36
18-crown-6	4.35	6.08	4.14	3.90
21-crown-7	2.54	4.35	3.27	2.80
24-crown-8	2.35	3.53	2.63	2.66

The binding constants for K^+ of various polyethers increases from left to right as shown in Figure 2 because compound **8** has only a chelate effect[14-16], but crownether **2** has both a chelate effect and a macrocyclic effect[14] and cryptand **9** has a chelate effect as well a macrobicyclic effect. The chelate effect is defined that multi-dentate complex is more stable than the complex formed with mono-dentate ligands. The stability constant, β, of a complex is defined as the overall formation constant that results from the addition of *n* ligands to a metal ion (eq. 2).

$$M + nL \rightleftharpoons ML_n \qquad \beta = \frac{[ML_n]}{[M]\,[L]^n} \qquad \text{(eq. 2)}$$

where M is metal and L is ligand. β is the stability constant of a complex.

A complex with a larger formation constant is favored thermodynamically by the relationship

$$\Delta G^o = -2.3RT \log \beta \qquad \text{(eq. 3)}$$

Where ΔG^o is changes in free energy, R is gas constant, T is temperature, and β is stability constant of a complex.

The standard free energy has an enthalpy component and an entropy component according to the realationship

$$\Delta G^o = \Delta H^o - T\Delta S^o \qquad \text{(eq. 4)}$$

Where ΔG^o is changes in free energy, ΔH^o is changes in enthalpy, T is temperature, and ΔS^o is changes in entropy.

The multi-dentate complexes have a smaller change in entropy than similar mono-dentate ligand complexes. This shows the formation of multi-dentate complex is more favorable than that of mono-dentate complex. Also, the macrobicyclic ligands have high stability and selectivity than other type ligands. The interaction between an analyte and the macrocyclic compound is always stronger than the interaction with non-cyclic compound, which is called the macrocyclic effect.[17] The strength of the interaction and the binding constant are strongly dependent on those effects in the binding of a macrocyclic receptor and an analyte.

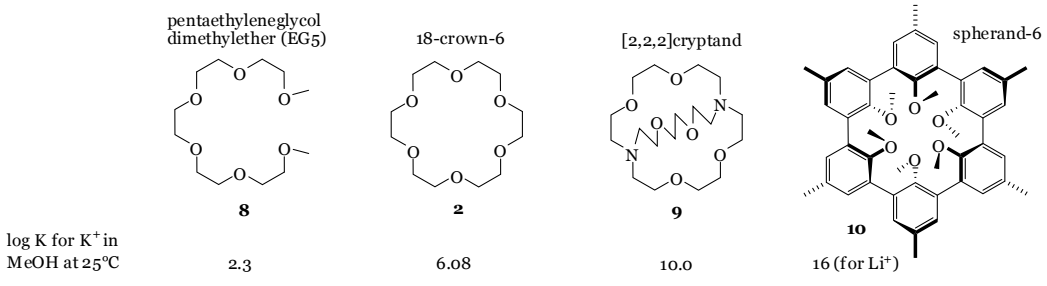

Figure 2 Comparison of binding constants for K^+ in MeOH at 25°C

1.3 Cavitands and Capsules

A cavitand[18-20] is described as a molecular container and is normally open at one end. The depth of cavity can be altered extending walls of the cavitand. The well-known cavitands are based on calixarenes and resorcinarenes shown in Figure 3. Calix[4]arene **11** is the parent compound of calixarenes and compound **12** is a basic structure of resorcinarenes where R can be various functional groups. Both calix[4]arene **13** and resorcin[4]arene **14** have intramolecular hydrogen-bonding interactions between OH groups in the upper or lower rim shown in Figure 4.

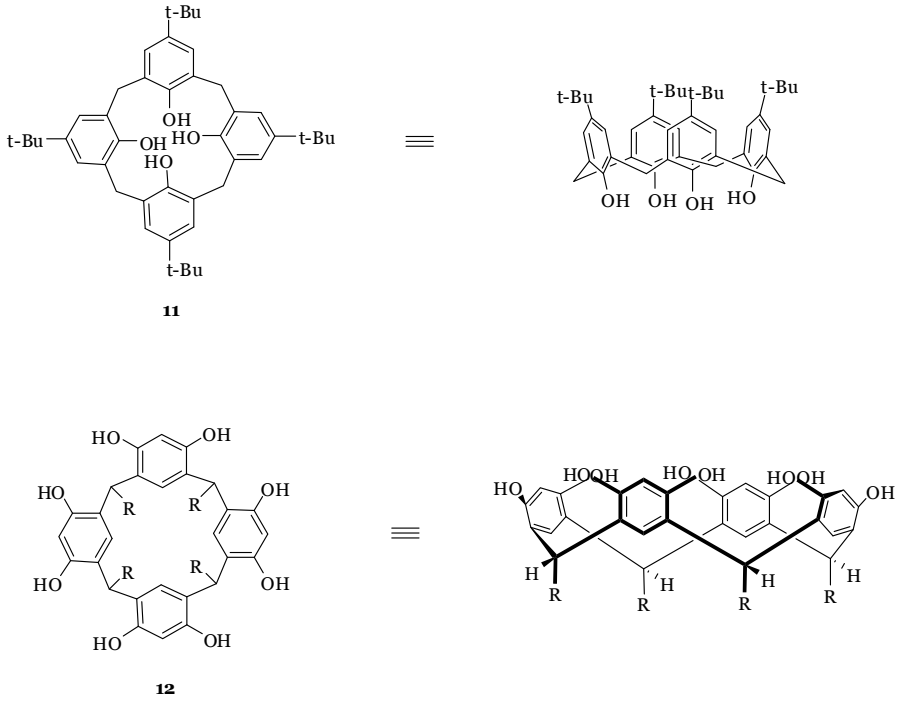

Figure 3 The structure of a calixarene and resorcinarene

Calixarenes are often used to prepare host molecules. The water soluble calixarene **15** has strong 1:1 complexes with bicyclic azoalkanes **15.1-15.4**.[21] The binding constants of protonated guests with calixarene **15** were determined by ^{1}H NMR titration at pD 2.4,

7.4, and 13.2, but all guests have the highest binding constants at pD 2.4 as shown in Figure 5. The reason is that all nitrogens were protonated in acidic condition.

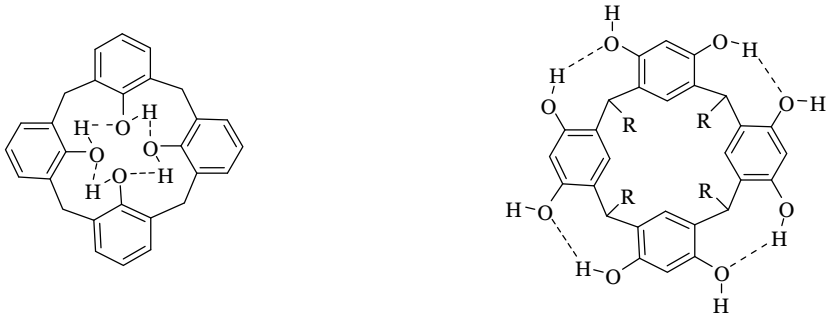

13 **14**

Figure 4 The hydrogen-bonding interaction of upper- and lower-rim in a calixarene and a resorcirnarene

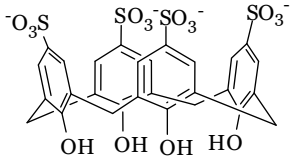

15

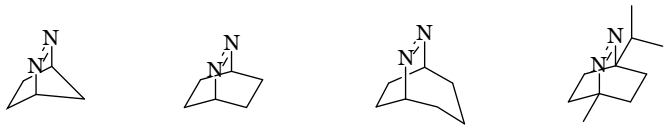

	15.1	**15.2**	**15.3**	**15.4**
K [M^{-1}]	490	4,300	15,000	3,300

Figure 5 The binding constant of bicyclic azoalkanes with water soluble calixarene at pD 2.4 in D_2O as determined by ^1H NMR titration

The calixarenes can be extended at their upper- and lower-rims and can bind a variety of analytes. Chen group reported[22] calix-aza-crown **16** attached with on dansyl group as a fluorophore that binds mercury ion (Hg^{2+}) selectively. Four amines have coordination with Hg^{2+} ion to form 16·Hg^{2+} shown in scheme 2. Calixarenes, calix-crowns,

and calix-aza-crowns do not have any fluorophore or chromophore. Therefore, the dansyl group was necessary for a fluorescence response. However, fluorescence was quenched after binding Hg^{2+} ion.

Scheme 2 The binding of calix-aza-crown with Hg^{2} $K_a = 1.31 \times 10^5\ M^{-1}$

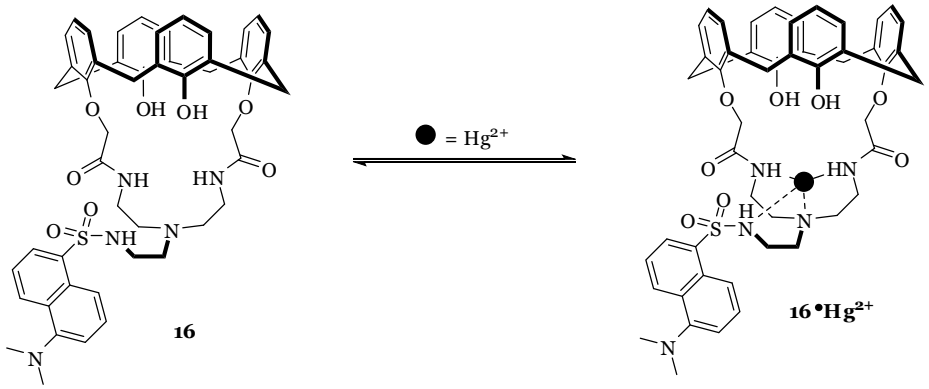

Calixarenes can also be functionalized at the upper-rim to increase their cavity volume. The Schatz group reported[23] that imidazolium-substituted calixarenes are efficient receptors for anions shown in Figure 6. The strength and selectivity of recognition depend on the binding of spherical (Cl^- and Br^-) and tetragonal ($H_2PO_4^-$ and HSO_4^-) anions.

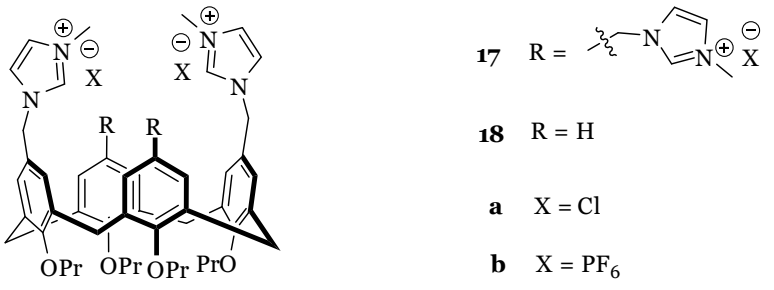

Figure 6 Imidazolium-substituted calixarenes as receptors for anions

The complex of $H_2PO_4^-$ and Cl^- needs two binding sites, and HSO_4^- and Br^- need at least three binding sites. The binding constants of compound **18** with HSO_4^- and Br^- are lower than those of compound **17** because their binding sites smaller than compound **18** shown in Table 3.

Table 3 Association constant (K_a) for anions with **17b** and **18b** in DMSO-d_6 at 298K

	K_a (M^{-1})			
Host	$H_2PO_4^-$	HSO_4^-	Cl^-	Br^-
17b	1,910	1,110	950	850
18b	1,980	200	900	200

The Poh group has prepared[24] rigid bowl-like cavitand **19** and the Glass group has reported[25] rigid calix[4]naphthalene **20** that have cavities wider than calixarenes and resorcarenes as shown in Figure 7. The cavitand was synthesized with naphthalenes; thus the receptors are termed calix[n]naphthalenes. The advantage of these cavitands is a wider cavity compared to regular calixarenes.

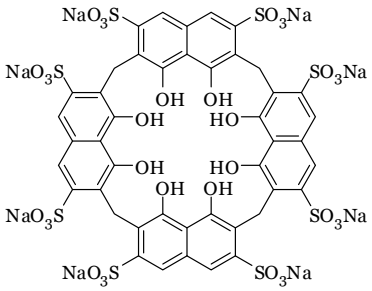

19

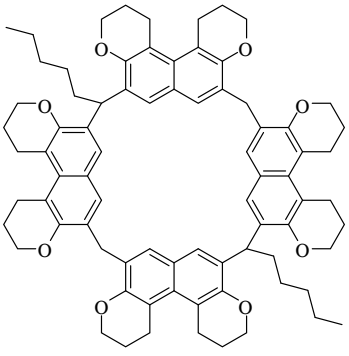

20

Figure 7 The structure of calix[n]naphthalene

The Rebek group has reported[26] a vase-like cavitand **21** extended from a resorcarene as shown in Figure 8. Compound **21** can bind neutral and cationic analytes by the encapsulation into a hydrophobic cavity. A variety of maleimide compounds encapsulate into compound **21** with hydrogen-bonding at the cavitand upper-rim. A dienophile, which was placed outside cavity, can be reacted with a diene and gives the Diels-Alder cycloaddition product. The reaction rate of the dienophiles bound in the cavity was accelerated by over 20-fold.

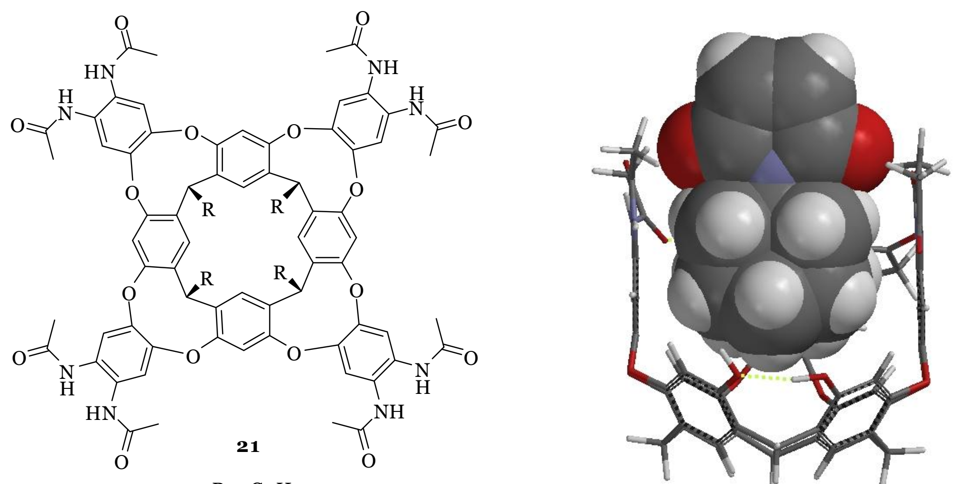

21

(a) R = $C_{11}H_{23}$ (b)

Figure 8 The deep cavitand (a) the structure of cavitand (b) the representation of binding cavitand with maleimide (3D model from Wavefunction Inc. software Spartan 06').

Scheme 3 The reaction mechanism and the binding constants K_a with a variety of maleimide **21a-21d**

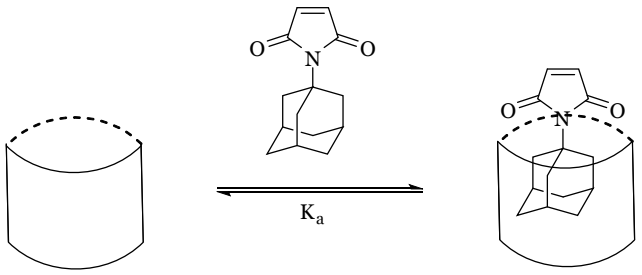

21

		The association constant K_a (M^{-1})
21a	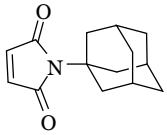	80
21b	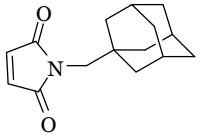	120
21c	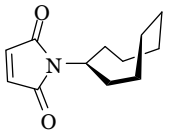	$> 10^4$
21d	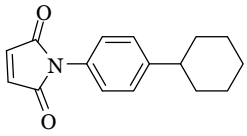	$> 10^4$

The Rebek group has synthesized[27] water soluble cavitand host **22** that has benzimidazole walls and carboxylic acid groups. The deep cavity was found to be well suited for the recognition of acetyl choline (**22a**), tetramethyl ammonium (**22b**), and choline (**22c**). Hydrophobic effects play a key role in the favorable complexation between the deep cavitand host and guests. The positive charge on the nitrogen has contact with

the water molecules and alkane groups encapsuled in the hydrophobic pocket and they have 1:1 binding as shown in Figure 9 and 10.

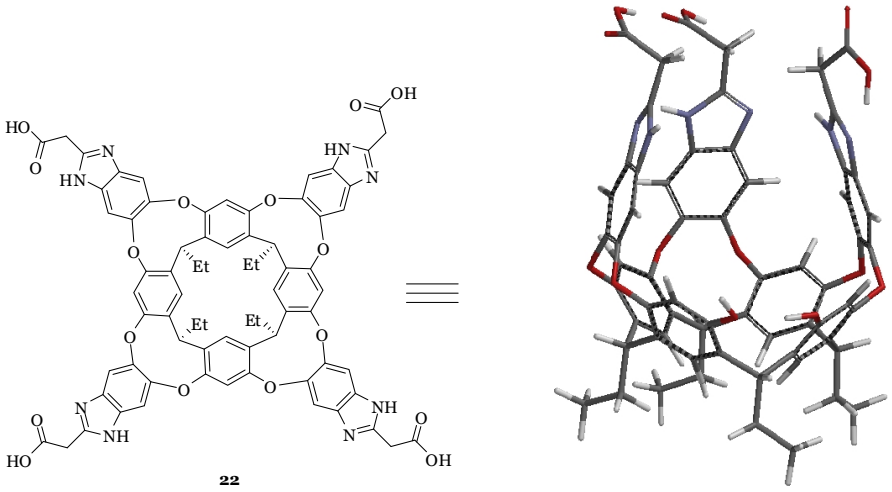

Figure 9 The structure of water soluble deep cavitand 22; one wall of the receptor has been removed for viewing clarity (3D model from Wavefunction Inc. software Spartan 06').

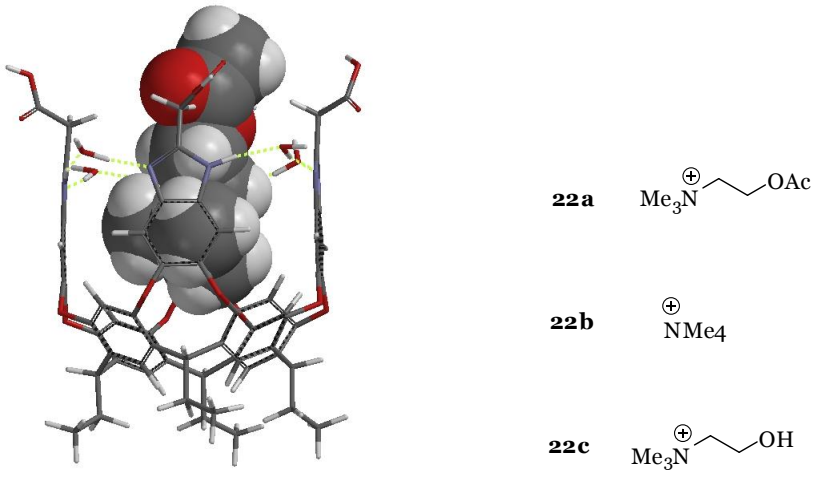

Figure 10 The complexation of water soluble cavitand **22-22a** and analytes (**22a – 22c**) (3D model from Wavefunction Inc. software Spartan 06').

1.4 Hydrophobic effect

The hydrophobic effect is an important binding interaction in supramolecular chemistry and molecular recognition. The tendency of non-polar molecules to self-associate in water rather than to dissolve individually is called the hydrophobic effect. Oil and water not mix together because of this hydrophobic effect. Amphiphilic molecules have both a hydrophobic region and a hydrophilic region. They form a micelle or bilayer in water as shown in Figure 11.

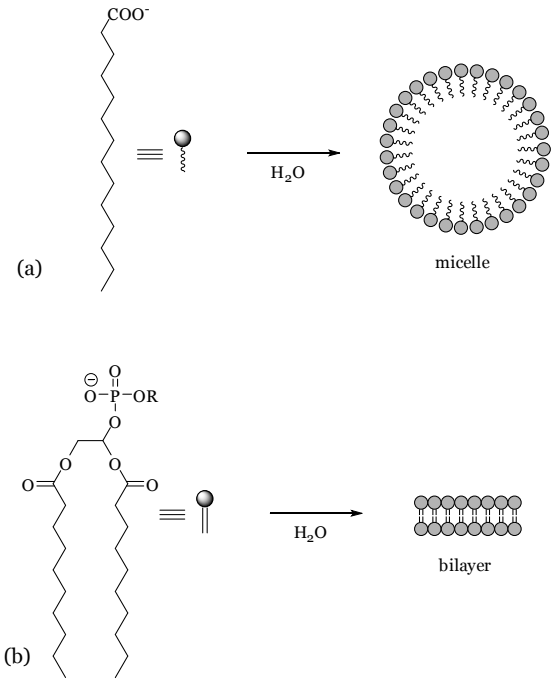

Figure **11** Examples of the aggregation driven by hydrophobic effect (a) micelle formation with an alkyl carboxylic acid (b) bilayer formation from the aggregation of a phospholipid

If two molecules of hydrocarbon are placed in water, the Gibbs free energy ΔG^o (eq. 4) is favorable ($\Delta G^o < 0$) for the aggregation. The enthalpy ΔH^o for the aggregation is

small and unfavorable ($\Delta H^o < 0$). Entropy ΔS^o for the aggregation is favorable ($\Delta S^o > 0$). Thus, hydrophobic association is entropy driven. Reducing the surface area by dimerization of two hydrocarbons (Figure 12) frees some of the ordered water and produces a favorable entropy for hydrocarbon aggregation.

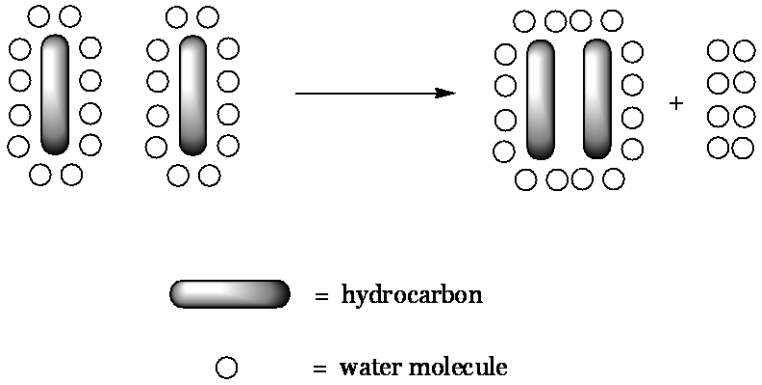

Figure **12** Dimerization of two hydrocarbons in water.

1.5 Conclusion

The field of molecular recognition studies non-covalent interaction between host and guest molecules that form stable complexes. The stability of the complexes relies on several factors such as the size and shape complementarity. The size and shape can be effective strategy in designing host-guest complexes. The dimerization of hydrophobic molecules in water is entropically favorable. Hydrophobic effect is one of important binding forces in supramolecular chemistry and molecular recognition.

Chapter 2. Chemical Sensing

2.1 Overview

Chemical sensing[4-6,28] involves the use of small molecules that provide a detectable response by a specific interaction with an analyte. A major goal is to introduce chemosensors into live cells to obtain information from cellular or sub-cellular structure and function. An ideal sensor would observe real-time biological processes without any interfering with the overall function of the cell.

The essential research issues[29] for making chemosensors are: (1) how sensors can bind the analyte selectively and (2) the relation between molecular and fluorescence changes.

A reversible interaction between the chemosensor and the analyte is essential for biological applications because it is necessary to sense both increases and decreases in analyte concentration.

2.2 Fluorescence as a Method for Detection

Fluorescence is a phenomenon in which a molecule absorbs a photon of light (excitation) and subsequently emits a photon (emission) at a longer wavelength than the one it absorbed.[29] The fluorescence process is illustrated in the Jablonski diagram shown in Figure 13. A molecule, atom, or ion at its ground state (S_0) could be excited to a higher

vibrational level of singlet excited state (S_1 or S_2). The molecule may undergo internal conversion that is the relaxation to the lowest energy excited state. Then, the electron may return to the ground vibrational state and emit a photon which is fluorescence. The absorption energy is greater than the energy of emission and the wavelength (λ) of emission is higher than the absorption wavelength. The Stoke shift is the difference between maxima of the excitation and emission spectrum. Stoke shifts depend on the structure of a fluorophore and its environment, such as a solvent.

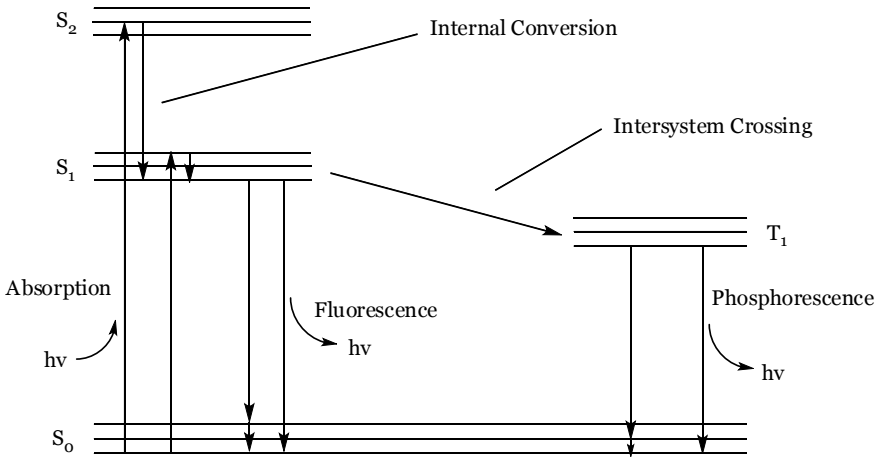

Figure 13 Jablonski diagram

Absorption of a photon does not always lead to fluorescence. The ratio of number of photons emitted to photons absorbed is the quantum yield (Φ) which gives the efficiency of the process. The maximum fluorescence quantum yield is 1.0 which means that all photons absorbed result in all photons emitted. Fluorescence quenching is the decrease of fluorescence intensity by the transfer of energy. The energy may transfer to another part of excited molecule or to another chemical species such as solvent.

If an electron at the S_1 state transfers by intersystem crossing to the triplet excited

state (T_1), phosphorescence may occur. This process occurs over much longer time periods than fluorescence because the lifetime at triplet state is long.

Chemosensors are widely used in sensing a variety of analytes by observing a change in fluorescence upon the binding of the analyte. There are many strategies which are photoinduced electron transfer (PET) quenching, π-system modulation, eximer formation, fluorescence resonance energy transfer (FRET), and environment sensitivity. Some of those strategies are discussed below.

2.3 Photoinduced Energy Transfer (PET) System

PET quenching occurs when the excitation of a fluorophore is followed by transfer of an electron from the HOMO of a donor (quenching element) into the HOMO of excited acceptor (fluorophore) as shown in Figure 14. When electrons are fully filled in the HOMO of a fluorophore, an electron transfers from the LUMO of a fluorophore to the HOMO of the donor. This process occurs when the energy level of the HOMO of donor is slightly higher than the HOMO of the fluorophore.

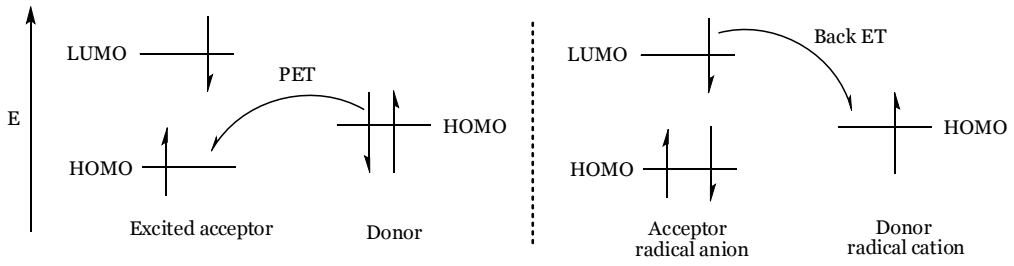

Figure 14 The frontier energy diagrams illustrating thermodynamics of PET and back electron transfer

The signaling of PET quenching is illustrated in Figure 15. The PET quenching sensors consist of a fluorophore linked to a receptor with a spacer. Before binding of an analyte by the receptor, the HOMO of a free receptor is slightly higher in energy than the HOMO of the flurophore. However, the HOMO of a bound receptor is slightly lower than the HOMO of the fluorophoe after binding. Because of this process, PET quenching systems have "off-on" switch system.

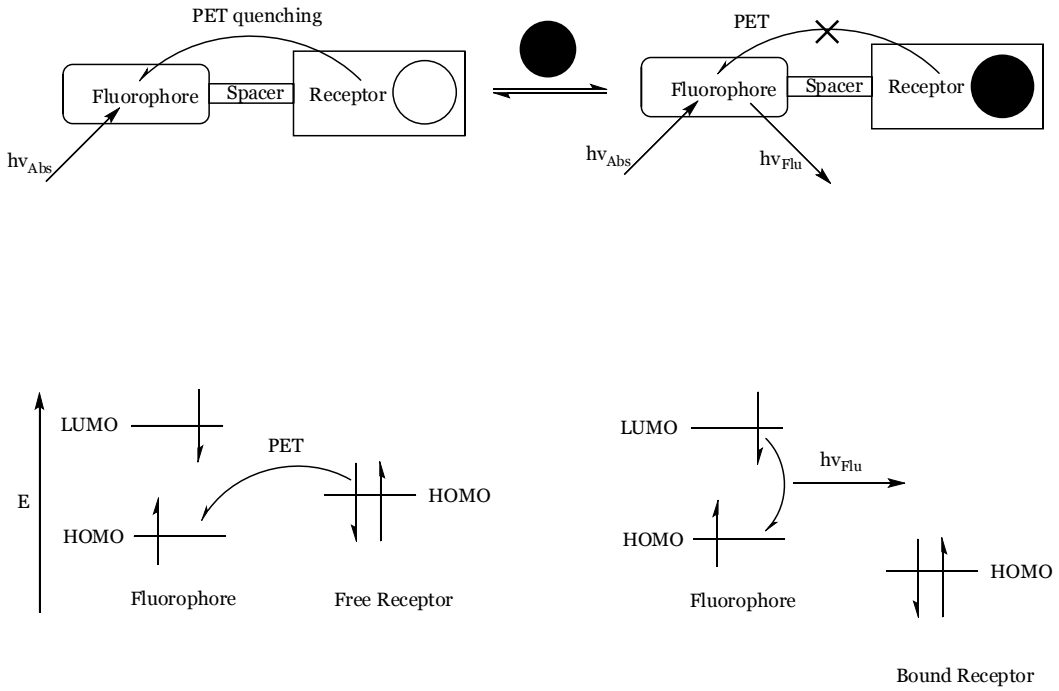

Figure 15 The "off-on" PET system and the energy diagram

The Czarnik group has reported[30,31] the anthracene based chemosensor **37** which is an "off-on" PET system as shown in Scheme 4. In the unbound state, the lone pair electrons on the nitrogens quench the fluorescence of the anthracene by PET. Therefore, the sensor has very low fluorescence intensity. Chelation of pyrophosphate causes a strong

hydrogen-bonding between the benzylic amines and the hydroxyl groups of the pyrophosphate. The hydrogen-bonding blocks the quenching of fluorescence by the lone pair electrons on the nitrogen and the anthracene emits strong fluorescence.

Scheme 4 Anion (pyrophosphate) sensing by a PET quenching mechanism

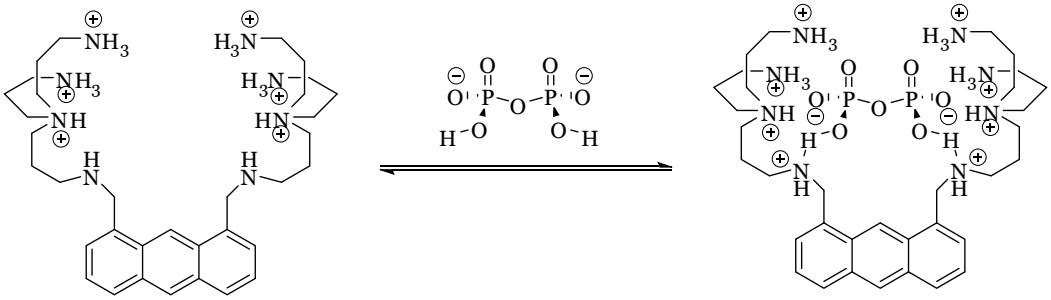

37

Low Fluorescence

37 • $H_2P_2O_7^{2-}$

Strong Fluorescence

The Shinkai group has prepared[32] boronic acid based PET quenching chemosensor **38** for sensing glucose as shown in Scheme 5. Before binding glucose, PET quenching of sensor **38** reduces the fluorescence intensity of the antheracence fluorophore. However, the fluorophore emits strong fluorescence upon the binding of glucose. The fluorescent species existed as both **38a** (2:1 complex between glucose and the sensor) and **38b** (1:1 complex), but the 2:1 complex is more stable than 1:1 complex in the binding of D-glucose. It was found that D-fructose binds in a fashion similar to **38a,** but D-galactose binds in a fashion similar to **38b**.

Scheme 5 The mechanism of the binding of glucose by a boronic acid based PET quenching chemosensor

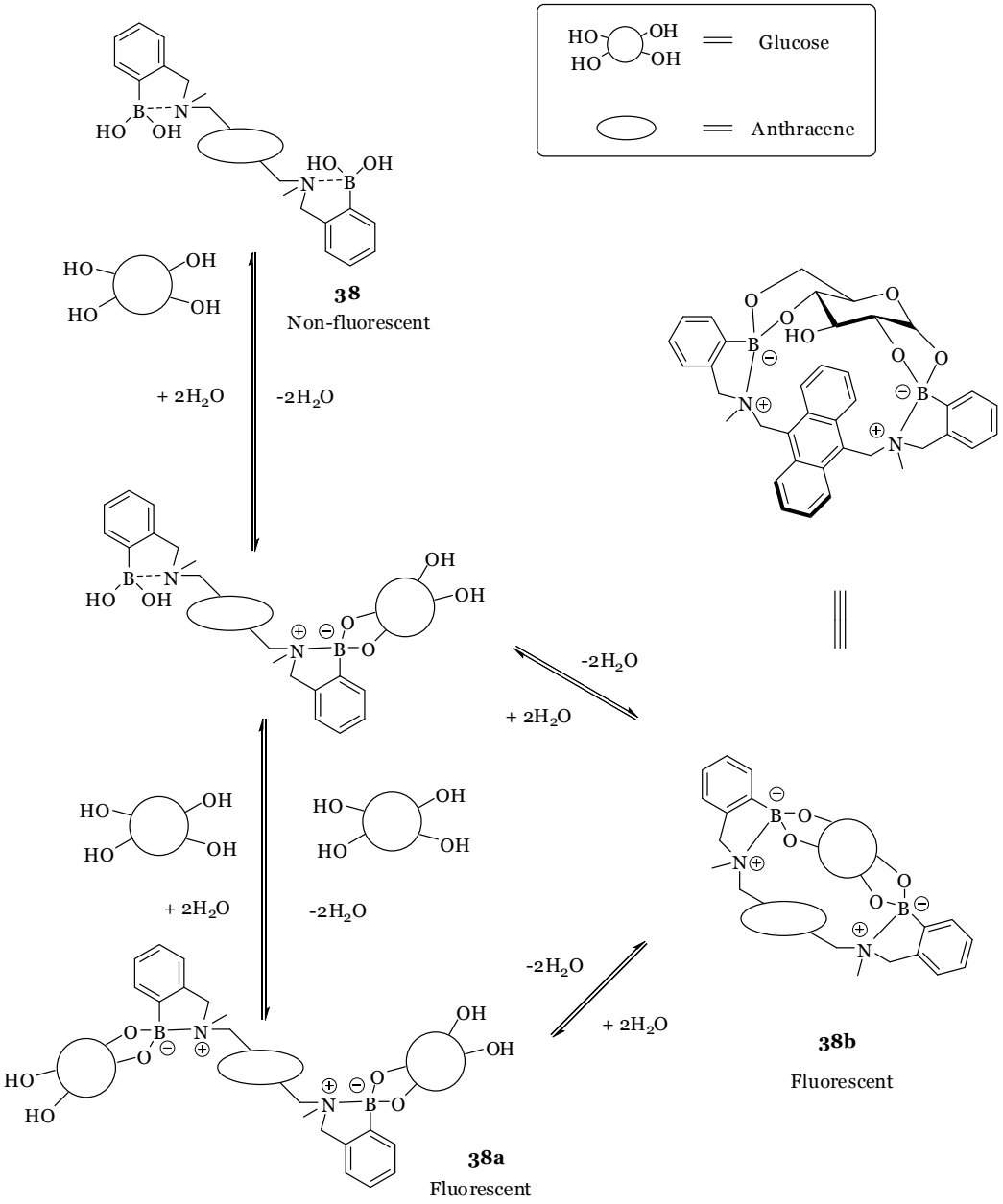

2.4 Excimers

Excimers are fluorophore dimers which are stable in the excited state. This occurs in solutions, pure liquids, intramolecular excimers, and sandwich dimers.[33] In the case of sandwich dimers, the energy transfers from one fluorophore in an excited state into another fluorophore. Pyrenes are usually used in excimer sensor systems with "turn-on" and "turn-off" systems.

The Kim group has published[34] a Cu^{2+} ion-induced self-assembly of a pyrenyl excimer system. If the pyrene monomers **39** meet Cu^{2+} ion, they form 2:1 complexes **39·Cu²⁺** and emit excimer fluorescence as shown in Scheme 6. An emission band increased at 460 nm upon the addition of Cu^{2+} and at 400 nm with various other metal cations. However, Cu^{2+} was more selectively detected than other metal ions.

Scheme 6 Cu^{2+} ion-induced self-assembly of a pyrenyl excimer system

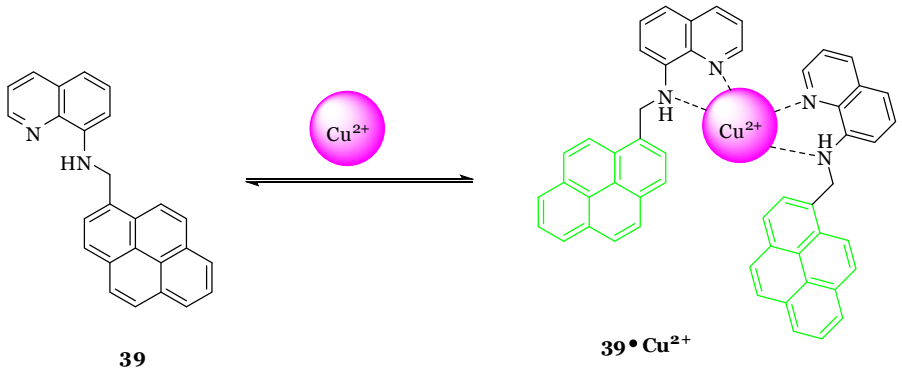

39 **39 • Cu²⁺**

As another example, the Kim group has synthesized[35,36] another excimer based calix-4-crown chemosensor for sensing certain metal ions. Two pyrenes are attached on the low-rim of the calix[4]arene which contains a crown ether moiety on the upper-rim. A calix-4-crown has strong excimer emission while it does not bind any analyte and the

excimer still turns on when a certain Group I metal ions (K^+, Li^+, and Cs^+) were sensed. But, the excimer turns off when other metal ions (Pb^{2+}, Ag^+, Mg^{2+}, Ca^{2+}, and Zn^{2+}) were bound lower-rim of the sensor because the distance between two pyrenes was increased. Therefore, this sensor can selectively detect a toxic Pb^{2+} ion.

Scheme 7 Excimer fluorescent chemosensor for sensing metal ions

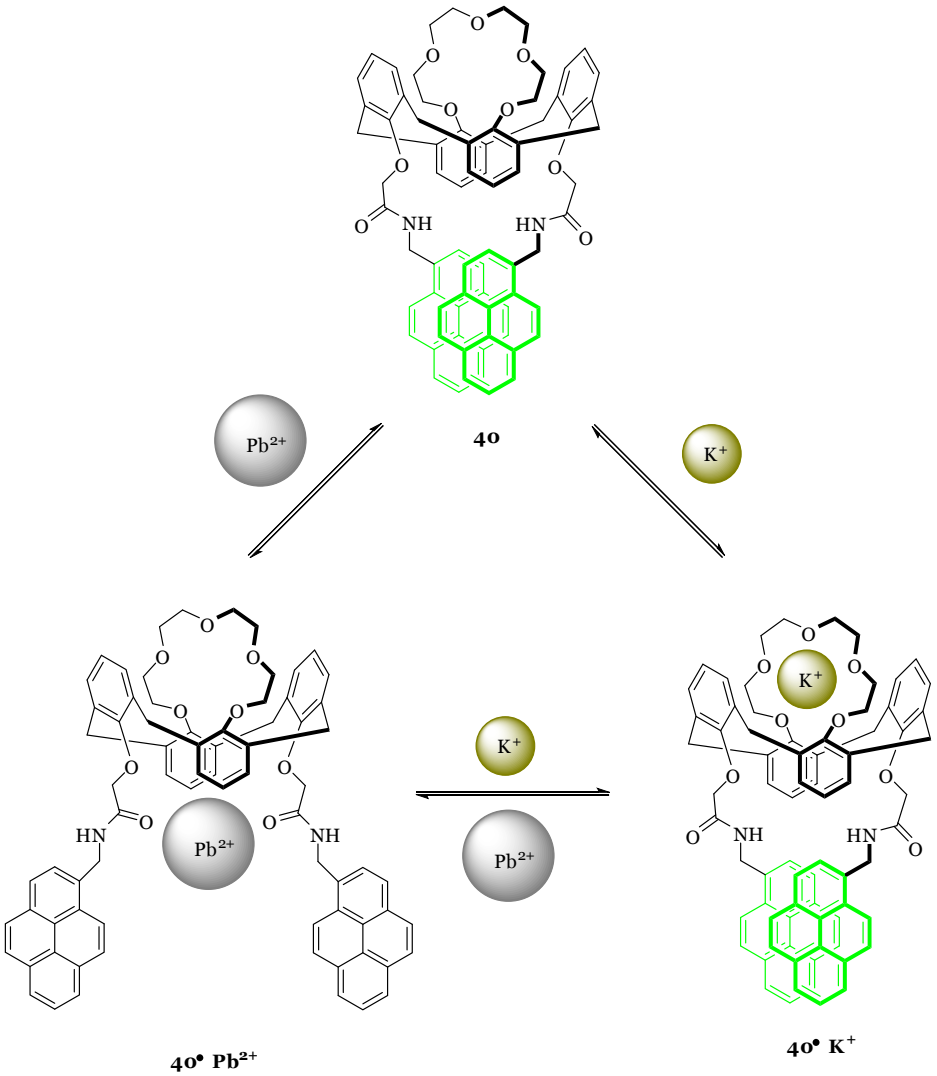

2.5 Conclusion

Fluorescent chemical sensing has been studied in a variety of fields for the past several decades. Many useful chemosensors have been introduced in order to monitor biological functions. The research and development of chemosensors are still needed to satisfy the demand of biological and environmental research.

Chapter 3. Lipids and Long-Chain Alkane Sensing

3.1 Lipids and Lipid Sensing

Lipids play an important role in biology.[37] They are hydrophobic or amphiphilic molecules. The functions of lipids are energy storage, forming the membranes between the intracellular and extracellular cells, hormones, and vitamins. Even though they are important in human life, certain lipids cause diseases such as cardiovascular diseases (CVD). Lipids are classified fatty acids, glycerides, non-glyceride lipids, and complex lipids as shown in Figure 16.

Fatty acids consist of a nonpolar hydrocarbon chain with a polar carboxylic acid at the end. They are amphiphatic which means part is soluble in water and part is not. The aliphatic chain can be saturated or unsaturated. Fatty acids play an important role in the life and death of cardiac cells because they are essential fuels for the mechanical and electrical activities of the heart. [38,39]

Glycerides are commonly known as acylglycerols which are formed from glycerol and fatty acids. They consist of neutral glycerides and phospholipids. Neutral glycerides could be mono-, di-, or triglycerids dependent on the number of ester groups on the hydroxyl groups of glycerides. These lipids serve as energy storage in adipose cells.[40] Phospholipids are a major component of cell membranes as they can form lipid bilayers. They are generally diglycerides linked to a phosphate group and a polar head group such as choline. In cell, phospholipids form membranes which serve as barriers to keep the inside and outside of a cell separate. The polar head of the molecules faces the inside of a cell as well as the outside of a cell, and then the non-polar fatty acid groups assemble

together and form a hydrophobic barrier.

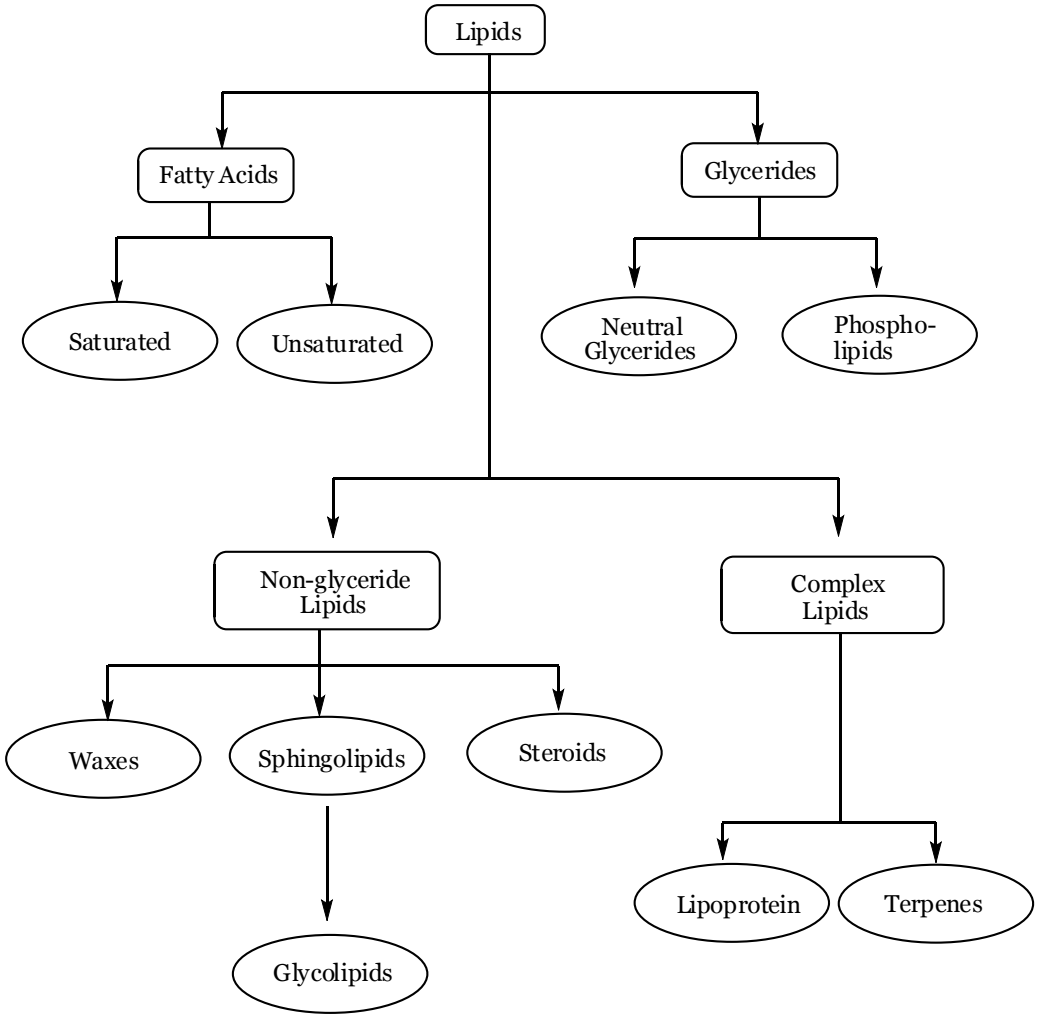

Figure 16 The classification of lipids

Nonglyceride lipids consist of waxes, sphingolipids, and steroids. Sphingolipids are based on sphingosine and are also a component of cellular membranes. The sphingolipids encompass sphongomyelins, which are a structural lipid of nerve cell membranes, and glycosphingolipids. Steroids are organic compounds that have a cyclopentia[a]phenanthrene skeleton or their derivatives.[41,42] Steroids encompass

cholesterol and various hormone. Cholesterols are needed to build and maintain cell membranes for all animals.[43] They are made in the liver and taken from dairy products. They are transported from liver to cells by the blood stream.

Lipoproteins are complex lipids found in blood plasma. They are coated with phospholipids and have cholesterols and triglycerids in their core. They consist of low-density lipoprotein (LDL), high-density lipoprotein (HDL), and very low-density lipoprotein (VLDL). VLDL is made in liver and transports lipids to tissues. Both LDL and HDL are made in the liver as well. LDL which is called "bad cholesterol" carries cholesterol to cells and HDL which is called "good cholesterol" scavenge excess cholesterol. Those are related with cardiovascular diseases (CVDs) such as coronary artery diseases (CADs). The main CAD is atherosclerosis.[40, 44]

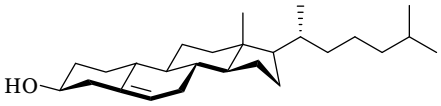

41 Cholesterol

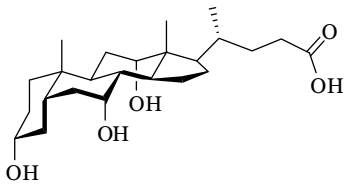

42 Cholic acid

43 Progesterone

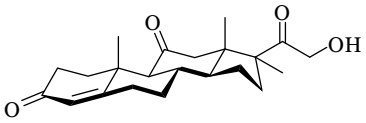

44 Cortisone

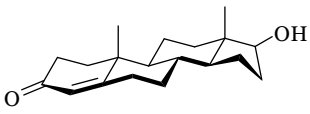

45 Testosterone

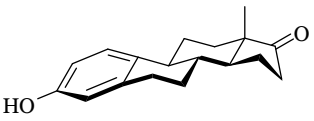

46 Estrone

Figure 17 Representatives of some steroids

Because of their biological importance, many scientists have tried to bind steroids, especially cholesterols.[45] Some of the important steroids are illustrated in Figure 15. The most common receptors for steroids are various size cyclodextrins (CDs) because they have hydrophobic cavity and are strongly soluble in water. There are α- (6 dextrins), β- (7 dextrins) , and γ-CD (8 dextrins), dependent on number of dextrin shown in Figure 18.

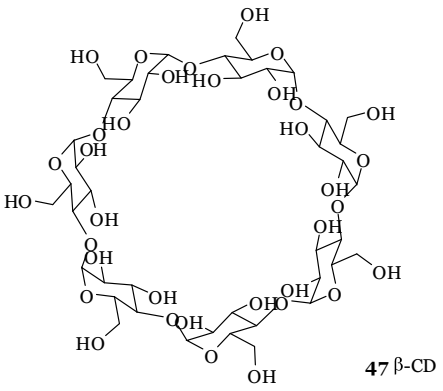

47 β-CD

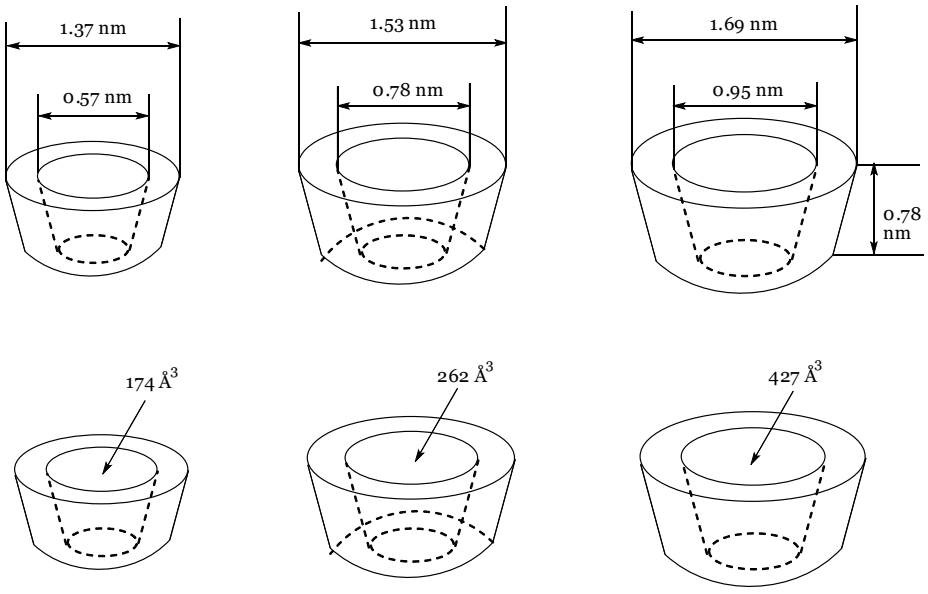

Figure 18 The structure of β-CD, approximate diameter, and cavity volume of α-, β-, γ-CD.[46]

The Breslow group has published[47] cholesterol receptors by means of the β-CD dimers shown in Figure 19. The association constant of β-CD for cholesterol is 300 times lower than β-CD dimer **48** as shown in Table 4. Cholesterol is encapsulated in the hydrophobic cavity of β-CD, but the dimer has a longer cavity than regular β-CD. This is the reason why the dimer has a higher association constant.

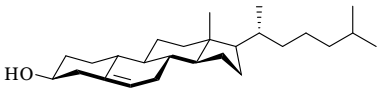

41 Cholesterol

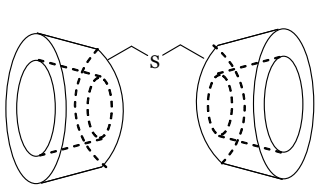

48

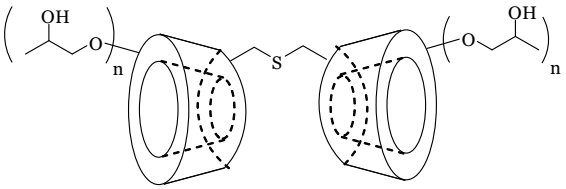

49

Figure 19 The structure of cholesterol and β-CD dimer receptors

Table 4 The binding constants of host-cholesterol complex in water at 25˚C

Host	K_a (M^{-1})
β-cyclodextrin (CD)	$1.7 \quad 10^4$
dimer **48**	$(5.54 \pm 0.76) \quad 10^6$
dimer **49**	$(1.47 \pm 0.62) \quad 10^5$

The Deiderich group has reported cyclophane **50** and **51** as a receptor for binding aromatic guests.[48,49] The distance between two meta hydrogens of cyclophane **50** is

approximately 4.3 Å and between the bridging oxygens is approximately 8.4 Å. The height of the wall is appoximatly 7 Å from lower methoxy to the upper one. Therefore, this cyclophane has an effective cavity for the tight encapsulation of guests. Cyclophane **50** is the better receptor for neutral steroids, but cyclophane **51** is more efficient in sensing anionic guests because it has four quaternary ammonium groups. The binding constant of cyclophnae **51** - ursodeoxycholic acid complex is 10 times higher than those of cyclophane **50** because cyclophane **51** has bigger cavity volume and diameter with two naphthalenes in their structure.

All steroid receptors use a hydrophobic cavity to encapsulate the hydrophobic steroids. This method is efficient to make a tight complex between a host and a steroid guest.

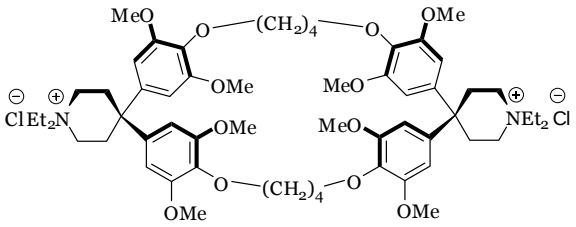

50

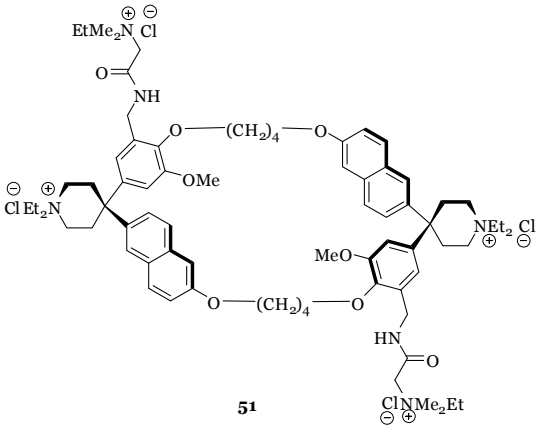

51

Table 5 The binding constants for cyclophane hosts and various steroids

Host	Guest	Binding Constants K_a (M^{-1})
50	Cholic acid	150
	Cortison	1,500
	Ursodeoxycholic acid	1,750
	Testosterone	3,500
51	Dehydrocholic acid	3,000
	Ursodeoxycholic acid	18,900
	Glycocholic acid	37,300
	Hyodeoxycholic acid	100,000

3.2 Low-Density Lipoproteins (LDLs) and Oxidized Phospholipids (OxPLs)

Lipoproteins are synthesized in the liver and intestines and are used to transfer lipids.[50] LDLs transport cholesterols from the liver to cells, and HDLs carry back excess cholesterols from cells to the liver. LDLs are related to coronary artery disease (CAD) such as atherosclerosis.[51] They have cholesterols and triglycerids in their core and are coated with phospholipids and an apoprotein B-100 (Apo-B100) in their surface. If the phospholipids on the surface of LDL particle are oxidized, the oxidized LDL may accumulate on the wall of the artery. Therefore, oxidized phospholipids are a potential predictor of coronary artery disease.[52-55]

Phophatidycholine (PC) is the main phospholipid on the surface of the LDL particle. Phospholipids can be oxidized by enzymes such as lipoxylgenase, myeloperoxidase, and NADPH oxidase.[56-58] The oxidation of 1-hexadecanoyl-2-eicosatetra-5',8',11',14'-enoyl-*sn*-

glycero-3-phosphocholine (PAPC) is shown in Scheme 8. The macrophage scavenger receptor CD 36 recognize oxidized phospholipids on the surface of oxidized LDL (oxLDL), causing then to absorb the LDL particle.[59]

Scheme 8 The oxidation reaction of phospholipids

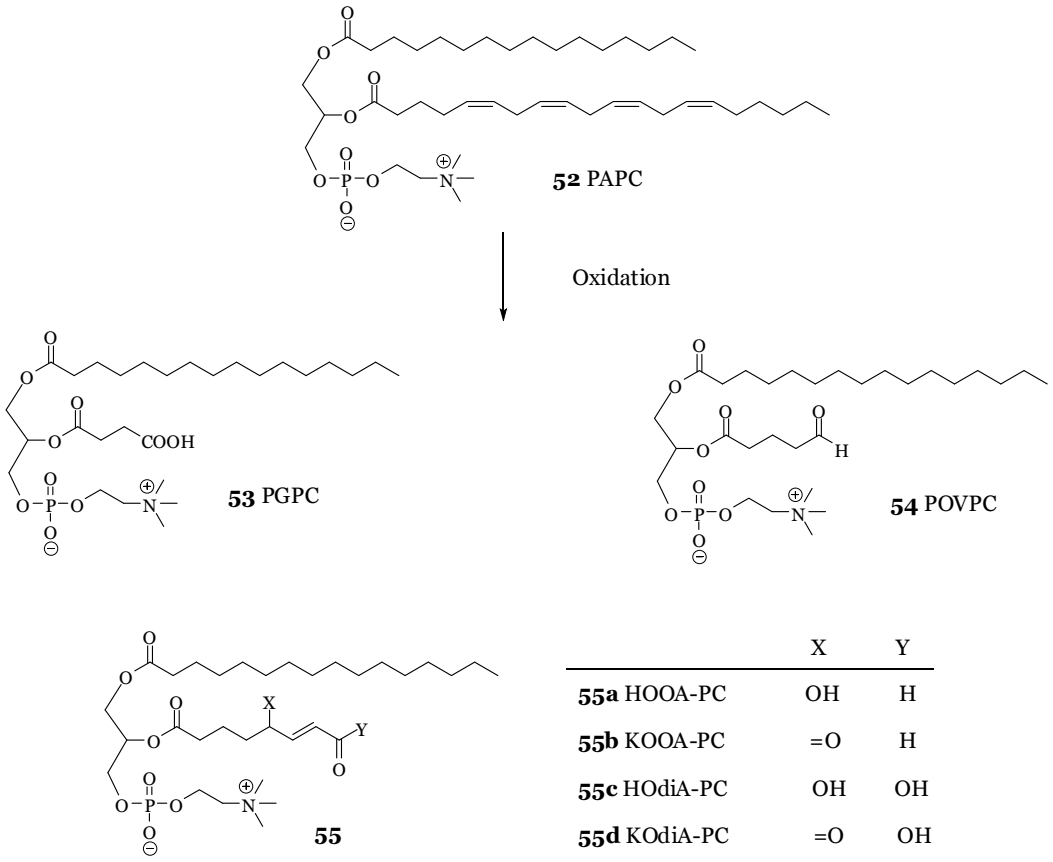

	X	Y
55a HOOA-PC	OH	H
55b KOOA-PC	=O	H
55c HOdiA-PC	OH	OH
55d KOdiA-PC	=O	OH

3.3 Long-Chain Alkane Sensing

The Gibb group has reported a cavitand **56** as a receptor for hydrophobic guests

including long-chain alkanes.[60,61] Hydrophobic effect[62,63] explains the binding between the cavitand **56** and guests. The shorter guests like pentane through heptanes formed 2:2 complexes, while guests longer than octane formed 2:1 complexes as shown in Scheme 9. However, octane is unique as it formed both 2:1 and 2:2 complexes.

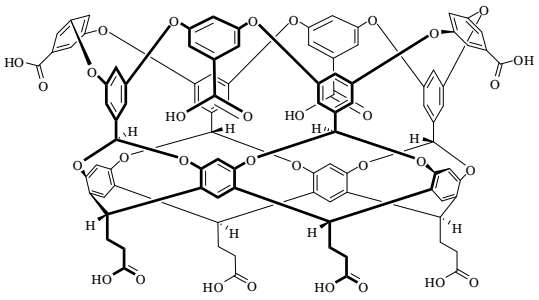

56

Scheme 9 The complexes of cavitand **56** and alkanes: 2:2 complex and 2:1 complex

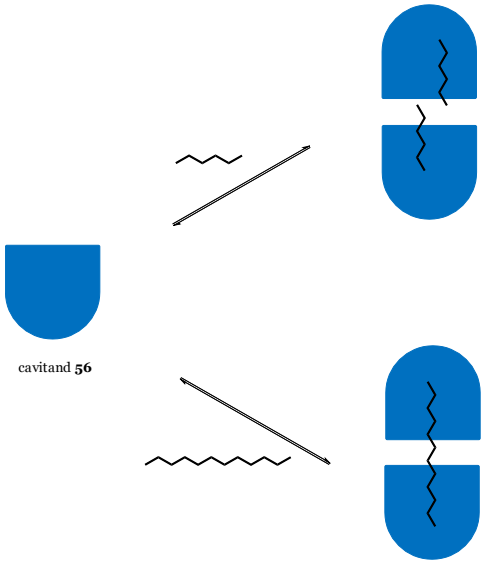

The Rebek group has reported a water-soluble cavitand **22** for the recognition of alkyl groups.[27,64-66] Dodecylphosphocholine (DPC) and sodium dedecylsulphate (SDS) have helical conformations when they bound in the hydrophobic cavity of a cavitand **22**.

When the host-guest complex was present in D_2O, the proton signal of the carbon atoms of the alkyl groups shifted up-field in the NMR spectra. The cavity volume is approximately 225 Å^3, and that of the helical alkane is about 126 Å^3. The coiled alkane chain inside the cavity has gauche strain which is approximately 0.5-0.6 kcal/mol. The structure of the complex was determined by NOe studies.

(a) 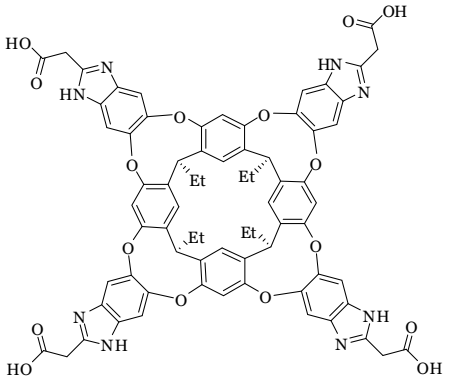

22

(b) 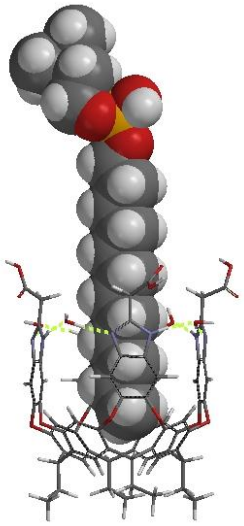

Figure 20 (a)The structure of water soluble cavitand **22** (b) and the complex with DPC (3D model from Wavefunction Inc. software Spartan 06').

The Rebek group has synthesized another cavitand **57** as a receptor for a variety of analytes such as anions,[67] aromatics,[68-72] and alkanes.[73] Long-chain alkanes can be encapsulated inside the cavity of dimeric capsule **58**. The length and volume of the capsule is 15 Å and 450 Å^3, respectively. On the other hand, the length of tetradecane (*n*-$C_{14}H_{30}$) is 14.8 Å when it was coiled. Therefore, the straight chain alkanes which are shorter than pentadecane (*n*-$C_{15}H_{32}$) can be sufficiently encapsulated in the dimeric capsule.

Scheme 10 The formation of capsule **58** by dimerization of cavitand **57** (3D model from Wavefunction Inc. software Spartan 06' and R group was eliminated for clarity).

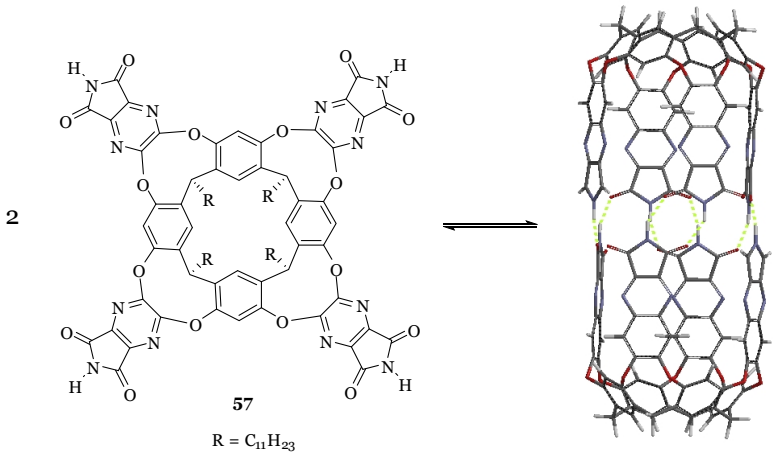

Glycoluril spacers **59a** and **59b** were added between dimeric capsule and the size of dimeric capsule was expanded. The capsule can be expanded based on the number of glycoluril spacers. The length of capsules is 15 Å (volume 450 Å^3), 22 Å (620 Å^3), 28 Å (810 Å^3), and 35 Å (980 Å^3) which added 0, 4, 8, and 12 glycoluril spacers, respectively.

Scheme 11 The structure of the expanded capsule **60** (3D model from Wavefunction Inc. software Spartan 06').

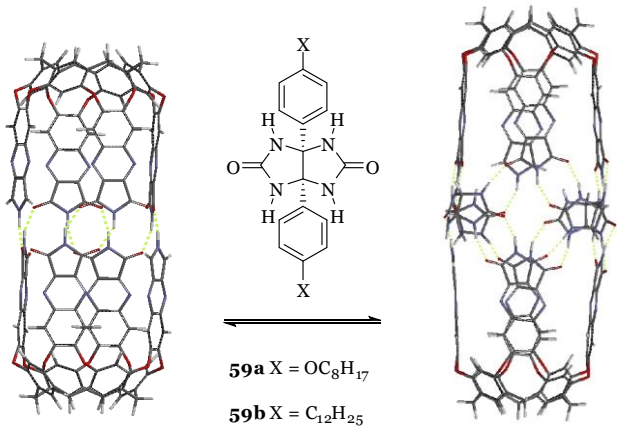

Table 6 The length and volume of the expanded capsule

Number of glycoluril spacer	Length (Å)	Volume (Å^3)
0	15	450
4	22	620
8	28	810
12	35	980

3.4 Conclusion

Lipid sensing is important for research and development of biological studies. Steroid recognition has been one of main lipid sensing so far. Alkane sensing is helpful for the recognition of phospholipids which are materials of cell membrane. However, receptors for alkanes do not have excellent selectivity to recognize between long straight chain alkanes and other alkanes. Therefore, the selective recognition of long straight chain alkane is important, but still needs more research.

Chapter 4. Prior Group Work

4.1 Molecular Tubes

The Glass group has prepared naphthalene based sensors which were named molecular tubes (**61**).[74] The aromatic rings constitute flat and rigid surfaces that would function suitably as the walls of the tubes. Because of the fluorescence of naphthalenes, the molecular tubes could act as fluorescent sensors. The bicyclic bridge links the naphthalene rings together in a rigid conformation. Moleuclar tubes have four carboxylic acid groups for water solubility.

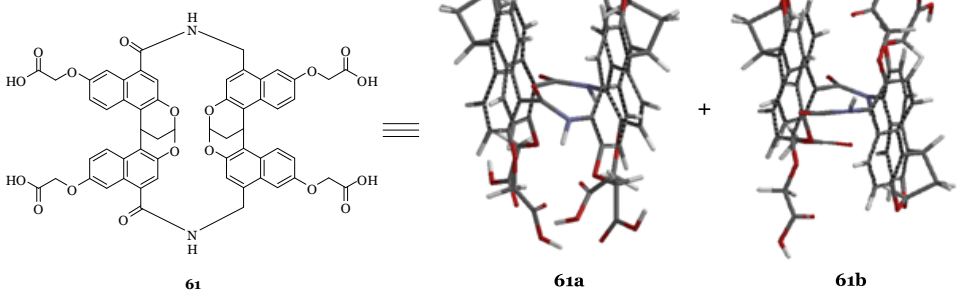

61 **61a** **61b**

The alkane chain of a variety of lipids could be encapsulated in the hydrophobic cavity of molecular tubes via the hydrophobic effect in water. The fluorescence of molecular tubes was enhanced or quenched based upon the type of hydrophobic guests. Molecular tube **61** has two different isomers: syn- (**61a**) and anti-isomer (**61b**). The association constant of dodecanoic acid was increased 1000 times greater the butyric acid. Also, straight chain

guests have higher association constants than branched chain guests because branch methyl group does not fit inside of the cavity. However, non-ionic and cationic guest, 1-heptanol and heptylamine, have pretty high binding constants such as 4,900 and 16,000 M^{-1}, respectively. The reason is that they do not have repulsion with carboxylates at the bottom of tubes.

Table 7 The association constants and fluorescence changes of molecular tubes with lipid guests

	Syn-isomer **61a**		Anti-isomer **61b**	
Lipid	K_a (M^{-1})	I_{sat} / I_0	K_a (M^{-1})	I_{sat} / I_0
acetic acid	-	-	-	-
butyric acid	17	1.25	18	0.92
hexanoic acid	100	1.14	72	0.32
octanoic acid	250	0.39	190	0.25
decanoic acid	3,500	0.48	3,800	0.32
dodecanoic acid	18,000	0.47	27,000	0.31
trans-3-octenoic acid	92	0.61	110	0.26
4-methyloctanoic acid	71	1.05	200	0.32
8-methylnenanoic acid	1,600	0.57	690	0.25
cyclohexane carboxylic acid	470	7.1	100	0.80
triethylene glycol	63	1.83	36	0.34
1-heptanol	4,900	0.28	6,700	0.19
cis-4-hepten-1-ol	1,200	1.32	5,200	0.58
heptylamine	16,000	0.42	16,000	0.11

4.2 Functionalizaing Molecular Tubes

Molecular tubes have excellent selectivity and fluorescence change upon the binding alkanes of various lengths. However, the molecular tubes only recognize the hydrophobic portion of the lipid. Many biologically important lipids have a unique head group. Therefore, it is necessary to add head group binding elements to the tube. We decided to functionalize the tube with one aldehyde group which could be elaborated into a number of binding elements.

Our first target was aldehyde **62**. Compound **62** was based on an allyl linked tube with an aldehyde at one open end. Interestingly, compound **62** was not completely symetrical like the other tubes and should be produced as a pair of enantiomers. However, the two enantiomers are similar and should bind chiral lipids very much the same.

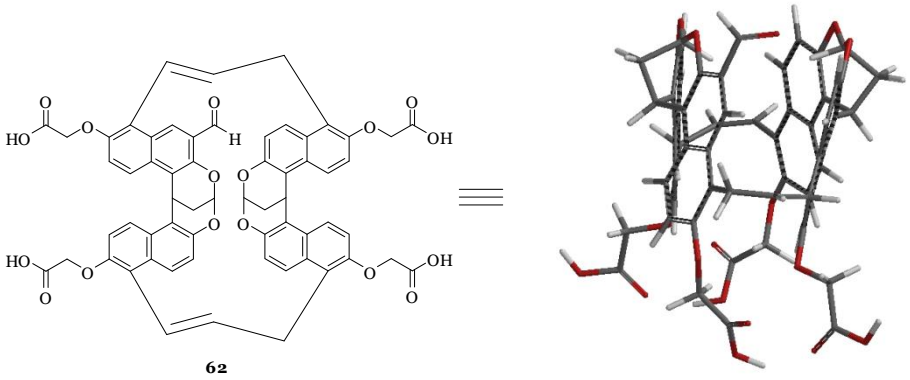

62

Therefore, 2,6-dihydroxynaphthalene **63** was converted into allyl-naphthalene dimer **64** by treatment with allyl bromide and a base followed by malonaldehyde bis(dimethyl)acetal. The allyl groups migrated to C 1 of the naphthalene group via a Claisen rearrangement and then compound **65** was obtained after reaction with ethyl

bromoacetate and sodium hydride (NaH). Formylation was attempted with a variety of reactions shown in Table 8. However, all attempts failed to provide the aldehyde product even at elevated temperature.

Scheme 12 Synthesis of allylic-formyl-naphthalene dimer **66**

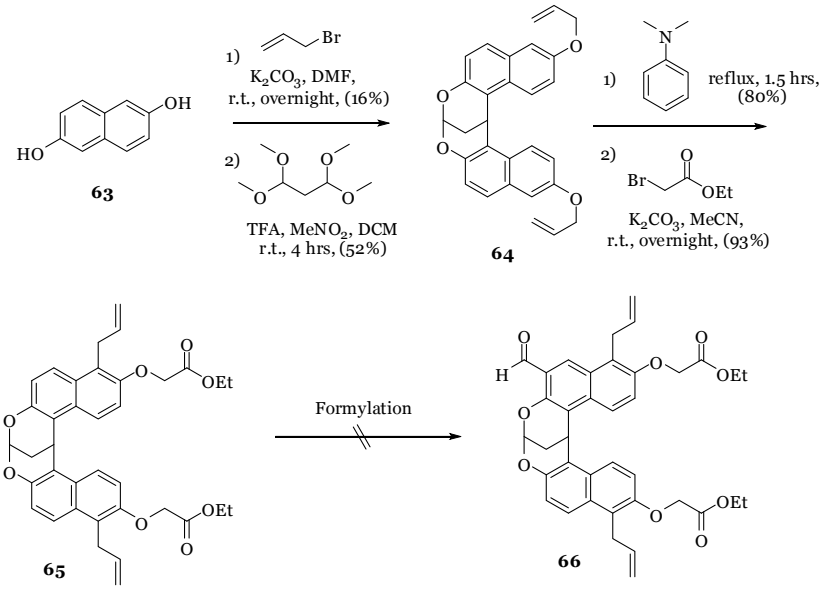

Table 8 Attempts to formylate on naphthalene dimer **65**

Reagents	Solvent	Temperature	Time	Results
$POCl_3$	DMF	r.t.	16 hrs	NR*
$POCl_3$	DMF	70˚C	14 hrs	NR
$Cl_2CHOCH_3/Ti(IV)Cl_4$	DCM	r.t.	16 hrs	NR
$Cl_2CHOCH_3/Ti(IV)Cl_4$	$ClCH_2CH_2Cl$	70˚C	16 hrs	NR
$(CF_3SO_2)_2O$	DMF	130˚C	18 hrs	NR
$C_6H_{12}N_4/H_2O$	CF3COOH	reflux	16 hrs	NR

(*NR : No Reaction)

Dimethoxyl dimer **67** was prepared as shown in Scheme **13**. Methoxy groups were used instead of the normal esters to avoid deprotection of the carbonyl in the subsequent step. Formylation was achieved with *n*-butyllithium (*n*-BuLi) / *N*, *N*'-dimethyl-formaldehyde (DMF) to give the desired product **68**. When tetrahydrofurane (THF) was used as a solvent, the ratio of product **68** and a side-product **69** was approximately 1:1. With diethyl ether (Et_2O), a 4:1 ratio was observed by ^{1}H-NMR. Unfortunately, these products were not separable by column chromatography. Therefore, the position of aldehyde was proved by reduction with sodium borohydride ($NaBH_4$) as shown in Scheme 14. The hydroxyl methyl compounds were separable and their regiochemistry was determined by ^{1}H-NMR.

Scheme 13 Synthesis of formylmethoxy naphthalene dimer **68**

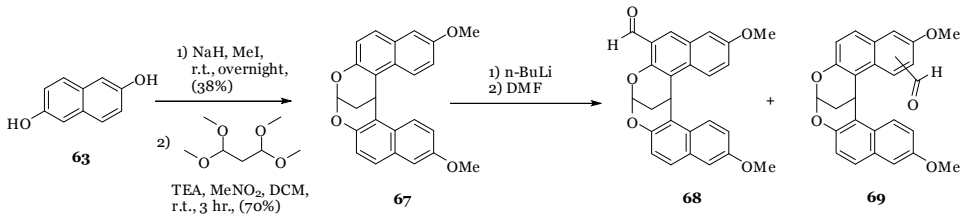

Scheme 14 Reduction of formylmethoxy naphthalene dimers **68** and **69**

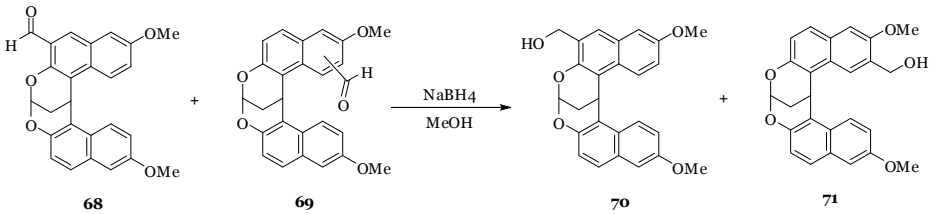

Unfortunately, compound **67** was highly soluble in THF, but was slightly soluble in Et_2O. An insoluble portion of compound **67** were not reacted in Et_2O. Due to the low yield of the reaction and difficulty in separation of the product, this route was abandoned.

4.3 Conclusion

The two isomers of the molecular tube are sufficient sensors for all types of lipids because they recognize lipids using a hydrophobic cavity in water. However, they do not have any other functional group for the recognition of more complex lipids. Their fluorescence is increased or decreased dependent on lipids.

Chapter 5. The Open-Tubes for Alkane Sensing

5.1 Designing Open-Tubes

The open-tube project was designed for the preparation of molecular tubes based on the naphthalene dimer. The disadvantages of the original molecular tubes were the difficulty in separating the isomers as well as low yield. Therefore, we decided to make open-tubes using naphthalene dimer **72** as a core group.

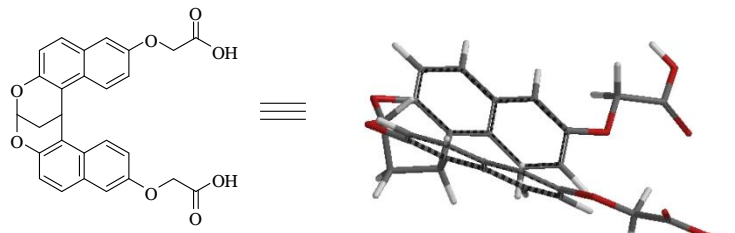

72

Compound **72** can be attached at the 1-positions on the naphthalene to produce an open, cleft-like structure **73** shown in Figure 21. These aromatic groups form the "walls" of the tube and might change fluorescence upon the binding of guests. Importantly, it becomes possible to easily add head-group binding elements to these aromatic groups.

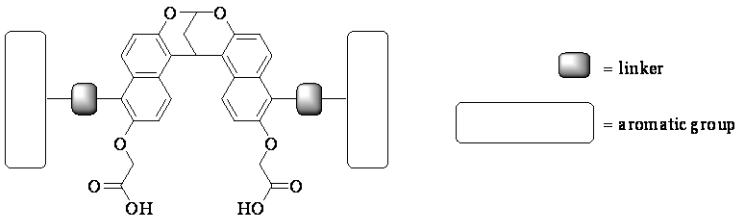

73

Figure 21: Representation of open-tubes

Scheme 15 Coupling reaction to synthesize molecular tube **61**

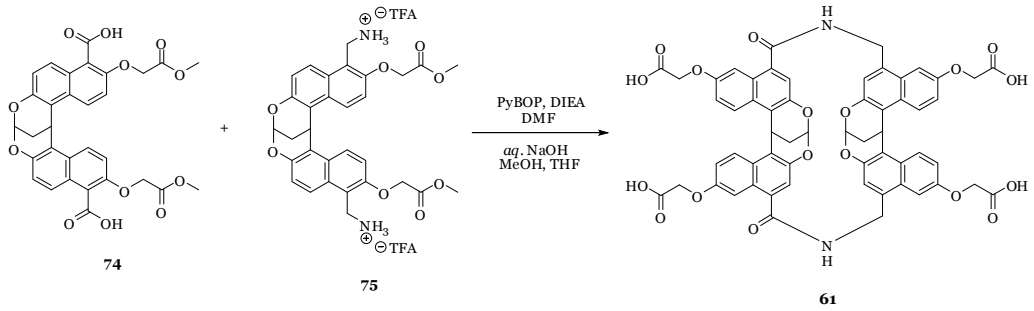

74 **75** **61**

Based on the species of amide coupling to produce closed-tube 61 (Scheme 15). We decided to use coupling chemistry to append the aromatic groups. Therefore, we would use a naphthalene dimer like **74** and an aromatic amine. Anthracene was the first attempted fluorophore. 9-Anthracene methanol **76** was converted into 9-bromomethyl anthracene **77** by reaction with phosphorous tribromide (PBr_3) in toluene in high yield. Bromide **77** was converted into 9-azidomethyl anthracene with sodium azide (NaN_3) in DMF in 100% yield. The azide was then reduced with 5% Pd/C and H_2 in methanol (MeOH) at r.t. for an hour and 9-aminomethyl anthracene **78** was obtained in 85% yield as shown in Scheme 16.

Scheme 16 Synthesis of 9-aminomethyl anthracene **78**

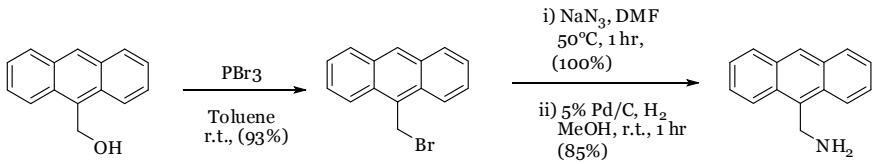

76 **77** **78**

Scheme 17 Synthesis of naphthalene dimer dicarboxylic acid **82**

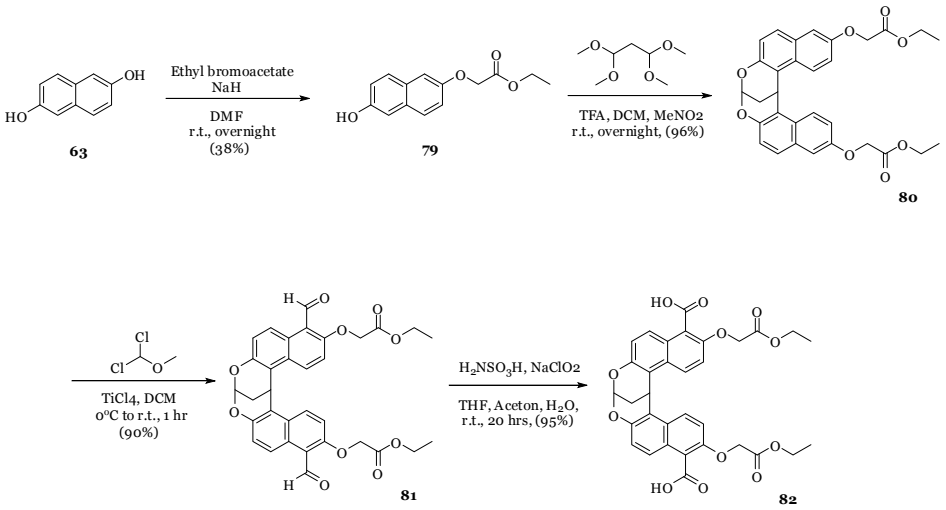

For the naphthalene core group, 2,6-hydroxynaphthalene was alkylated with ethyl bromoacetate and sodium hydride (NaH) and obtained mono-alkylated product **79** in 38% (Scheme 17). Then, compound **79** was dimerized with malonaldehyde bis(dimethyl)acetal in trifluoroacetic acid (TFA), dichloromethane (DCM), and nitromethane ($MeNO_2$). Compound **80** was formylated with α, α-dichloromethoxymethyl ether and titanium tetrachloride ($TiCl_4$) followed by oxidation with sulfamic acid and sodium chlorite to give naphthalene core compound **82**. Compound **78** and **82** were reacted under typical condition, but the reaction did not give the desired product.

Therefore, the naphthalene core was appended with an amine functional group and reacted with 9-anthracene carboxylic acid. Aldehyde compound **81** was reacted with *t*-butoxycarbamate, triethylsilane (TES) to obtain BOC-protected amine compound **83** (Scheme 18). Then, BOC group was deprotected with TFA in DCM. Without work-up, coupling of amine **83** and anthracene carboxylic acid was accomplished using benzotriazol-1-yl-oxytripyrrolidinophosphonium hexafluorophosphate (PyBOP) and diisopropylethylamine (DIEA) in DMF. Saponification of compound **84** was achieved with 6 M-NaOH in MeOH and THF to give acid product **85**.

Scheme 18 Synthesis of anthracene fluorophore open-tube **85**

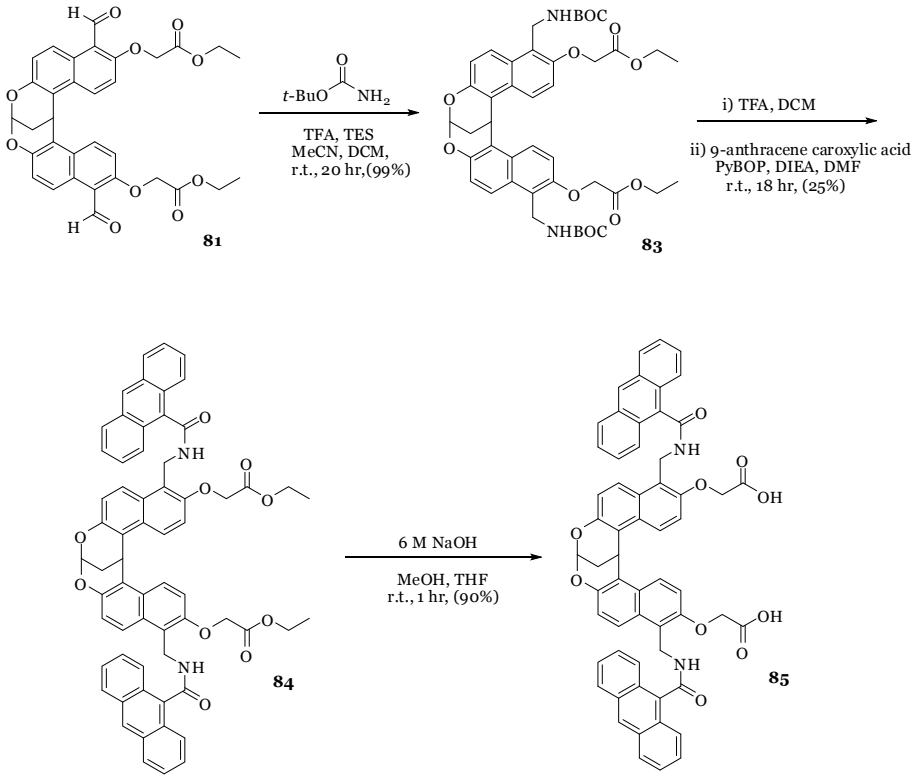

Unfortunately, the fluorescent properties of **85** were poor. The fluorescent emission was not stable, possibly due to intramolecular photoreaction of the anthracene groups. Therefore, a new fluorophore was needed.

We decided to append other aromatic groups, such as dansyl group and functionalized anthracenes. Compound **83** was reacted with TFA in DCM to remove BOC-group followed by the reaction with dansyl chloride and DIEA in DCM to give the desired product **86** in 40%. Saponification of compound **86** was achieved with 6 M-NaOH in MeOH and THF to give acid product **87** in 67%. The fluorescent emission of compound **87** was also not stable.

Scheme 19 Synthesis of dansyl fluorophore open-tube **87**

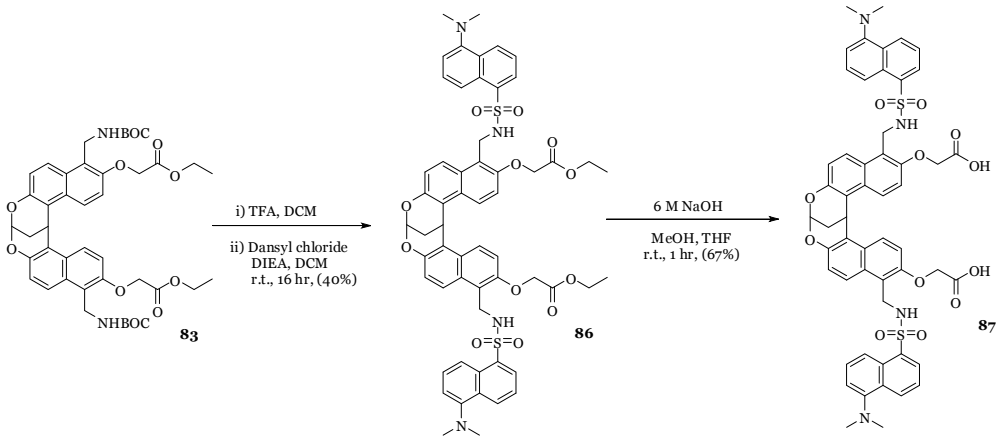

We would use functionalized anthracene like 10-bromoanthracene-9-carboxylic acid **88** and 9,10-anthracene dicarboxylic acid **89**. The BOC group of compound **83** was deprotected by treatment with TFA in DCM. Without work-up, coupling of amine **83** and 10-bromoanthracene-9-carboxylic acid **88** was accomplished using hydroxybenzotriazole (HOBt) and DIEA in DMF in 16% yield. Saponification of compound **90** was achieved with 0.15 M-LiOH in MeOH and THF to give acid product **91** in 97% (Scheme 20).

Scheme 20 Synthesis of 9-bromoanthracene fluorophore open-tube **91**

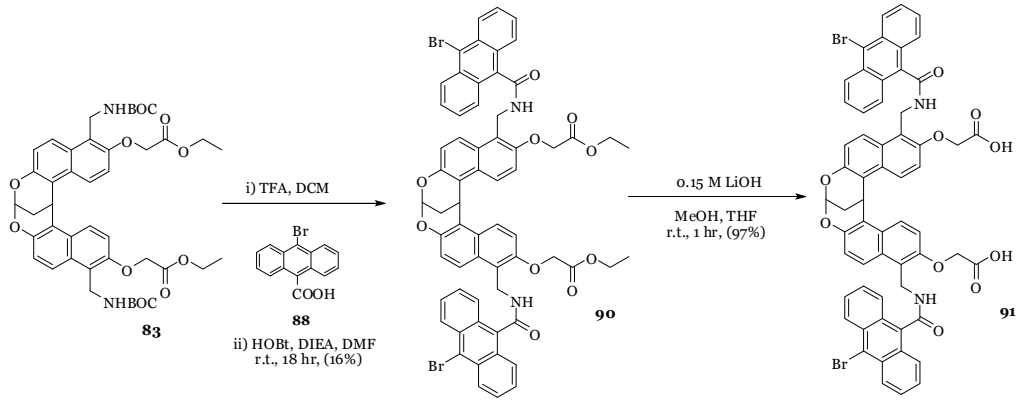

9,10-Dibromoanthracene **92** was achieved lithium-halogen exchange by treatment with *n*-BuLi in Et_2O to give 9,10-dilithioanthracene intermediate. Then, the intermediate was poured into dry ice to give the desired product **89** (Scheme 21).

Scheme 21 Synthesis of 9,10-anthracene dicarboxylic acid **89**

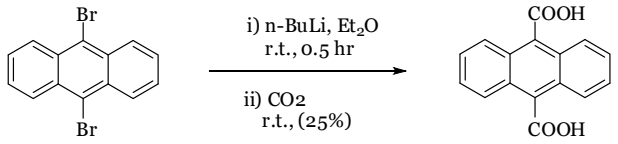

92 **89**

Coupling of amine **83** and 9,10-anthracene dicarboxylic acid **89** was accomplished using HOBt and DIEA in DMF. However, this reaction did not produce the desired product **93** and compound **83** was recovered (Scheme 22).

Scheme 22 Attempt to append 9-anthroic acid at compound **93**

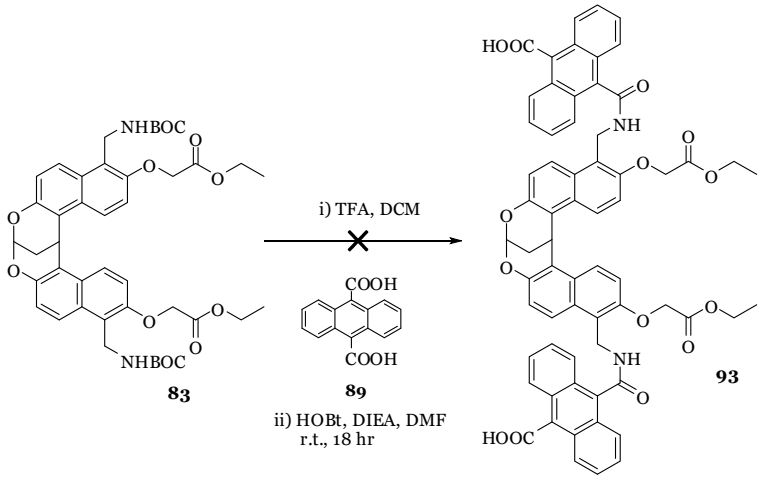

83 **89** **93**

5.2 Synthesis of Open-Tubes

The next open-tube was designed as shown in Scheme 23. The one carbon linker prevents the aromatic side groups from interacting and carbazoles are known to be competent fluorophores.

Scheme 23 The retrosynthesis of carbazole fluorophore open-tubes (3D model from Wavefunction Inc. software Spartan)

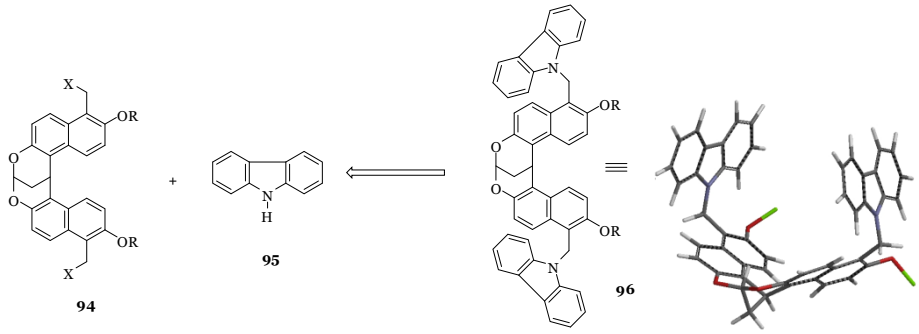

As shown in Scheme 24, alkylation of 2,6-dihydroxynaphthalene with ethylbromo acetate and NaH in DMF gave compound **79** in 38% yield followed by dimerization with malonaldehyde bis(dimethyl)acetal in TFA, DCM, and $MeNO_2$ to afford alkylated-naphthalene dimer **80** in 90% yield. We first attempted to convert compound **80** directly into compound **97** using formaldehyde/HBr. These conditions worked well in a related case (Scheme 25), but for compound **80**, no product was obtained. This is likely due to side reaction of the ester. Therefore, compound **80** was formylated with α, α-dichloromethoxymethyl ether and $TiCl_4$ in DCM gave aldehyde compound **81** in 96% yield. Then, aldehyde **81** was reduced by sodium borohydride ($NaBH_4$) in EtOH and THF at 0˚C for half an hour to obtain alcohol product followed by bromination with phosphorous tribromide (PBr_3) in DCM gave compound **97**.

Scheme 24 Synthesis of bromomethyl naphthalene dimer **97**

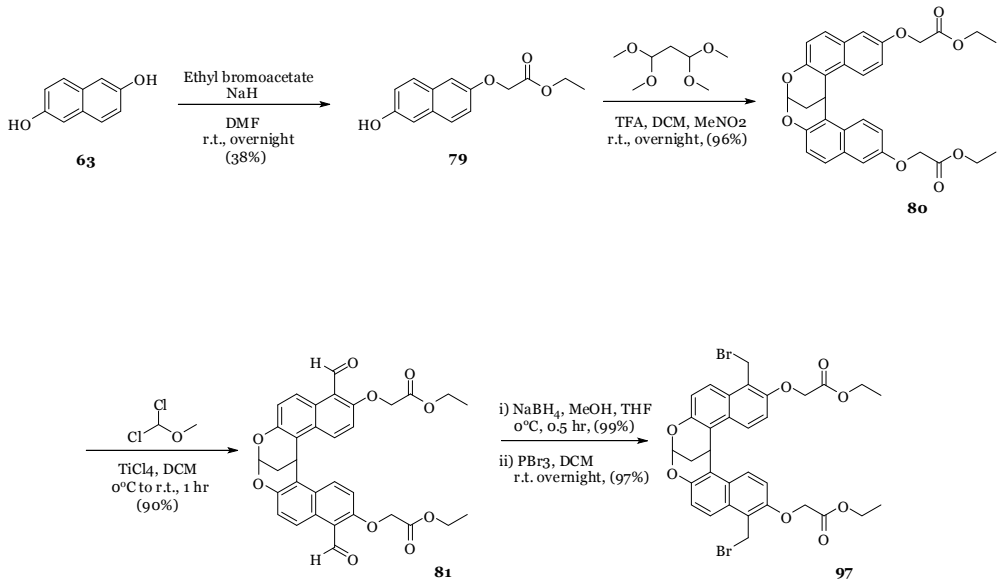

63 **79** **80** **81** **97**

Scheme 25 Attempts bromomethylation on naphthalene dimer

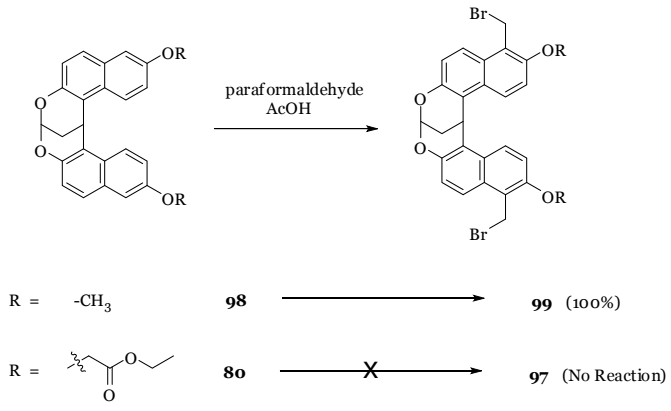

For the aromatic group, carbazole **100** was commercially available and dibenzocarbazole **101** was synthesized shown in Scheme 26. Refulxing β-tetralone **104** with hydrazine in 6 M-HCl and H_2O gave tetrahydro-dibenzocarbazole **105**.[75] Compound **105** was oxidized with iodine (I_2) and propylene oxide in benzene with light (hv) and dibenzocarbazole **101** was obtained in 71% yield.[76]

Scheme 26 Synthesis of dibenzocarbazole **101**

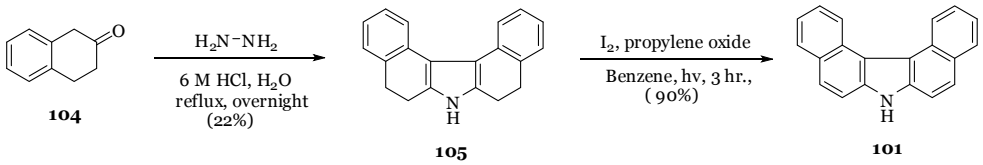

Scheme 27 Synthesis of carbazole and dibenzocarbazole fluorophore open-tubes

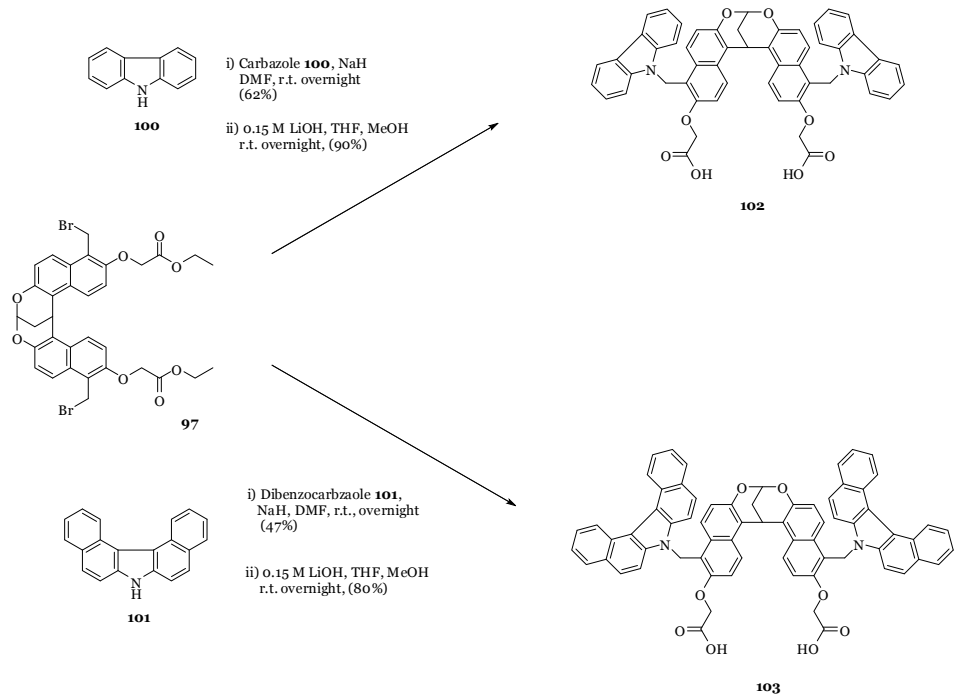

Carbazole **100** was coupled with bromomethyl naphthalene core **97** using NaH in DMF followed by saponification with 0.15 M-LiOH in THF and MeOH to give the desired product **102** in 56% yield over two steps. Also, dibenzocarbazole **101** gave compound **103** with the same reaction conditions in 38% yield over two steps shown in Scheme 27.

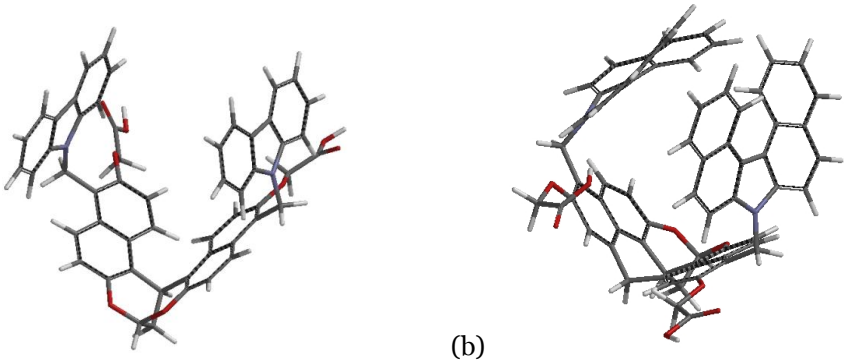

(a) (b)

Figure 22 The 3D structure of (a) open-tube **102** and (b) open-tube **103** (3D model from Wavefunction Inc. software Spartan 06')

5.3 Recognition of Alkane Sensing

The open-tubes were titrated with various lipid guests. Titrations were performed in buffered water (20 mM HEPES) at pH 8.4 with host concentration of 1 10^{-6} M. The changes in the fluorescence emission were observed for most guests as shown in Table 9. The fluorescence of the host was enhanced upon the addition of guest as shown in Figure 24 - 27.

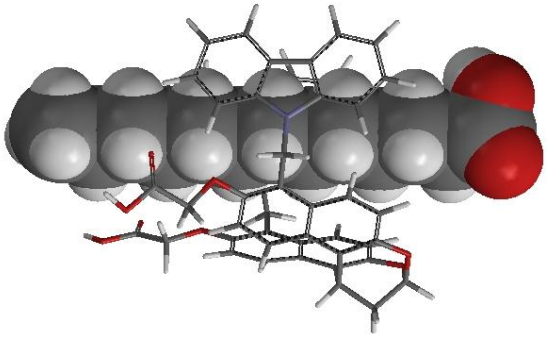

Figure 23 The binding complex of open-tube **102** and dodecanoic acid (3D model from Wavefunction Inc. software Spartan 06')

Table 9 Association constants of carbazole-sensor **102** and dibenzocarbazole-sensor **103** with lipid guests (20 mM HEPES; pH = 8.4; [host] = 1 10^{-6} M; λ_{ex} = 355 nm; λ_{em} = 400 nm for **102**; λ_{em} = 405 nm for **103**)

Entry	Guest	K_a (M^{-1})	
		Sensor 102	**Sensor 103**
1	Acetic acid	460	100
2	Butyric acid	1,400	350
3	Hexanoic acid	2,960	6,600
4	Octanoic acid	5,300	9,580
5	Decanoic acid	39,700	10,700
6	Dodecanoic acid	396,000	114,000
7	1-Heptanol	1,840,000	9,170,000
8	*cis*-4-Heptene-1-ol	306,000	110,000
9	*trans*-3-Octenoic acid	67,500	16,600
10	4-Methyloctanoic acid	20,000	104,000
11	Cyclohexane carboxylic acid	7,640	9,880

Longer straight chain lipids were bound with higher affinity than shorter lipids (entry 1-6). The greater hydrophobic surface of longer chain lipids renders them less soluble in water. As shown entry 7 and 8, alcohols had much higher association constant because they have less repulsion with carboxylates of the sensors. The branched lipids (entry 10), 4-methyloctanoic acid, had lower association constants than straight chain lipids such as octanoic acid because of methyl branching group. We believe that the changes in fluorescence of the open-tubes occur because the fluorophores are surrounded by water in the unbound state, but the water is expelled upon lipid binding.

Scheme **28** The representation of a non-cooperative binding host

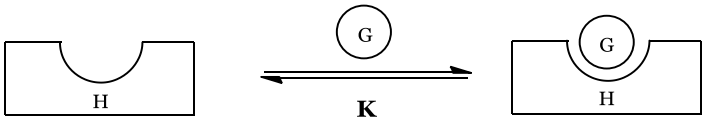

A non-cooperative host typically possesses the binding profile as shown in Scheme 28. A non-cooperative binding is most accurately described by a form of the Langmuir isotherm (eq. 5).[77] Eq. 5 is a rectangular hyperbola with $[G]_f$ being the concentration free guest. The observed response, which is typically from spectroscopic measurements, is given by y and the range from 0 to y_{max}.

$$y = \frac{y_{max}[G]_f}{K_d + [G]_f} \qquad \text{(eq. 5)}$$

$$H + G \rightleftharpoons H \bullet G \qquad \text{(eq. 6)}$$

Eq. 6 is represented the equilibrium equation of a simple host-guest binding equilibrium which is a single site binding. The binding constant is expressed in eq. 1.

$$K_a = \frac{[H \bullet G]}{[H]\,[G]} \qquad \text{(eq. 1)}$$

The total concentration of H and G gives mass balance eq. 7 and 8.

$$[H]_t = [H]_f + [H \bullet G] \quad \text{(eq. 7)}$$

$$[G]_t = [G]_f + [H \bullet G] \quad \text{(eq. 8)}$$

Where $[H]_t$ is the total concentration of H, $[G]_t$ is the total concentration of G, $[H]_f$ is the concentration of the free H, and $[G]_f$ is the concentration of the free G.

Binding constants were determined by plotting fluorescence of the sensor versus the concentration of lipid, and fitting to a single site binding isotherm. A binding isotherm is the theoretical change in the concentration of one component as a function of the concentration of another component at constant temperature. The experiment is performed holding the concentration of host relative constant while varying the concentration of the guest (eq. 9).

$$[H \bullet G] = \frac{[H]_t K_a [G]_f}{1 + K_a [G]_f} \quad \text{(eq. 9)}$$

Where $[H]_t$ is the concentration of the total host, $[G]_f$ is the concentration of the free guest, and K_a is the association constant.

Typically for low $[H]_t$, it is possible to use $[G]_t$ since $[G]_f$ is similar. When K_a becomes high, one can no longer assume $[G]_t = [G]_f$.

Replacing eq. 9 into eq. 8 yields a quadratic equation (eq. 10).[78]

$$K_a[G]_f^{\,2} = (1 - [G]_t + [H]_t)[G]_f - [G]_t = 0 \quad \text{(eq. 10)}$$

The real root of eq. 10 is expressed in eq. 11 which defines the concentration of free guest ($[G]_f$) based on Ka and total concentration of host ($[H]_t$) and the total concentration of guest ($[G]_t$).

$$[G]_f = \left[\frac{-(1 - [G]_t + [H]_t) + \sqrt{(1 - [G]_t + [H]_t)^2 - 4K_a[G]_t}}{2K_a} \right] \quad \text{(eq. 11)}$$

We can change eq. 11 dissociation constant dependable equation. The dissociation constant of the complex is

$$K_d = \frac{[H]_f [G]_f}{[H \bullet G]} \quad \text{(eq. 12)}$$

Replacing eq. 7 and eq. 8 in eq. 12 yields quadratic equation for the concentration of free guest (eq. 17)

$$K_d = \frac{([H]_t - [H \bullet G]) [G]_f}{([G]_t - [G]_f)} \quad \text{(eq. 13)}$$

$$K_d = \frac{[H]_t [G]_f - [G]_t [G]_f + [G]_f^2}{([G]_t - [G]_f)} \quad \text{(eq. 14)}$$

$$K_d ([G]_t - [G]_f) = [H]_t [G]_f - [G]_t [G]_f + [G]_f^2 \quad \text{(eq. 15)}$$

$$[G]_f^2 + ([H]_t - [G]_t + K_d) [G]_f - K_d[G]_t = 0 \quad \text{(eq. 16)}$$

$$[G]_f = \left[\frac{-([H]_t - [G]_t + K_d) + \sqrt{([H]_t - [G]_t + K_d)^2 + 4K_d[G]_t}}{2} \right] \quad \text{(eq. 17)}$$

Substitution eq. 17 into eq. 5 yields

$$y = \frac{y_{max} \left[\frac{-([H]_t - [G]_t + K_d) + \sqrt{([H]_t - [G]_t + K_d)^2 + 4K_d[G]_t}}{2} \right]}{K_d + \left[\frac{-([H]_t - [G]_t + K_d) + \sqrt{([H]_t - [G]_t + K_d)^2 + 4K_d[G]_t}}{2} \right]} \quad \text{(eq. 20)}$$

where y is the change in fluorescence intensity, y_{max} is the change in fluorescence intensity at the excess of guest, K_d is the dissociation constant, $[H]_t$ is the total concentration of host, $[G]_t$ is the total concentration of guest.

The eq. 20 can be used as the input for a user-defined function in the nonlinear fitting function of Graphpad Prism which will then determine the value of K_d and y_{max} from best-fit curve. The simple form of the binding isotherm was used for most guests. However, for sensor **102** ● decanoic acid, sensor **102** ● 1-heptanol, and sensor **103** ● 1-heptanol, the quadratic form was used.

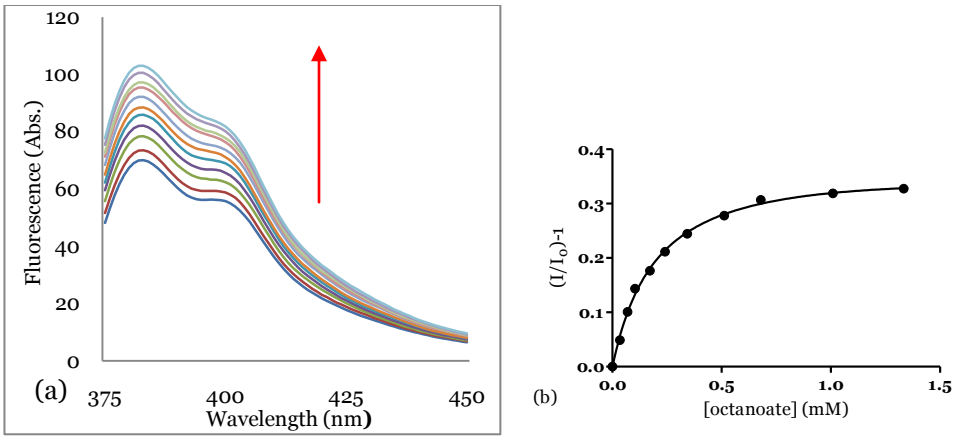

Figure 24 Fluorescence titration of carbazole-sensor **102** with octanoic acid in buffer (20 mM HEPES; pH = 8.4; [**102**] = 1 10^{-6} M; λ_{ex} = 355 nm); a) Fluorescence emission upon the addition of octanoic acid; b) Fit of the titration data at λ_{em} = 400 nm to a single site binding isotherm

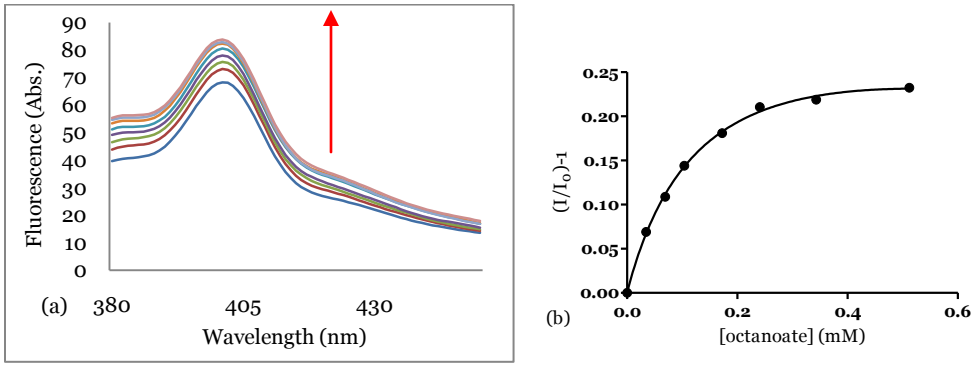

Figure 25 Fluorescence titration of dibenzocarbazole-sensor **103** with octanoic acid in buffer (20 mM HEPES; pH = 8.4; [**103**] = 1 10^{-6} M; λ_{ex} = 355 nm); a) Fluorescence emission upon the addition of octanoic acid; b) Fit of the titration data at λ_{em} = 405 nm to a single site binding isotherm

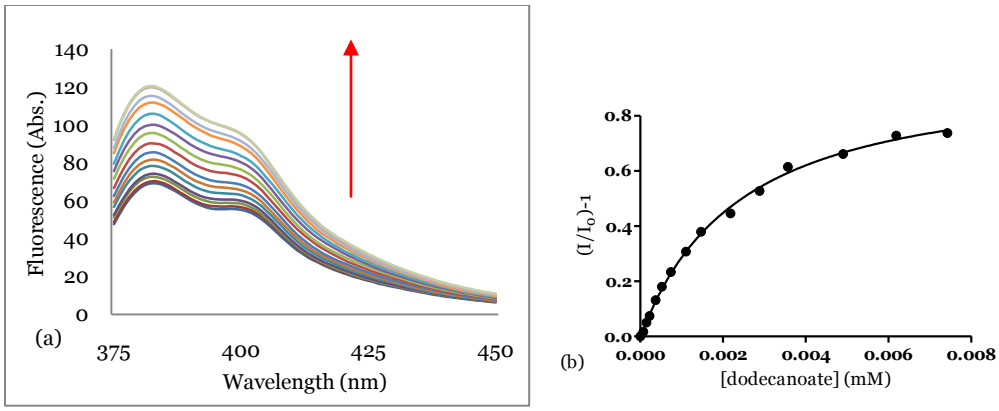

Figure 26 Fluorescence titration of carbazole-sensor **102** with dodecanoic acid in buffer (20 mM HEPES; pH = 8.4; [**102**] = 1 10^{-6} M; λ_{ex} = 355 nm); a) Fluorescence emission upon the addition of dodecanoic acid; b) Fit of the titration data at λ_{em} = 400 nm to a single site binding isotherm

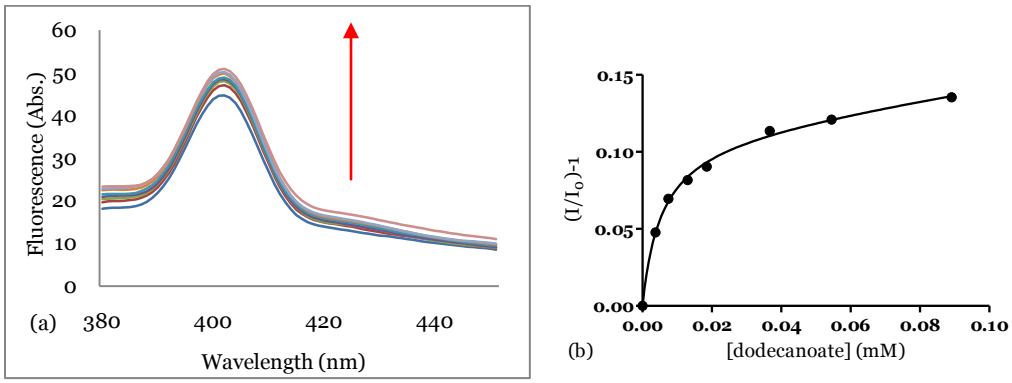

Figure 27 Fluorescence titration of dibenzocarbazole-sensor **103** with dodecanoic acid in buffer (20 mM HEPES; pH = 8.4; [**103**] = 1 10^{-6} M; λ_{ex} = 355 nm); a) Fluorescence emission upon the addition of dodecanoic acid; b) Fit of the titration data at λ_{em} = 405 nm to a single site binding isotherm

5.4 Conclusion

A series of receptors for the recognition of various lipids has been synthesized. The open-tube **102** and **103** were easily synthesized and purified compared to molecular tubes which are the previous host for the recognition of lipids. The open-tube **102** and **103** were tested by fluorescence titration with a variety of lipids. The fluorescence intensity of the host compounds increased upon the addition lipid guests and showed higher binding constants than those of molecular tubes. However, they have a lower selectivity for lipids. More polar functional group increase water solubility of the host and the specific binding site such as amine may increase the selectivity for the recognition of lipids.

Chapter 6. Experimental

6.1 Experimental Procedures

General Fluorescence Procedures. Fluorescence spectra were obtained on a Shimadzu RF-5301 PC spectrofluorimeter. A solution of sensor (10^{-6} M) were prepared in buffer solution (20 mM HEPES, adjusted to pH = 8.4). This solution was placed in a cuvette (1 mL). The sample was then titrated with a solution of the lipid (1-900 mM in 20 mM HEPES, adjusted to pH = 8.4 with 10^{-6} M sensor). The fluorescence change and corresponding concentration of guest were recorded. This data was fit to a single site binding isotherm using Graphpad Prism 3.03.

General Synthetic Procedures. All reactions were performed in dried glassware under nitrogen atmosphere unless otherwise noted. Tetrahydrofuran (THF), benzene, and toluene were distilled from sodium benzophenone ketyl under nitrogen immediately before use. Dichloromethane (DCM) and triethylamine (TEA) were distilled from calcium hydride under nitrogen immediately before use. Flash column chromatography was carried out with 32-63 μm silica gel. NMR spectra were run with a Bruker ARX-250 MHz, DRX-300 MHz, or DRX-500 MHz in $CDCl_3$ or DMSO-d_6 using tetramethylsilane (TMS) as a reference. IR spectra were run with a Thermo Scientific Auxiliary Equipment Module (AEM) for Nicolet FT-IR spectrometers. Mass spectra were run with a Bruker Apex-Qe FTMS at the Old Dominion University in Norfolk, VA.

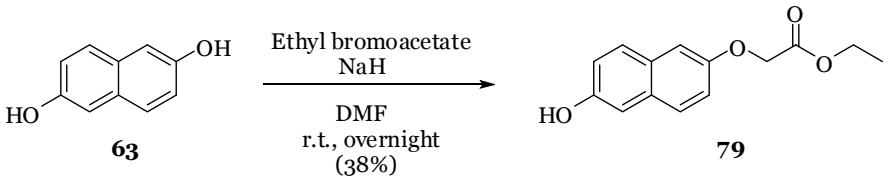

63 **79**

Mono-alkylated compound 79: NaH (1.37 g, 60% in mineral oil, 34.25 mmol) was added into a DMF (100 mL) in a flame dried flask, and stirred for 10 min. Then, 2,6-dihydroxynaphthalene (5 g, 31.22 mmol) in DMF (50 mL) was dropwise added into the solution by means of an addition funnel for 30 min. The reaction mixture was stirred at room temperature for 1 hr, and ethyl bromoacetate (5.4 mL, 34.25 mmol) was slowly added into the reaction. The reaction mixture was stirred at room temperature overnight. DMF was removed *in vacuo*, and the crude product was extracted with EtOAc (500 mL × 3) and 10% HCl from the remaining residue. The organic layers were dried over Na_2SO_4 and filtered. After removal the solvents *in vacuo*, crude product was purified by chromatography (5% Et_2O/DCM). White powdered solid was obtained (2.92 g, 11.86 mmol, 38%). m.p.: 133-135°C; ^{1}H-NMR (500 MHz, $CDCl_3$) δ: 7.59 (d, 1H, *J* = 8.5 Hz, Ar-$\underline{H}_f$), 7.56 (d, 1H, *J* = 9.0 Hz, Ar-$\underline{H}_c$), 7.18 (dd, 1H, *J* = 9.0, 2.5 Hz, Ar-$\underline{H}_a$), 7.09 (d, 1H, *J* = 2.5 Hz, Ar-$\underline{H}_b$), 7.07 (dd, 1H, *J* = 6.0 Hz, *J* = 2.5 Hz, Ar-$\underline{H}_e$), 7.03 (d, 1H, *J* = 2.0 Hz, Ar-$\underline{H}_d$), 5.07 (s, 1H, -O$\underline{H}$), 4.71 (s, 2H, -O$\underline{CH_2}$COO), 4.30 (q, 2H, *J* = 7.5 Hz, -O$\underline{CH_2}CH_3$), 1.31 (t, 3H, *J* = 7.1 Hz, -OCH$_2\underline{CH_3}$); ^{13}C-NMR (125 MHz, $CDCl_3$) δ: 169.2, 154.2, 152.3, 130.4, 129.3, 128.5, 128.1, 119.1, 118.3, 109.7, 107.5, 65.6, 61.5, 14.2; IR (KBr, cm^{-1}): 3383, 3031, 2982, 2937, 2908, 1732, 1605, 1527, 1442, 1380, 1352, 1327, 1204, 1160, 1119, 1074, 1025; HRMS for M^+ calcd. For $(C_{14}H_{14}O_4)Na^+$ 269.0784, found 269.0778

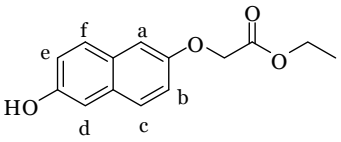
f
a
e
O
O
O
b
HO
d
c

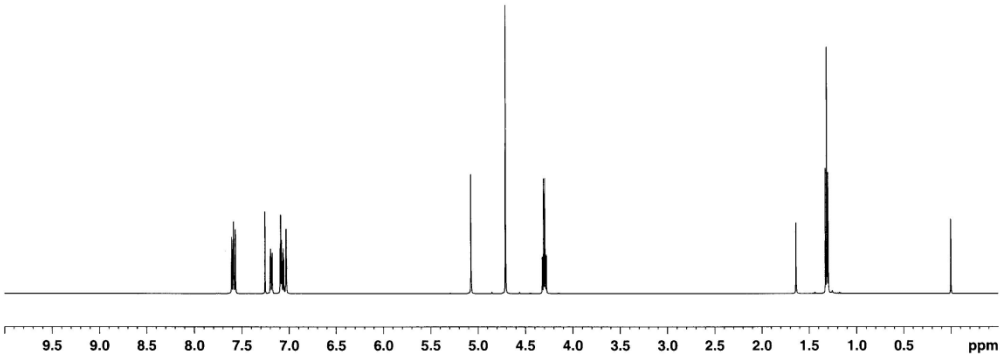
9.5 9.0 8.5 8.0 7.5 7.0 6.5 6.0 5.5 5.0 4.5 4.0 3.5 3.0 2.5 2.0 1.5 1.0 0.5 ppm

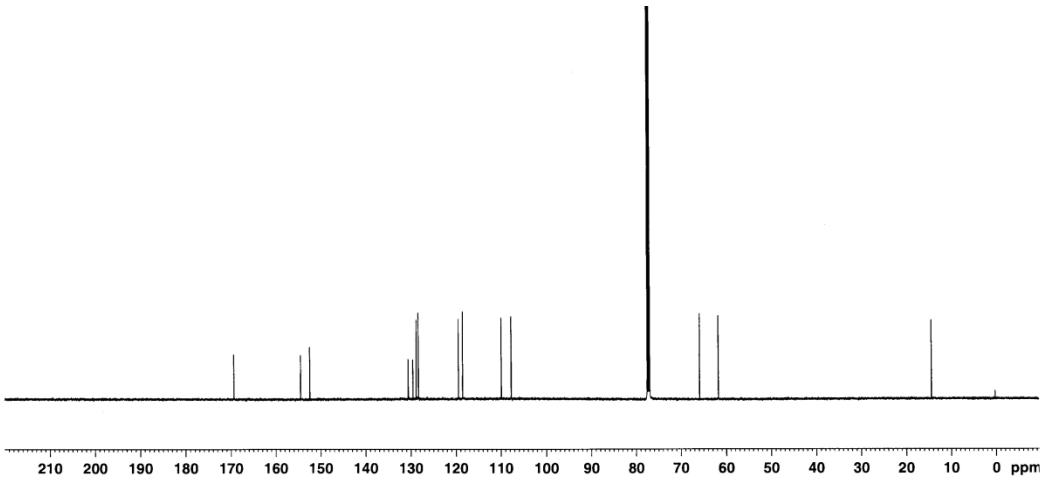
210 200 190 180 170 160 150 140 130 120 110 100 90 80 70 60 50 40 30 20 10 0 ppm

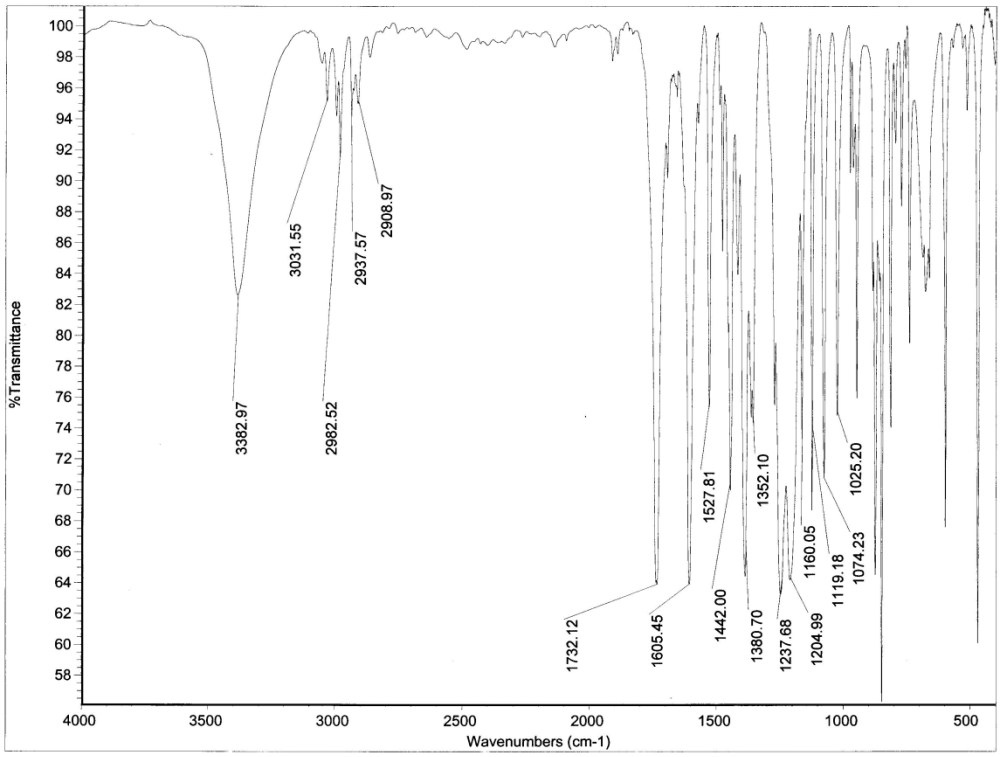
%Transmittance
Wavenumbers (cm-1)
3382.97
3031.55
2982.52
2937.57
2908.97
1732.12
1605.45
1527.81
1442.00
1380.70
1352.10
1237.68
1204.99
1160.05
1119.18
1074.23
1025.20

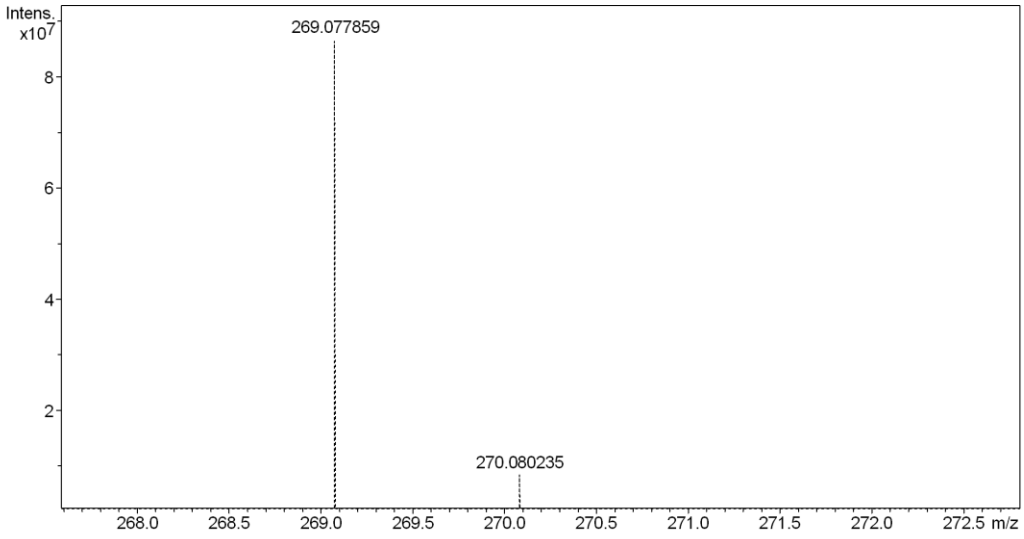
Intens.
x10^7
269.077859
270.080235
m/z

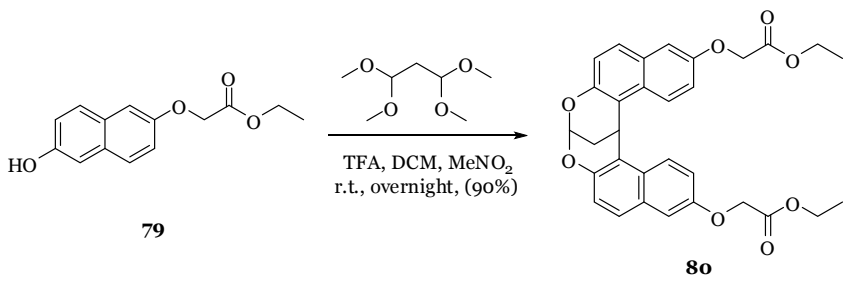

79 **80**

Dimer compound 80: Compound **79** (1.93 g, 7.83 mmol) was dissolved in TFA (10 mL), nitromethane (20 mL), and DCM (100 mL). Malonaldehyde bis(dimethylacetal) (0.8 mL, 4.70 mmol) in DCM (50 mL) was added dropwise into the solution by an addition funnel over 45 min. After the addition was complete, the reaction mixture was stirred at room temperature overnight. The reaction mixture was poured over crushed ice, followed by the slow addition of 1M NaOH and $NaHCO_3$ until pH of the solution reached ca. 8. The crude product was extracted with DCM (300 mL × 3), and the organic layers were dried over Na_2SO_4, and then filtered. Solvents were removed *in vacuo*, and the residue was purified by chromatography (DCM). The white powered solid was obtained (1.87 g, 3.53 mmol, 90%). m.p.: 154-156˚C; ^{1}H-NMR (500 MHz, $CDCl_3$) δ: 8.45 (d, 2H, *J* = 9.3 Hz, Ar-$\underline{H_e}$), 7.44 (d, 2H, *J* = 8.9 Hz, Ar-$\underline{H_c}$), 7.29 (dd, 2H, *J* = 8.9 Hz, 2.5 Hz, Ar-$\underline{H_a}$), 7.12 (d, 2H, *J* = 9.0 Hz, Ar-$\underline{H_d}$), 6.98 (d, 2H, *J* = 2.7 Hz, Ar-$\underline{H_b}$), 6.23 (s, 1H, -$O_2\underline{CH}CH_2CHAr_2$), 5.23 (s, 1H, -$O_2CHCH_2\underline{CH}Ar_2$), 4.65 (s, 4H, -O$\underline{CH_2}$CO), 4.26 (t, 4H, *J* = 7.2 Hz, -O$\underline{CH_2}CH_3$), 2.38 (t, 2H, *J* = 2.5 Hz, -$O_2CH\underline{CH_2}CHAr_2$), 1.27 (t, 6H, *J* = 7.1 Hz, -$OCH_2\underline{CH_3}$); ^{13}C-NMR (125 MHz, $CDCl_3$) δ: 168.9, 154.0, 149.0, 131.4, 127.3, 126.8, 124.4, 119.0, 118.7, 118.5, 108.7, 91.4, 65.6, 61.4, 26.7, 22.8, 14.1; IR (KBr, cm^{-1}): 2982, 2933, 1748, 1605, 1511, 1421, 1384, 1262, 1229, 1202, 1196, 1180, 1106, 1090, 1013; HRMS for M^+ calcd. For $(C_{31}H_{28}O_8)Na^+$ 551.1676, found 551.1664

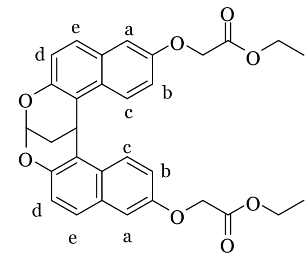

e
a
d
b
c
c
b
d
e
a
O
O
O
O
O
O
O
O

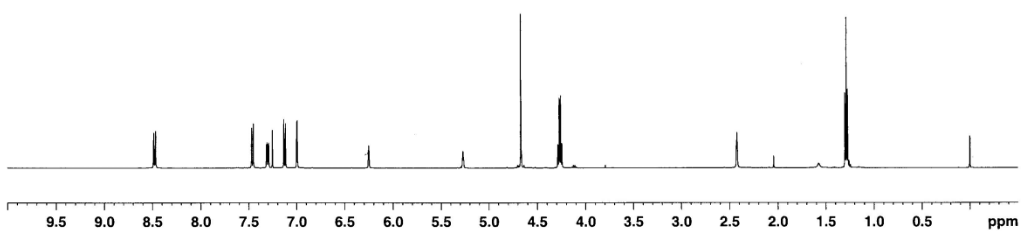

9.5 9.0 8.5 8.0 7.5 7.0 6.5 6.0 5.5 5.0 4.5 4.0 3.5 3.0 2.5 2.0 1.5 1.0 0.5 ppm

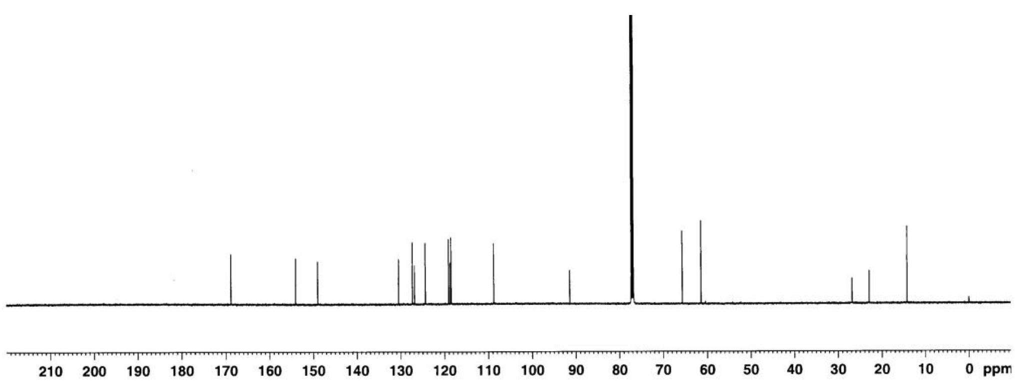

210 200 190 180 170 160 150 140 130 120 110 100 90 80 70 60 50 40 30 20 10 0 ppm

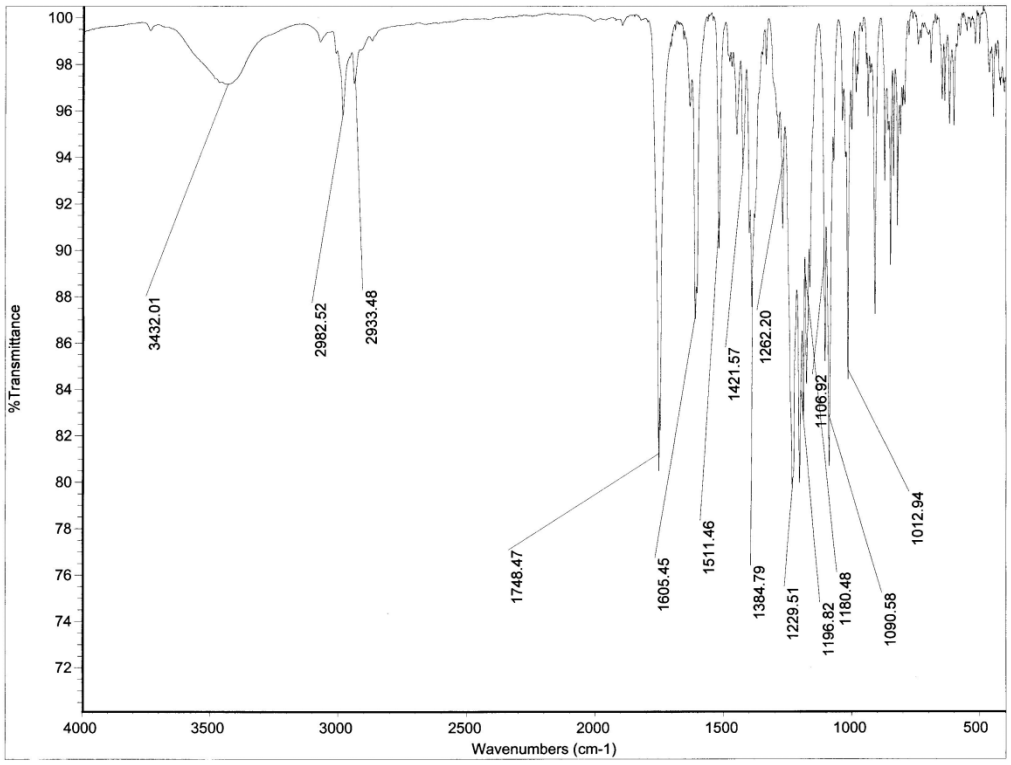
%Transmittance
Wavenumbers (cm-1)
3432.01
2982.52
2933.48
1748.47
1605.45
1511.46
1421.57
1384.79
1262.20
1229.51
1196.82
1180.48
1106.92
1090.58
1012.94

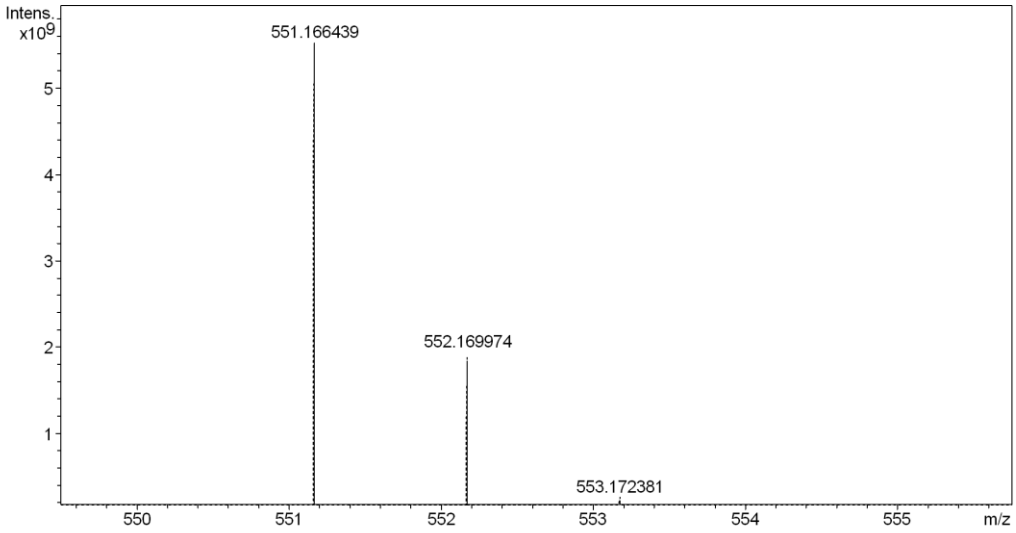
Intens.
x10^9
551.166439
552.169974
553.172381
m/z

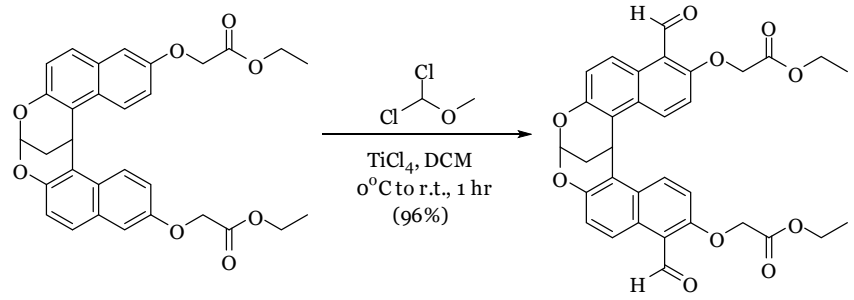

80 **81**

Dialdehyde compound 81: Dimer **80** (695 mg, 1.32 mmol) compound was dissolved in DCM (120 mL) in a flame dried flask under nitrogen, and cooled down to 0°C in an ice-bath. Following addition of α,α-dichloromethyl methyl ether (0.5 mL, 5.26 mmol), $TiCl_4$ (5.3 mL, 1.0 M in DCM, 5.26 mmol) was added *via* syringe. After the addition at 0°C, the reaction mixture was warmed to room temperature and stirred for 1 hr. After the reaction mixture was cooled down to 0°C, it was poured into a solution of saturated $NaHCO_3$. The crude product was extracted with DCM (100 mL × 3), and the organic layer was dried over Na_2SO_4 and filtered. Solvents were removed *in vacuo*, and the residue was purified by column chromatography (DCM to 10% Et_2O/DCM). The greenish yellow powdered solid was obtained (738 mg, 1.26 mmol, 96%). m.p.: 172-173˚C; ^{1}H-NMR (500 MHz, $CDCl_3$) δ: 10.87 (s, 1H, -Ar<u>CHO</u>), 9.05 (d, 2H, *J* = 9.5 Hz, Ar-<u>H_b</u>), 8.60 (d, 2H, *J* = 9.5 Hz, Ar-<u>H_c</u>), 7.25 (d, 2H, *J* = 5.0 Hz, Ar-<u>H_d</u>), 7.16 (d, 2H, *J* = 7.5 Hz, Ar-<u>H_a</u>), 6.24 (s, 1H, -O_2<u>CH</u>CH_2CHAr_2), 5.17 (s, 1H, -O_2CHCH_2<u>CH</u>Ar_2), 4.80 (d, 4H, 3.5 Hz, -O<u>CH_2</u>CO), 4.26 (q, 2H, *J* = 7.0 Hz, -O<u>CH_2</u>CH_3), 2. 40 (s, 2H, -O_2CH<u>CH_2</u>$CHAr_2$), 1.27 (t, 3H, *J* = 7.0 Hz, -OCH_2<u>CH_3</u>); ^{13}C-NMR (125 MHz, $CDCl_3$) δ: 191.9, 168.2, 160.0, 149.5, 130.5, 127.7, 126.8, 125.5, 122.1, 118.5, 118.3, 113.6, 91.1, 66.5, 61.7, 26.6, 22.8, 14.1; IR (KBr, cm^{-1}): 3440, 2974, 1758, 1671, 1597, 1519, 1384, 1206, 1187, 1102, 1060, 1021; HRMS for M^+ calcd. For $(C_{33}H_{28}O_{10})Na^+$ 607.1574, found 607.1573

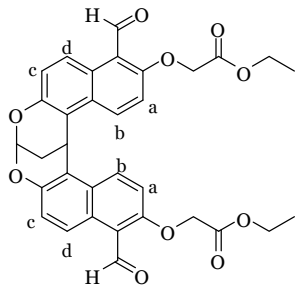
H
O
O
O
O
d
c
a
b
O
b
a
c
O
O
O
d
H
O

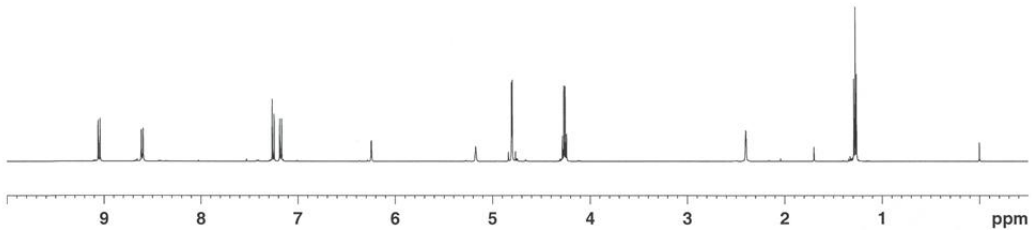
9
8
7
6
5
4
3
2
1
ppm

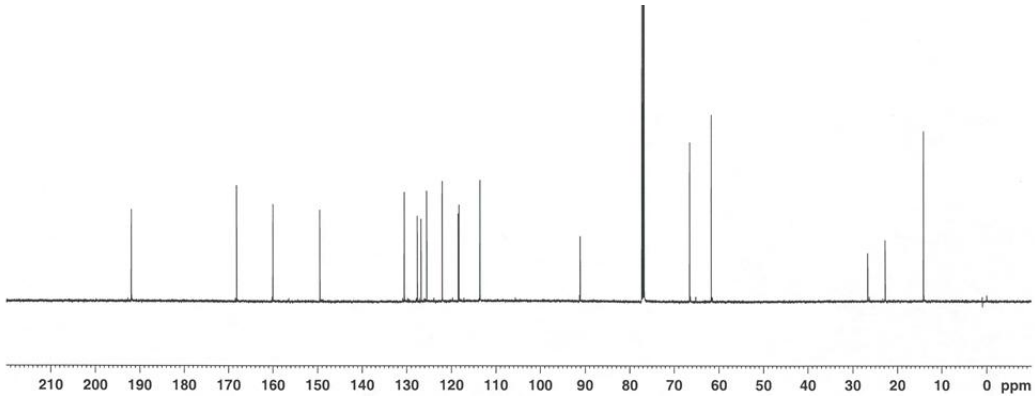
210
200
190
180
170
160
150
140
130
120
110
100
90
80
70
60
50
40
30
20
10
0 ppm

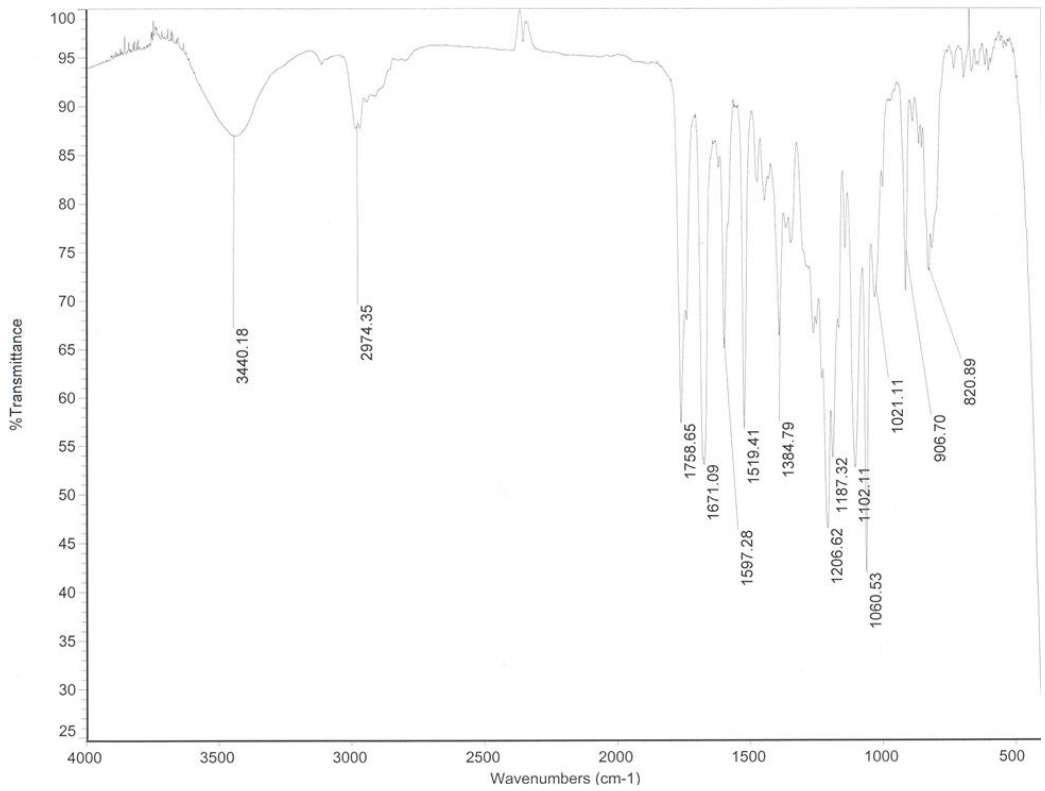
%Transmittance
Wavenumbers (cm-1)
3440.18
2974.35
1758.65
1671.09
1597.28
1519.41
1384.79
1206.62
1187.32
1102.11
1060.53
1021.11
906.70
820.89

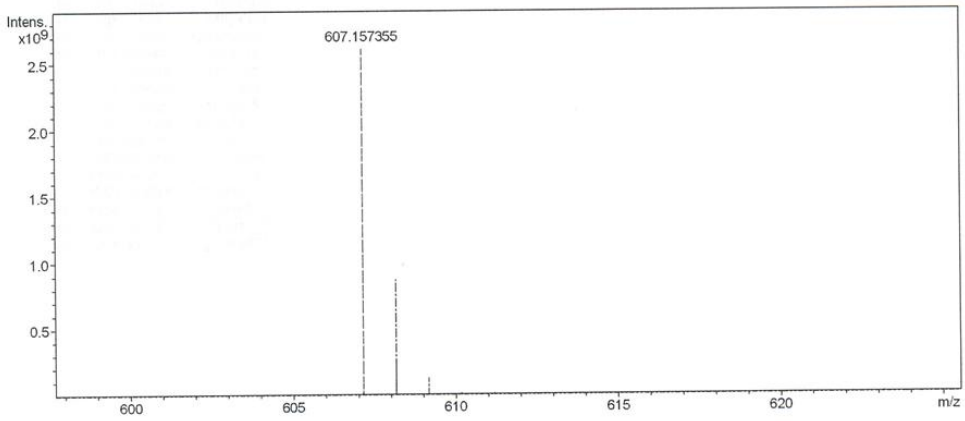
Intens.
x10^9
607.157355
m/z

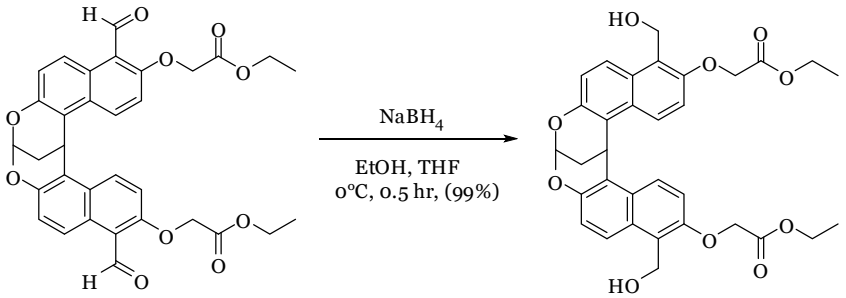

81

Dimethanol compound: Dialdehyde **81** (394 mg, 0.67 mmol) was dissolved in EtOH (40 mL) and THF (40 mL) in a dried flask under nitrogen, and then the solution was cooled down to 0°C. Sodium borohydride ($NaBH_4$)(64 mg, 1.69 mmol) was slowly added into the solution, and the reaction mixture was stirred at 0°C for 0.5 hrs. 10% HCl was slowly added to quench the reaction, and the crude product was extracted with DCM (50 mL × 4). The residue was purified by chromatography (10% Et_2O/DCM). The white powdered solid was obtained (393 mg, 0.67 mmol, 99%). m.p.: 144-145˚C; ^{1}H-NMR (500 MHz, $CDCl_3$) δ: 8.45 (d, 2H, *J* = 9.5 Hz, Ar-$\underline{H_b}$), 7.95 (d, 2H, *J* = 9.0 Hz, Ar-$\underline{H_d}$), 7.20 (d, 2H, *J* = 4.5 Hz, Ar-$\underline{H_c}$), 7.18 (d, 2H, *J* = 4.0 Hz, Ar-$\underline{H_a}$), 6.25 (s, 1H, -$O_2\underline{CH}CH_2CHAr_2$), 5.25 (s, 1H, -$O_2CHCH_2\underline{CH}Ar_2$), 5.10 (q, 4H, 15.5 Hz, 12.0 Hz, -Ar$\underline{CH_2}$OH), 4.77 (dd, 4H, 16.5 Hz, 8.5 Hz, -O$\underline{CH_2}$CO), 4.20 (q, 2H, *J* = 7.5 Hz, *J* = 7.0 Hz, -O$\underline{CH_2}CH_3$), 2.40 (s, 2H, -$O_2CH\underline{CH_2}CHAr_2$), 1.25 (t, 3H, *J* = 7.0 Hz, -$OCH_2\underline{CH_3}$); ^{13}C-NMR (125 MHz, $CDCl_3$) δ: 170.1, 152.0, 149.4, 129.4, 127.9, 125.5, 124.6, 124.4, 119.9, 118.9, 115.2, 91.6, 67.4, 61.9, 55.8, 27.2, 23.2, 14.3; IR (KBr, cm^{-1}): 3427, 2966, 1742, 1600, 1520, 1404, 1287, 1207, 1164, 1106, 1061; HRMS for M^+ calcd. For $(C_{33}H_{32}O_{10})Na^+$ 611.1887, found 611.1881

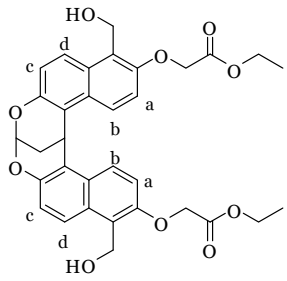
HO
d
c
O
O
O
a
b
b
O
a
c
O
O
d
HO
O

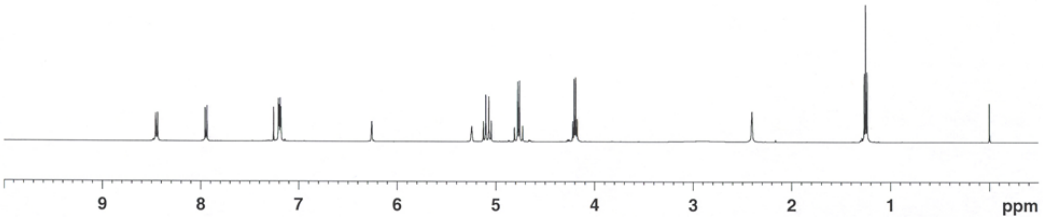
9
8
7
6
5
4
3
2
1
ppm

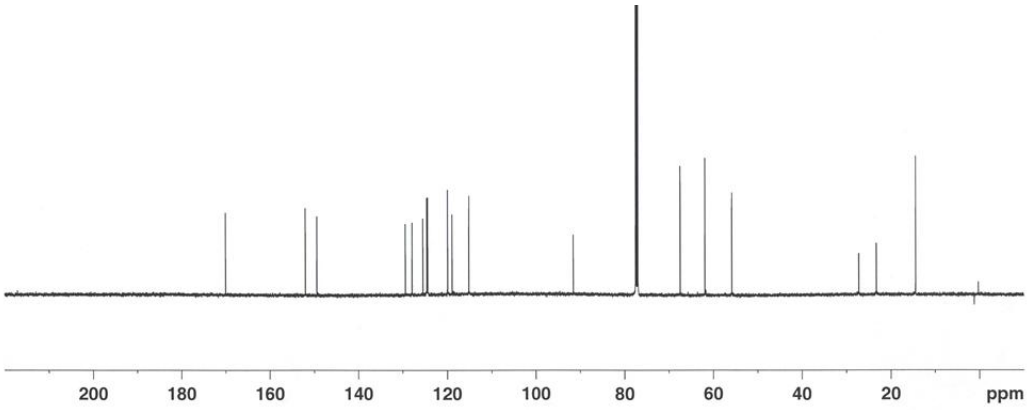
200
180
160
140
120
100
80
60
40
20
ppm

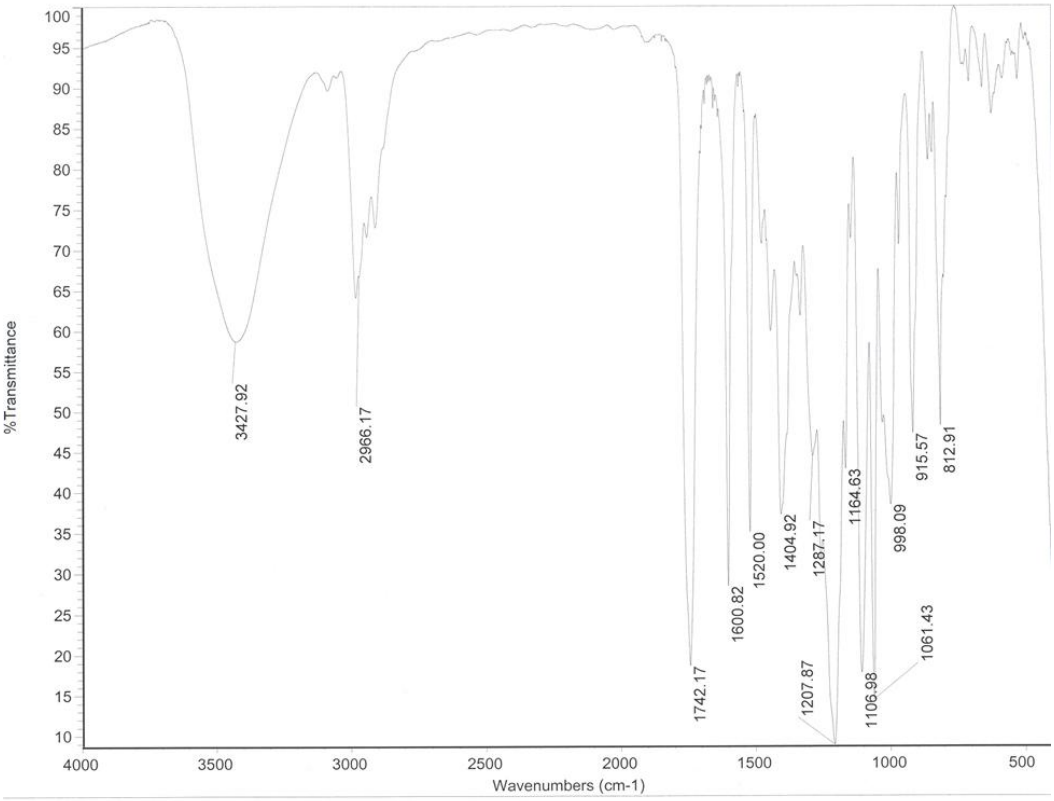
%Transmittance
Wavenumbers (cm-1)
3427.92
2966.17
1742.17
1600.82
1520.00
1404.92
1287.17
1207.87
1164.63
1106.98
1061.43
998.09
915.57
812.91

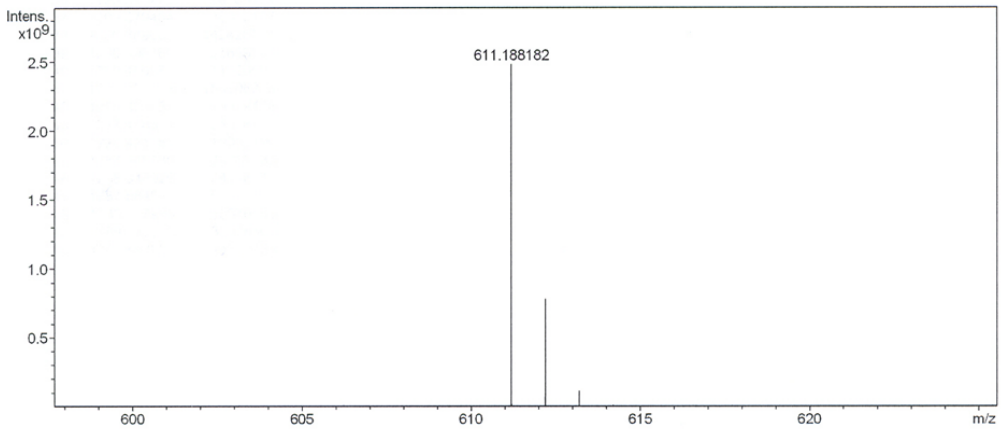
Intens.
x10^9
611.188182
m/z

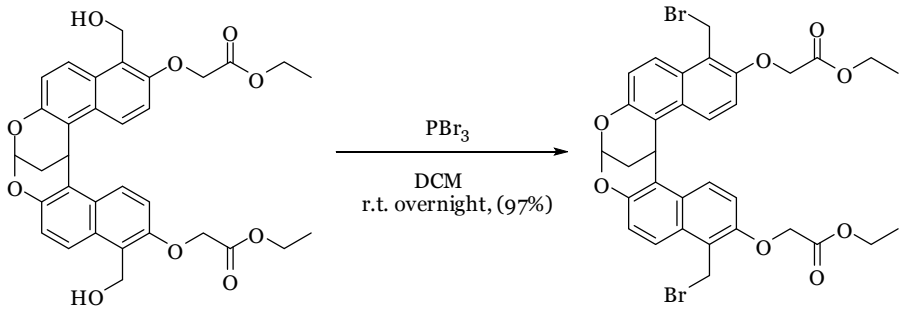

97

Dibromide compound 97: Dimethanol product (340 mg, 0.58 mmol) was dissolved in DCM (75 mL). Then, phosphorous tribromide (PBr_3) (0.11 mL, 1.45 mmol) was slowly added into the solution. The reaction mixture was stirred at room temperature overnight. After the reaction complete, saturated $NaHCO_3$ was slowly added into the reaction mixture to quench. The crude product was extracted with DCM (50 mL × 3), and the organic layers were dried over Na_2SO_4 and filtered. Solvents were removed *in vacuo*, the pure beige color solid was obtained without further purification (400 mL, 0.56 mmol, 97%). m.p.: 174-176˚C; ^{1}H-NMR (500 MHz, $CDCl_3$) δ: 8.43 (d, 2H, *J* = 9.5 Hz, Ar-$\underline{H_b}$), 7.81 (d, 2H, *J* = 9.0 Hz, Ar-$\underline{H_c}$), 7.26 (d, 2H, *J* = 9.5 Hz, Ar-$\underline{H_d}$), 7.15 (d, 2H, 9.5 Hz, Ar-$\underline{H_a}$), 6.21 (s, 1H, -$O_2\underline{CH}CH_2CHAr_2$), 5.18 (s, 1H, -$O_2CHCH_2\underline{CH}Ar_2$), 5.03 (dd, 4H, 46.5 Hz, 10.5 Hz, -Ar$\underline{CH_2}$Br), 4.78 (s, 4H, -O$\underline{CH_2}$CO), 4.25 (q, 4H, *J* = 7.5 Hz, *J* = 7.0 Hz, -O$\underline{CH_2}CH_3$), 2.33 (s, 2H, -$O_2CH\underline{CH_2}CHAr_2$), 1.23 (t, 3H, *J* = 7.0 Hz, -$OCH_2\underline{CH_3}$); ^{13}C-NMR (125 MHz, $CDCl_3$) δ: 168.8, 151.7, 149.2, 128.3, 127.3, 125.0, 123.4, 120.9, 119.9, 118.8, 114.4, 91.2, 66.8, 61.4, 26.6, 24.7, 22.8, 14.1; IR (KBr, cm^{-1}): 3436, 2974, 2933, 1754, 1599, 1520, 1443, 1406, 1379, 1292, 1259, 1201, 1164, 1152, 1102, 1061, 1026; HRMS for M^+ calcd. For $(C_{33}H_{30}Br_2O_8)Na^+$ 735.0199, found 735.0195

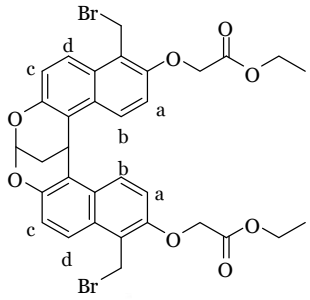
Br
d
c
O
O
O
a
b
b
O
a
c
O
O
O
d
Br

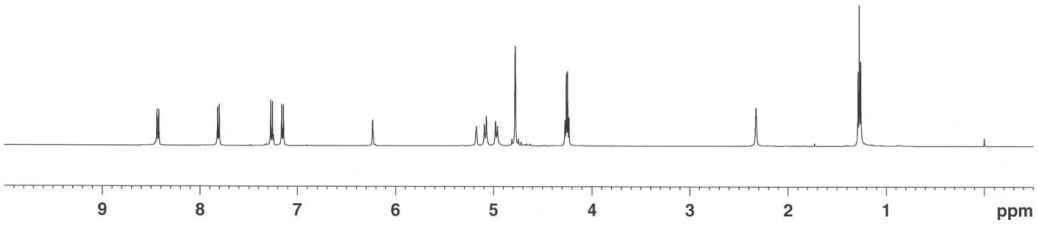
9
8
7
6
5
4
3
2
1
ppm

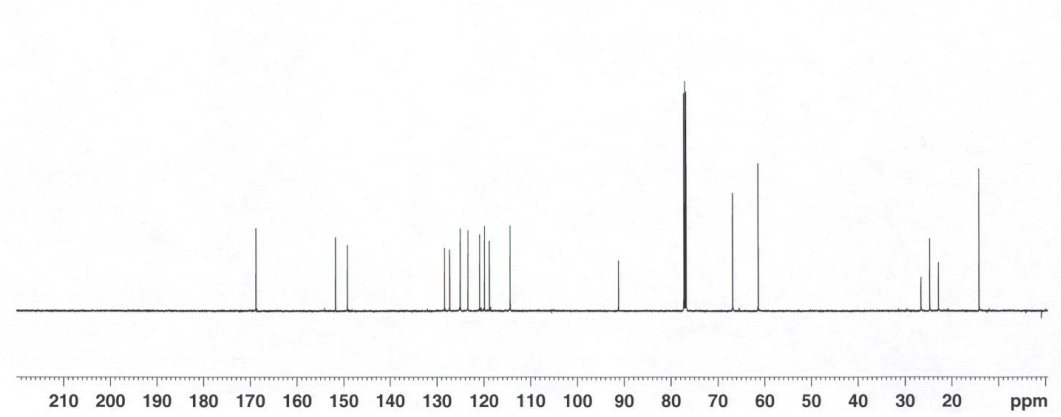
210
200
190
180
170
160
150
140
130
120
110
100
90
80
70
60
50
40
30
20
ppm

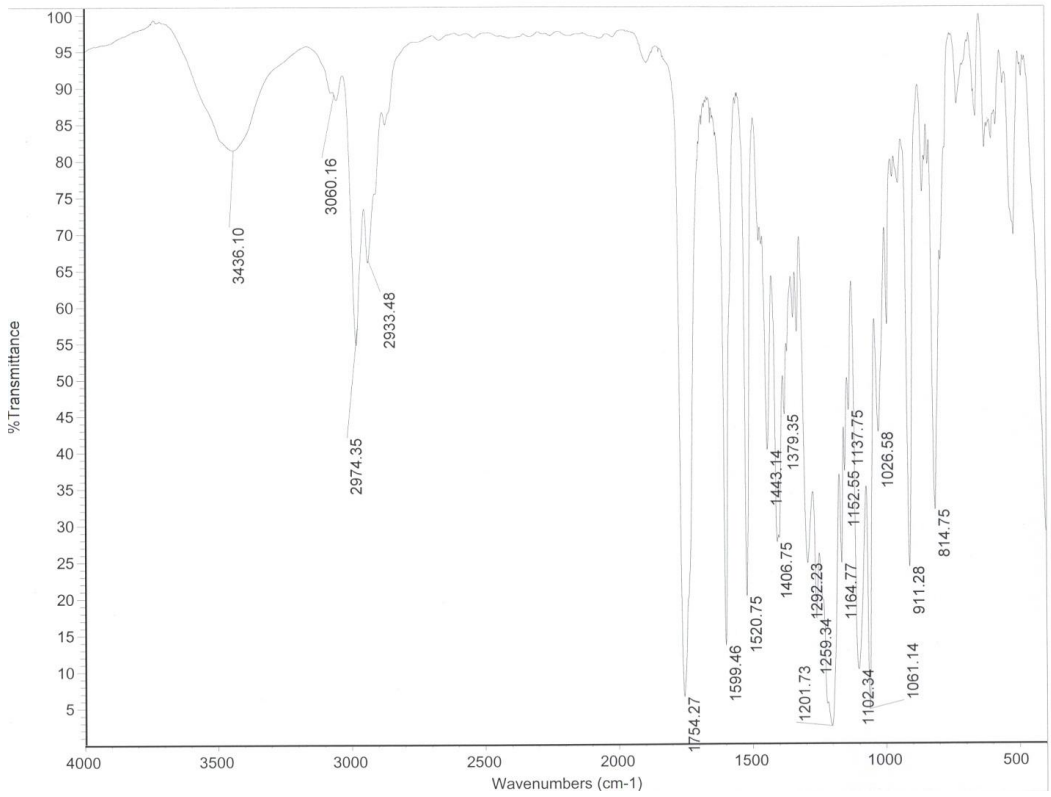
%Transmittance
Wavenumbers (cm-1)
3436.10
3060.16
2974.35
2933.48
1754.27
1599.46
1520.75
1443.14
1406.75
1379.35
1292.23
1259.34
1201.73
1164.77
1152.55
1137.75
1102.34
1061.14
1026.58
911.28
814.75

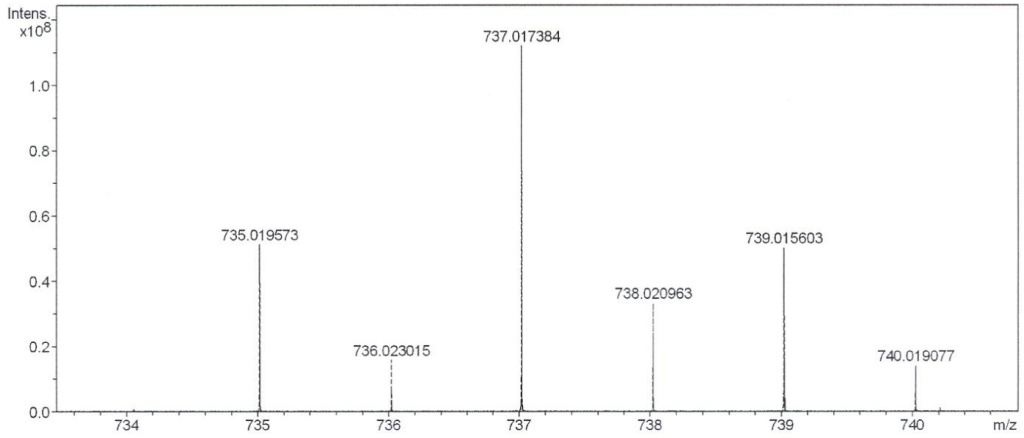
Intens.
x10^8
737.017384
735.019573
739.015603
738.020963
736.023015
740.019077
m/z

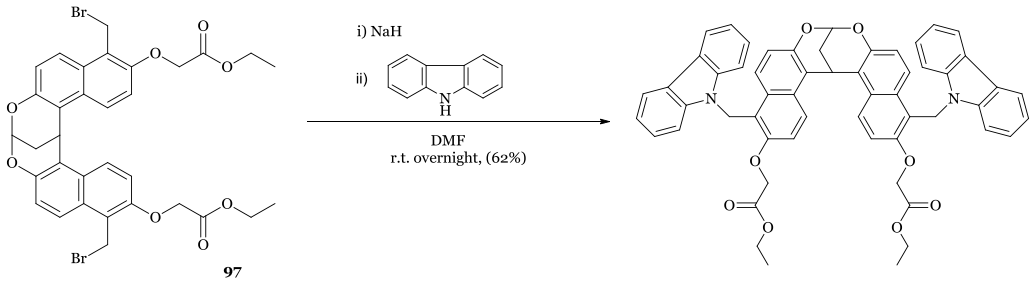

97

Carbazole Open-Tube ester: NaH (21 mg, 60% in mineral oil, 0.53 mmol) was added into DMF (20 mL) in a flame dried flask, and stirred for 10 min. Then, carbazole (105 mg, 0.63 mmol) in DMF (20 mL) was slowly added into the solution *via* syringe over 5 min. After the solution stirred at room temperature for 1 hr, dibromide compound (150 mg, 0.21 mmol) in DMF (20 mL) was added dropwise into the reaction over 10 min. The reaction mixture was stirred at room temperature overnight. DMF was removed *in vacuo*, and the crude product was extracted with DCM (50 mL × 4) and 10% HCl from the remaining residue. The organic layers were dried over Na_2SO_4 and filtered. After removal the solvents *in vacuo*, crude product was purified by column chromatography (20% hexanes/DCM to DCM). White powdered solid was obtained (115 mg, 0.13 mmol, 62%). m.p.: 277-280˚C; ^{1}H-NMR (500 MHz, $CDCl_3$) δ: 8.48 (d, 2H, *J* = 9.5 Hz, Ar-$\underline{H_b}$), 8.02 (d, 4H, *J* = 8.0 Hz, Ar-$\underline{H_{h,\,i}}$), 7.57 (d, 2H, *J* = 9.0 Hz, Ar-$\underline{H_c}$), 7.30 (m, 8H, 7.5 Hz, Ar-$\underline{H_{f,\,g,\,j,\,k}}$), 7.21 (d, 2H, *J* = 9.0 Hz, Ar-$\underline{H_d}$), 7.14 (t, 4H, *J* = 7.0 Hz, Ar-$\underline{H_{e,\,l}}$), 6.92 (d, 2H, *J* = 9.0 Hz, Ar-$\underline{H_a}$), 6.13 (s, 1H, -$O_2\underline{CH}CH_2CHAr_2$), 5.51 (dd, 4H, *J* = 86 Hz, *J* = 15 Hz, -Ar$\underline{CH_2}$N), 5.18 (s, 1H, -$O_2CHCH_2\underline{CH}Ar_2$), 4.56 (s, 4H, -O$\underline{CH_2}$CO), 4.18 (q, 4H, *J* = 7.0 Hz, -O$\underline{CH_2}CH_3$), 2.29 (s, 2H, -$O_2CH\underline{CH_2}CHAr_2$), 1.20 (t, 3H, *J* = 7.0 Hz, -$OCH_2\underline{CH_3}$); ^{13}C-NMR (125 MHz, $CDCl_3$) δ: 169.1, 152.6, 148.9, 140.8, 129.5, 127.3, 125.5, 124.4, 123.4, 122.9, 119.9, 119.8, 119.6, 118.8, 118.7, 113.9, 109.6, 91.1, 66.6, 61.4, 38.5, 26.8, 22.9, 14.1; IR (KBr, cm^{-1}): 3444, 3043, 2970, 2929, 1754, 1621, 1599, 1519, 1482, 1462, 1452, 1399, 1378, 1323, 1271, 1201, 1164, 1105, 1063, 1029; HRMS for M^+ calcd. For $(C_{57}H_{46}N_2O_8)Na^+$ 909.3146, found 909.3133

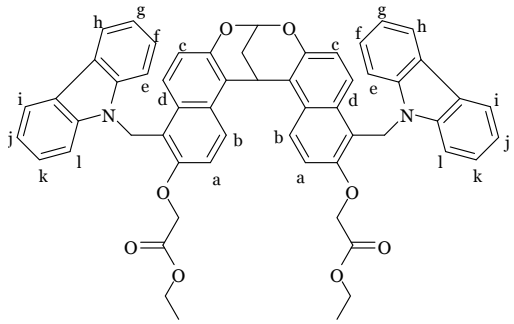
h
g
f
e
i
j
k
l
N
d
c
O
O
c
d
b
a
O
O
O
O
O
O
b
a
g
f
h
e
i
j
k
l
N

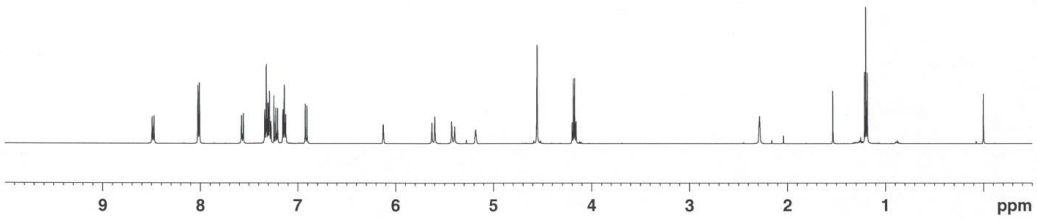
9
8
7
6
5
4
3
2
1
ppm

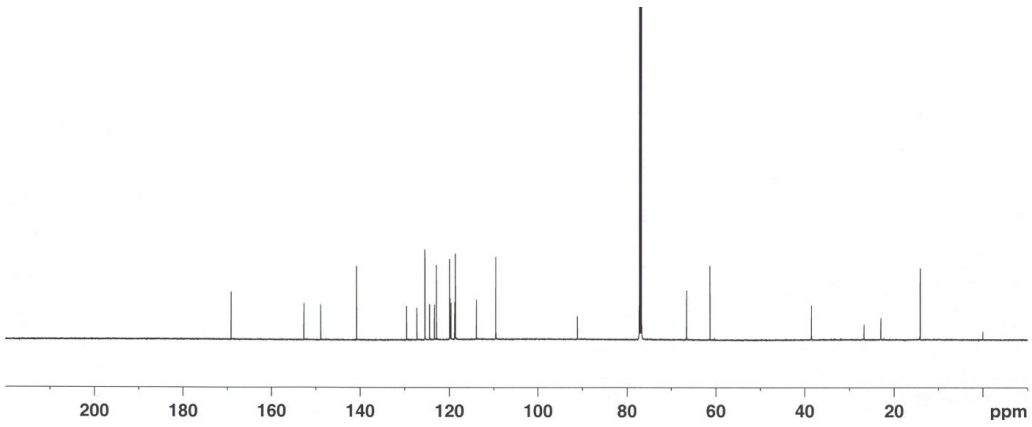
200
180
160
140
120
100
80
60
40
20
ppm

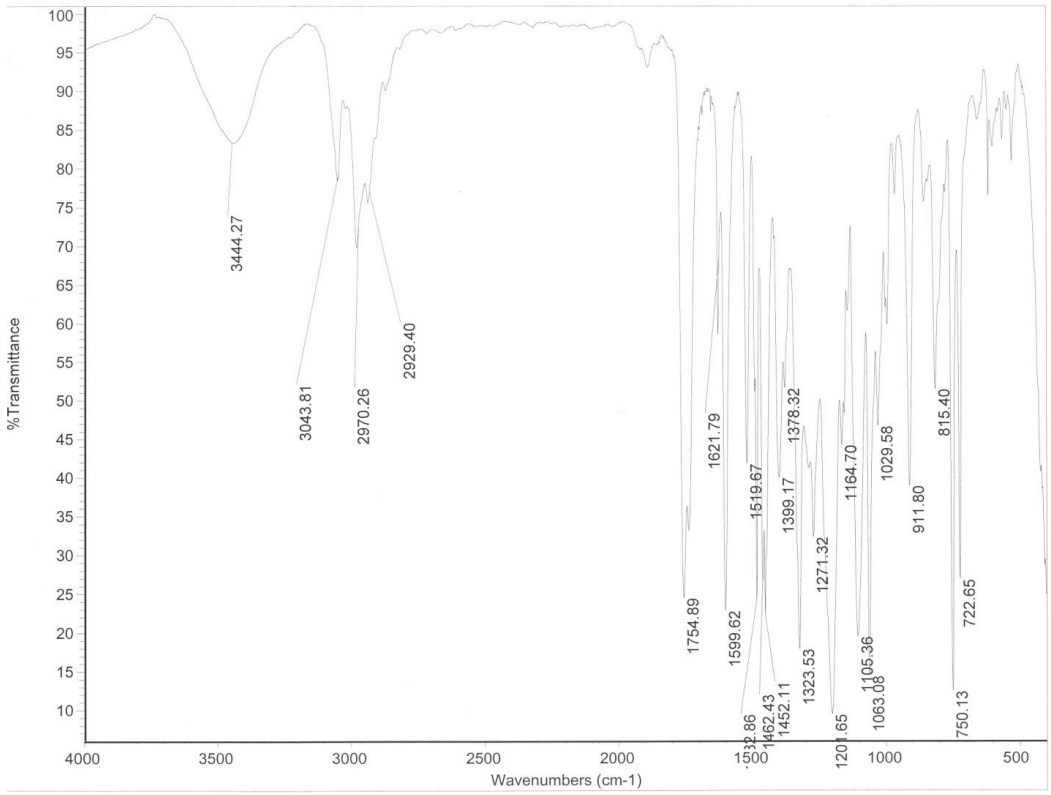
%Transmittance
Wavenumbers (cm-1)
3444.27
3043.81
2970.26
2929.40
1754.89
1621.79
1599.62
1519.67
1462.43
1452.11
1399.17
1378.32
1323.53
1271.32
1201.65
1164.70
1105.36
1063.08
1029.58
911.80
815.40
750.13
722.65

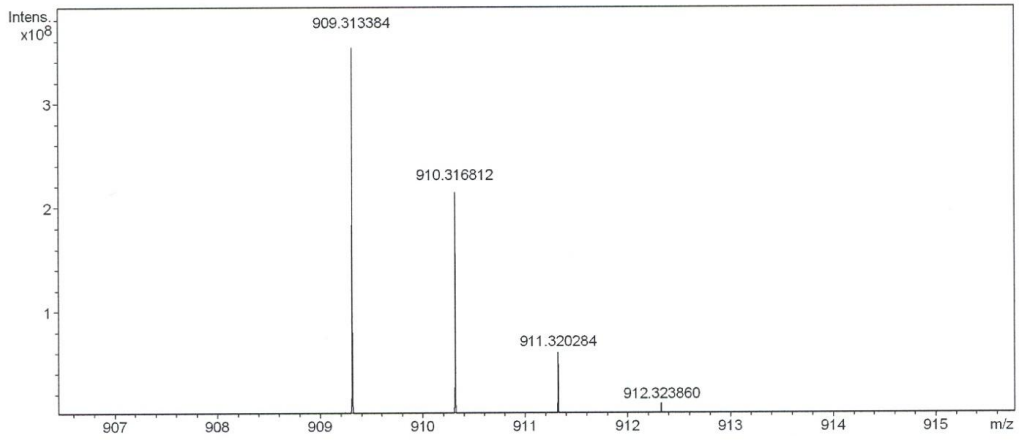
Intens.
x10^8
909.313384
910.316812
911.320284
912.323860
m/z

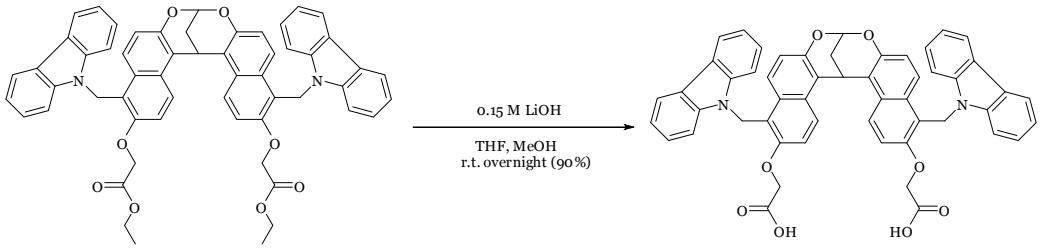

102

Carbazole Open-Tube 102: Open-Tube ester (20 mg, 0.023 mmol) was dissolved in THF (4 mL) and MeOH (1.5 mL), then 0.15 M LiOH (1 mL) was added into the solution. The reaction mixture was stirred at room temperature for 1 hr. 10% HCl was added into the reaction to quench, and then crude product was extracted with DCM (30 mL × 3). The organic layers were dried over Na_2SO_4, and filtered. Solvents were removed *in vacuo*, the residue was dissolved in distilled DCM, and then pentane was slowly added into the solution to give pure white product (17 mg, 0.021 mmol, 90%). m.p.: 277˚C (Dec.); ^{1}H-NMR (500 MHz, DMSO-d_6) δ: 8.81 (d, 2H, *J* = 9.5 Hz, Ar-$\underline{H}_b$), 8.12 (d, 4H, *J* = 7.5 Hz, Ar-$\underline{H}_{h, i}$), 7.63 (d, 6H, *J* = 8.5 Hz, Ar-$\underline{H}_{c, e, l}$), 7.54 (d, 2H, 9.5 Hz, Ar-$\underline{H}_d$), 7.33 (t, 4H, 7.5 Hz, Ar-$\underline{H}_{f, k}$), 7.16 (t, 4H, *J* = 7.5 Hz, Ar-$\underline{H}_{g, j}$), 6.86 (d, 2H, *J* = 9.0 Hz, Ar-$\underline{H}_a$), 6.23 (s, 1H, -$O_2\underline{CH}CH_2CHAr_2$), 5.92 (q, 4H, *J* = 15.5 Hz, -Ar$\underline{CH_2}$N), 5.58 (s, 1H, -$O_2CHCH_2\underline{CH}Ar_2$), 4.94 (q, 4H, *J* = 16.5 Hz, *J* = 14 Hz, -O$\underline{CH_2}$CO), 2.30 (s, 2H, -$O_2CH\underline{CH_2}CHAr_2$); ^{13}C-NMR (125 MHz, DMSO-d_6) δ: 171.3, 153.5, 148.9, 141.1, 129.7, 127.6, 126.4, 126.2, 123.9, 123.0, 120.4, 119.9, 119.7, 119.5, 118.8, 115.3, 110.7, 91.6, 66.8, 38.9, 26.9, 22.6; IR (KBr, cm^{-1}): 3423, 3047, 2908, 1744, 1625, 1599, 1519, 1482, 1462, 1442, 1399, 1321, 1229, 1204, 1102, 1061, 1021; HRMS for M^+ calcd. For $(C_{53}H_{38}N_2O_8)Na^+$ 853.2520, found 853.2504

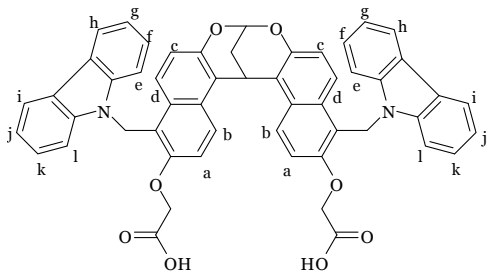
h
g
f
c
O
O
c
f
g
h
e
d
d
e
i
N
N
i
j
b
b
j
l
l
k
k
a
a
O
O
O
O
OH
HO

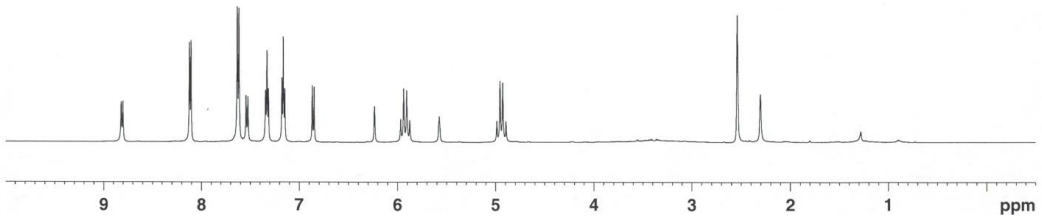
9
8
7
6
5
4
3
2
1
ppm

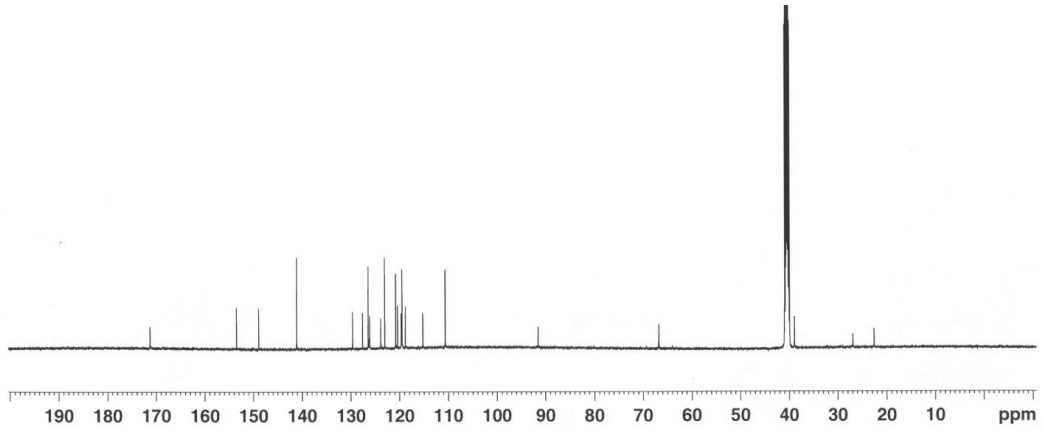
190
180
170
160
150
140
130
120
110
100
90
80
70
60
50
40
30
20
10
ppm

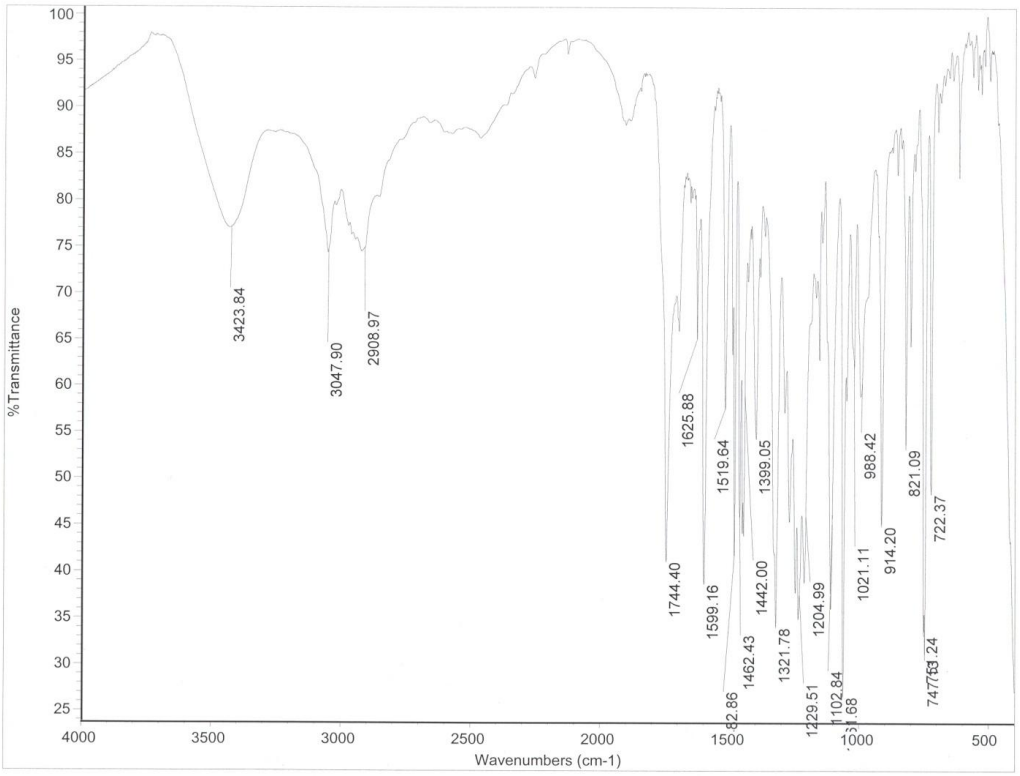
%Transmittance
Wavenumbers (cm-1)
3423.84
3047.90
2908.97
1744.40
1625.88
1599.16
1519.64
1462.43
1442.00
1399.05
1321.78
1229.51
1204.99
1102.84
1021.11
988.42
914.20
821.09
747.63
722.37

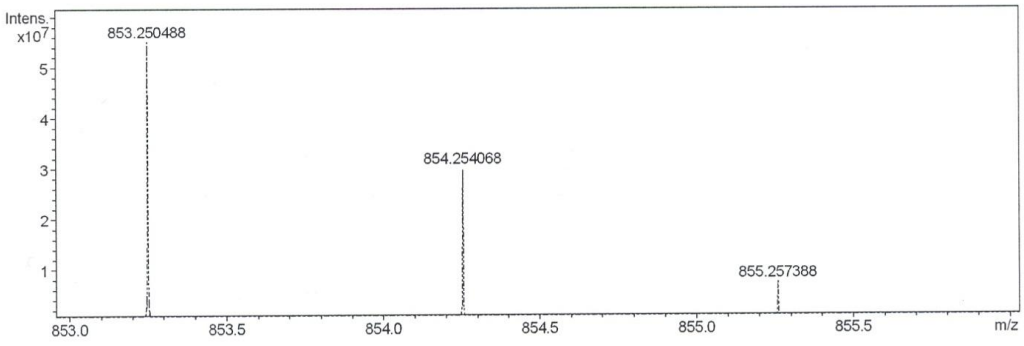
Intens.
x10^7
853.250488
854.254068
855.257388
m/z

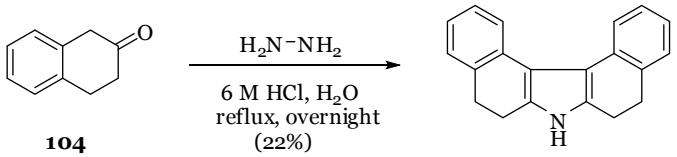

104 **105**

5,6,8,9-Tetrahydro-7H-dibenzo[c,g]carbazole compound 105: Anhydrous hydrazine (0.1 mL, 3.42 mmol), and 6 M-HCl (3 mL) were stirred under reflux for 30 min. β-tetralone (1 g, 6.84 mmol) was slowly added over 5 min. and the mixture was stirred under reflux overnight, then cooled to room temperature and extracted with EtOAc (50 mL 4). Brown color crude powder was obtained and recrystallized in benzene to give light brown product (401 mg, 1.48 mmol, 22%) m.p.: 249-250°C[75]; ^{1}H-NMR (500 MHz, DMSO-d_6) δ: 11.04 (s, 1H, -NH), 7.56 (d, 2H, 7.5 Hz, Ar-H_a), 7.25 (d, 2H, 7.5 Hz, Ar-H_d), 7.17 (t, 2H, *J* = 7.5 Hz, Ar-H_b), 7.01 (t, 2H, *J* = 7.5 Hz, Ar-H_c), 2.91 (dt, 8H, *J* = 125.5 Hz, *J* = 7.5 Hz, *J* = 7.0 Hz, -ArCH_2CH_2Ar-); ^{13}C-NMR (125 MHz, DMSO-d_6) δ: 134.8, 132.1, 128.9, 127.1, 124.5, 123.4, 114.4, 30.86, 22.5; IR (KBr, cm^{-1}): 3411, 3060, 2994, 2933, 2872, 2819, 1597, 1523, 1478, 1462, 1421, 1376, 1303, 1180, 1155, 1004; HRMS for M^+ calcd. For $(C_{20}H_{17}N)Na^+$ 294.1253, found 294.1249

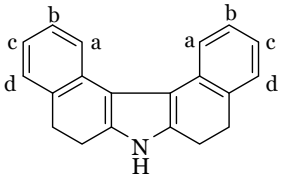
b
a
c
d
b
a
c
d
N
H

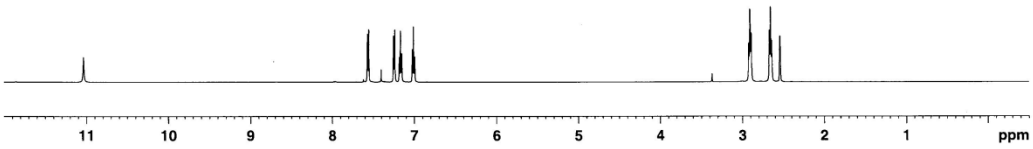
11
10
9
8
7
6
5
4
3
2
1
ppm

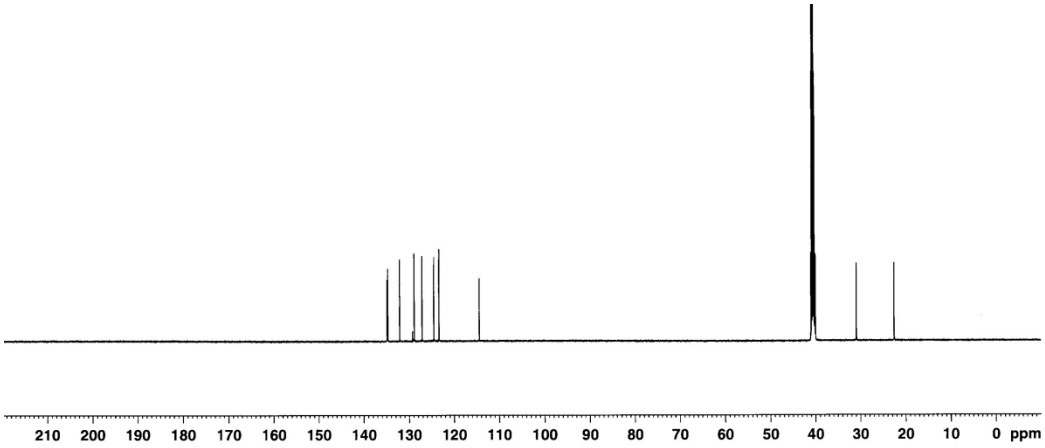
210
200
190
180
170
160
150
140
130
120
110
100
90
80
70
60
50
40
30
20
10
0 ppm

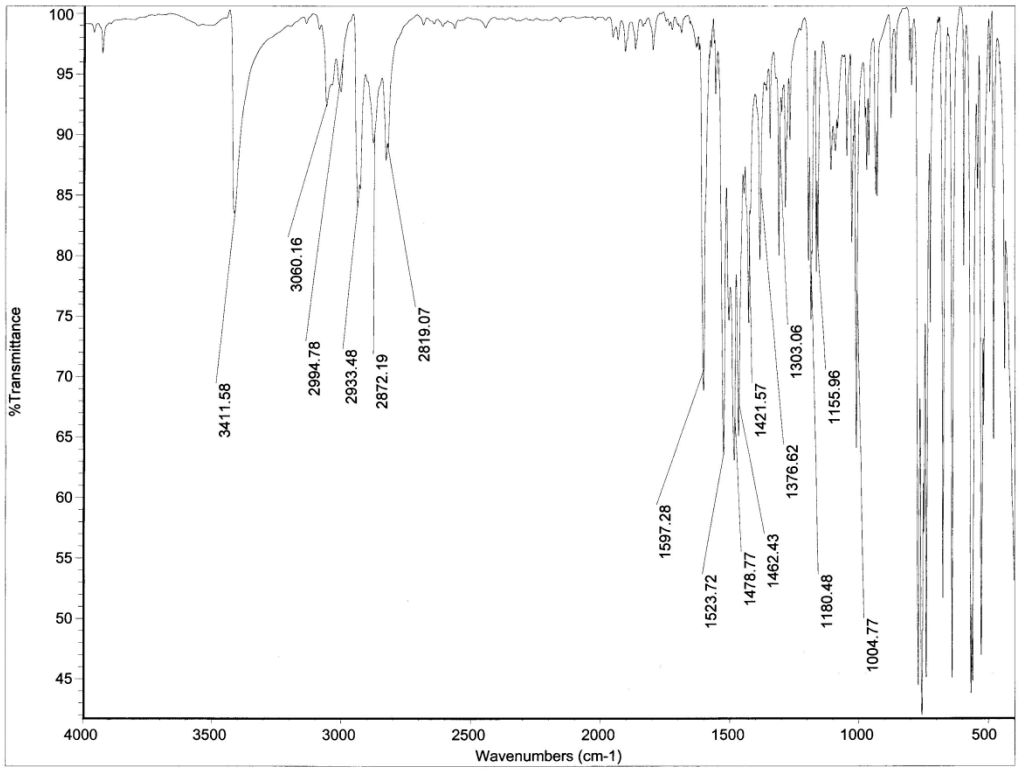
%Transmittance
Wavenumbers (cm-1)
3411.58
3060.16
2994.78
2933.48
2872.19
2819.07
1597.28
1523.72
1478.77
1462.43
1421.57
1376.62
1303.06
1180.48
1155.96
1004.77

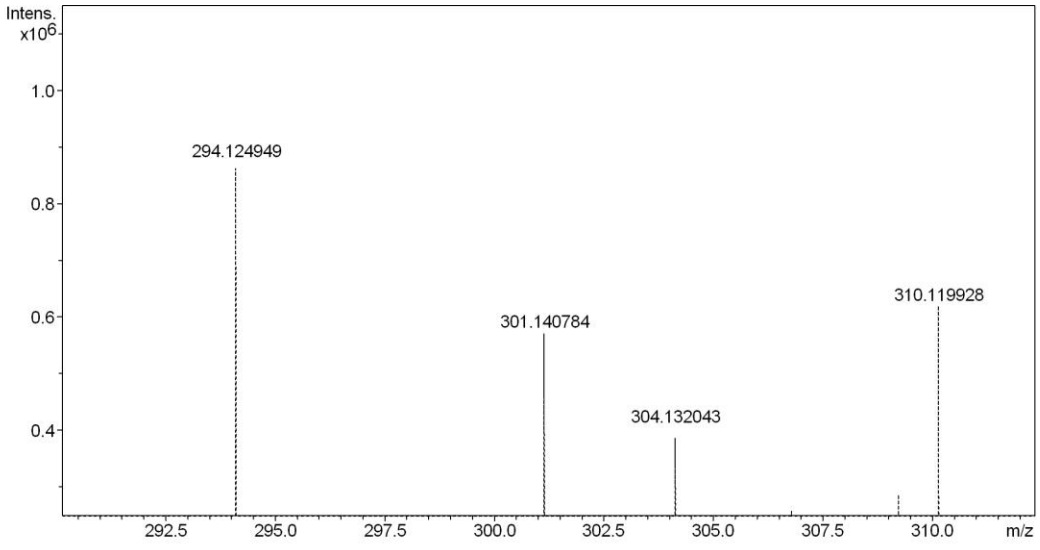
Intens.
x10^6
294.124949
301.140784
304.132043
310.119928
m/z

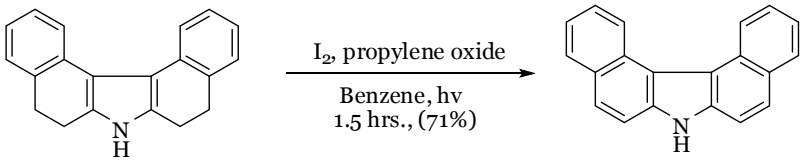

105 **101**

7H-Dibenzo[c,g]carbazole 101: Tetrahydrocarbazole **105** (100 mg, 0.37 mmol) and iodine (187 mg, 0.74 mmol) were dissolved in benzene (50 mL) and N_2 gas was bubbled for 15 min. Propylene oxide (6 mL, 88.72 mmol, 240 eq.) was added into the mixture *via* syringe and lamp was turned on. The mixture was stirred under N_2 flow for 1.5 hours. Crude product was extracted with DCM (50 mL 3) and 10% $Na_2S_2O_3{\cdot}5H_2O$ (100 mL). The organic layers were dried over Na_2SO_4 and filtered. After removal the solvents *in vacuo*, crude product was purified by column chromatography (DCM). Brown powdered solid was obtained (70 mg, 0.26 mmol, 71%). m.p.: 154°C[75]; ^{1}H-NMR (500 MHz, DMSO-d_6) δ: 12.38 (s, 1H), 9.13 (d, 2H, 8.5 Hz, Ar-$\underline{H}_a$), 8.14 (d, 2H, 8.0 Hz, Ar-$\underline{H}_d$), 7.97 (d, 2H, 9.0 Hz, Ar-$\underline{H}_f$), 7.88 (d, 2H, *J* = 8.5 Hz, Ar-$\underline{H}_b$), 7.75 (t, 2H, *J* = 7.5 Hz, Ar-$\underline{H}_c$), 7.55 (t, *J* = 7.5 Hz, Ar-$\underline{H}_e$); ^{13}C-NMR (125 MHz, DMSO-d_6) δ: 137.5, 130.3, 130.2, 129.6, 127.2, 126.3, 125.1, 123.8, 117.1, 114.6; IR (KBr, cm^{-1}): 3366, 3043, 2958, 2925, 2851, 1613, 1523, 1462, 1376, 1315, 1249, 1200, 1041, 1008; HRMS for M^+ calcd. For $(C_{20}H_{13}N)Na^+$ 268.1120, found 268.1117

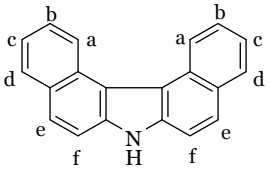
b
b
c
a
a
c
d
d
e
e
N
H
f
f

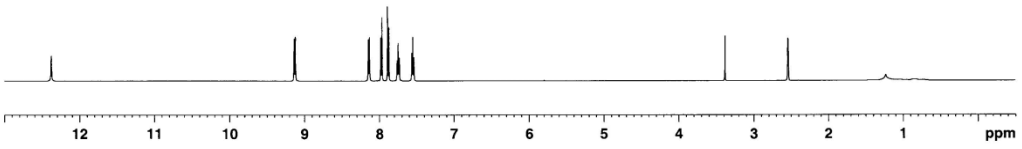
12
11
10
9
8
7
6
5
4
3
2
1
ppm

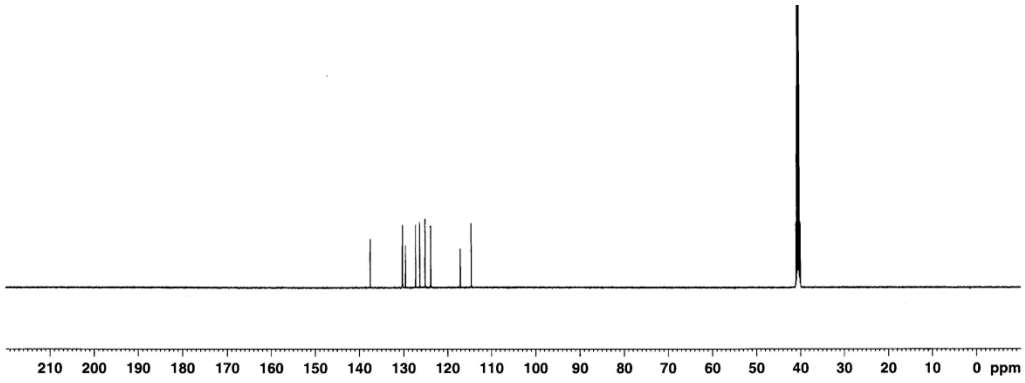
210
200
190
180
170
160
150
140
130
120
110
100
90
80
70
60
50
40
30
20
10
0 ppm

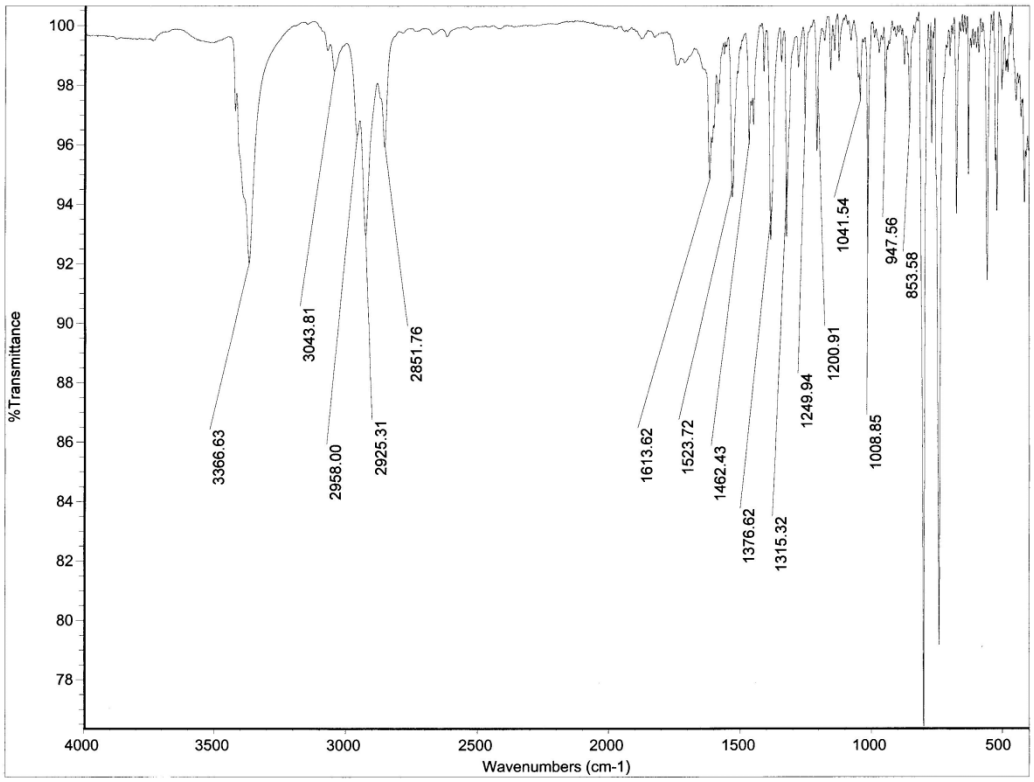
%Transmittance
Wavenumbers (cm-1)
3366.63
3043.81
2958.00
2925.31
2851.76
1613.62
1523.72
1462.43
1376.62
1315.32
1249.94
1200.91
1041.54
1008.85
947.56
853.58

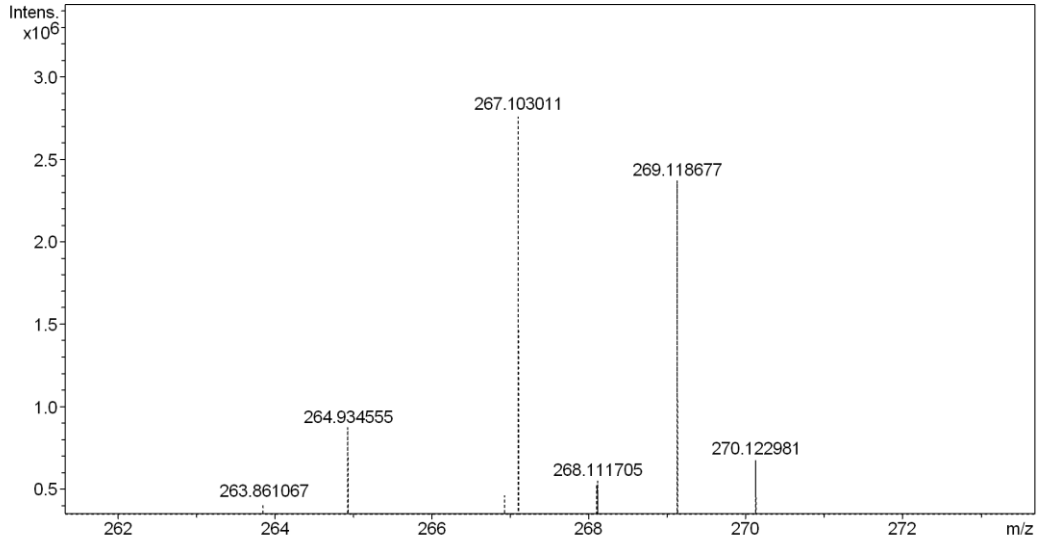
Intens.
x10^6
m/z
267.103011
269.118677
264.934555
270.122981
268.111705
263.861067

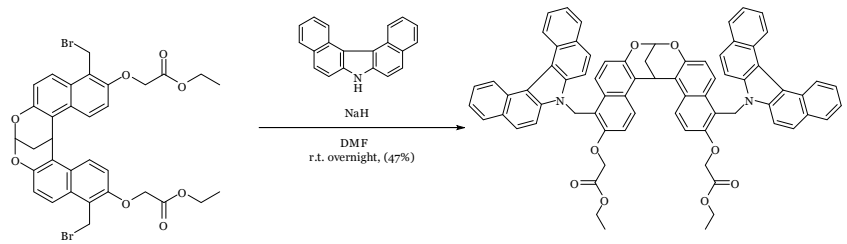

Dibenzocarbazole Open-Tube ester: NaH (14 mg, 60% in mineral oil, 0.35 mmol) was added into a DMF (20 mL) in a flame dried flask, and stirred for 10 min. Then, dibenzocarbazole (113 mg, 0.42 mmol) in DMF (20 mL) was slowly added into the solution via syringe over 5 min. After the solution stirred at room temperature for 1 hr, dibromide **97** (100 mg, 0.14 mmol) in DMF (20 mL) was added dropwise into the reaction over 10 min. The reaction mixture was stirred at room temperature overnight. DMF was removed *in vacuo*, and the crude product was extracted with DCM (50 mL × 3) and 10% HCl from the remaining residue. The organic layers were dried over Na_2SO_4 and filtered. After removal the solvents *in vacuo*, crude product was purified by column chromatography (20% hexanes/DCM to DCM). White powdered solid was obtained (71 mg, 0.07 mmol, 47%). ^{1}H-NMR (500 MHz, $CDCl_3$) δ: 9.02 (d, 4H, *J* = 8.0 Hz, Ar-$\underline{H}_{j, p}$), 8.82 (d, 2H, *J* = 9.5 Hz, Ar-$\underline{H}_b$), 8.06 (d, 4H, *J* = 8.0 Hz, Ar-$\underline{H}_{g, m}$), 8.01 (d, 4H, 9.0 Hz, Ar-$\underline{H}_{e, k}$), 7.86 (d, 4H, 9.0 Hz, Ar-$\underline{H}_{i, o}$), 7.69 (t, 6H, *J* = 7.5 Hz, Ar-$\underline{H}_{c, h, n}$), 7.53 (t, 4H, *J* = 7.5 Hz, Ar-$\underline{H}_{f, l}$), 7.51 (d, 2H, *J* = 7.0 Hz, Ar-$\underline{H}_d$), 6.87 (d, 2H, *J* = 9.0 Hz, Ar-$\underline{H}_a$), 6.22 (s, 1H, -$O_2\underline{C}\underline{H}CH_2CHAr_2$), 6.15 (q, 4H, *J* = 16.5 Hz, *J* = 14 Hz, -Ar$\underline{CH_2}$N), 5.59 (s, 1H, -$O_2CHCH_2\underline{C}\underline{H}Ar_2$), 4.94 (q, 4H, *J* = 20.5 Hz, *J* = 16.5 Hz, -O$\underline{CH_2}$CO), 4.18 (q, 4H, *J* = 7.0 Hz, -O$\underline{CH_2}CH_3$), 2.29 (s, 2H, -$O_2CH\underline{CH_2}CHAr_2$), 1.19 (t, 3H, *J* = 7.0 Hz, -$OCH_2\underline{CH_3}$); ^{13}C-NMR (125 MHz, $CDCl_3$) δ: 169.2, 152.7, 148.6, 137.7, 129.5, 129.4, 128.9, 128.5, 127.2, 126.6, 125.9, 125.7, 124.5, 123.5, 123.2, 120.0, 119.5, 118.6, 116.3, 114.6, 112.5, 91.1, 66.2, 61.2, 38.9, 26.3, 22.4, 14.1; IR (KBr, cm^{-1}): 3436, 3047, 2970, 2952, 1750, 1728, 1599, 1515, 1442, 1392, 1372, 1323, 1254, 1201, 1103, 1057; HRMS for M^+ calcd. For $(C_{73}H_{54}N_2O_8)Na^+$ 1109.3772, found 1109.3741

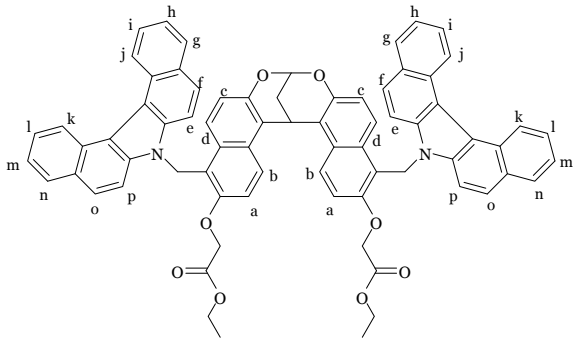
h
i
g
j
f
c
O
O
c
l
k
e
d
d
e
k
l
m
N
b
b
N
m
n
p
o
a
a
p
o
n
O
O
O
O
O
O

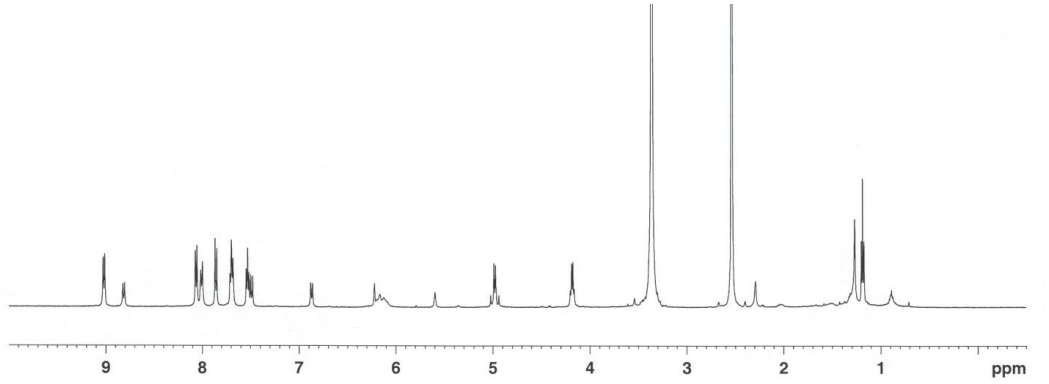
9
8
7
6
5
4
3
2
1
ppm

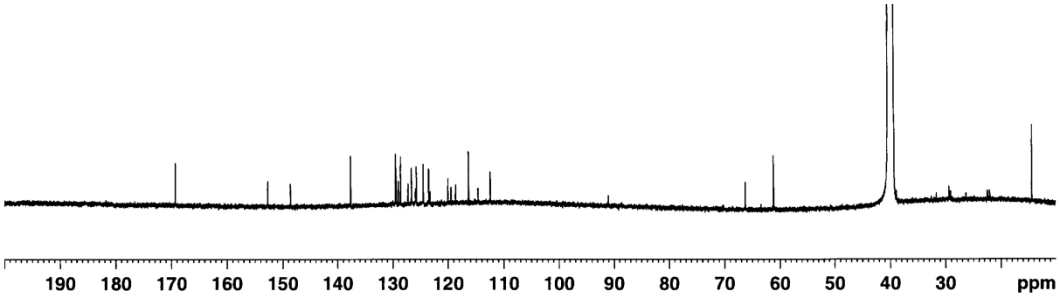
190
180
170
160
150
140
130
120
110
100
90
80
70
60
50
40
30
ppm

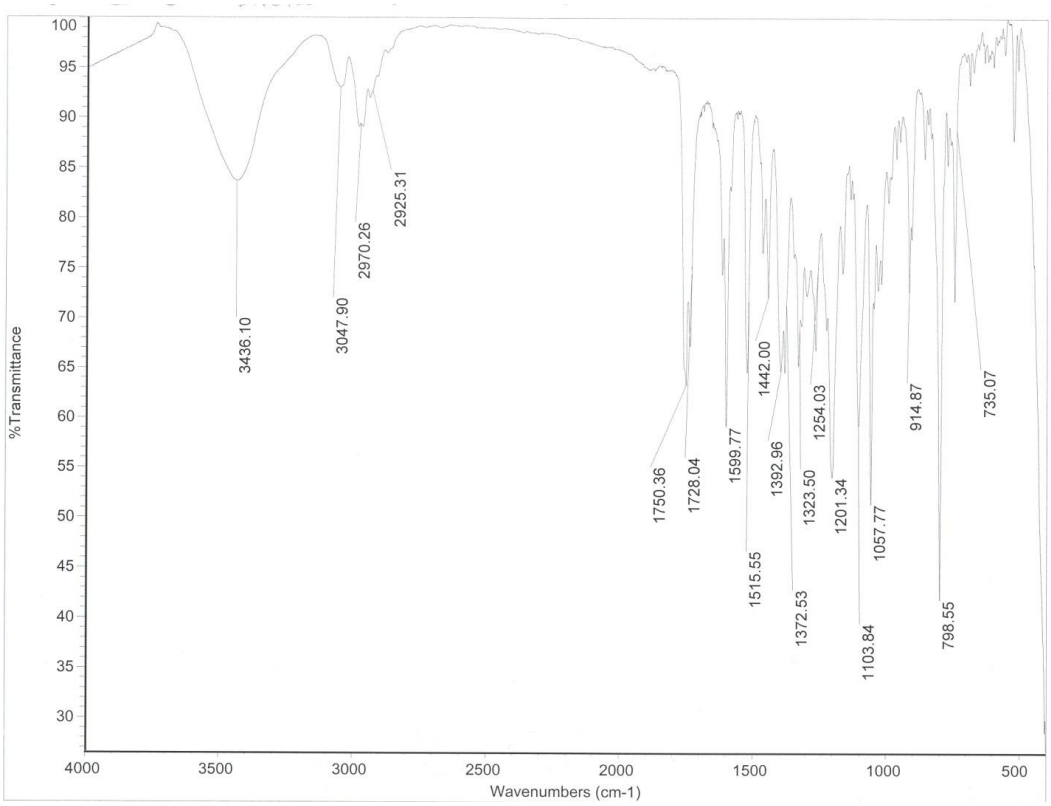
%Transmittance
Wavenumbers (cm-1)
3436.10
3047.90
2970.26
2925.31
1750.36
1728.04
1599.77
1515.55
1442.00
1392.96
1372.53
1323.50
1254.03
1201.34
1103.84
1057.77
914.87
798.55
735.07

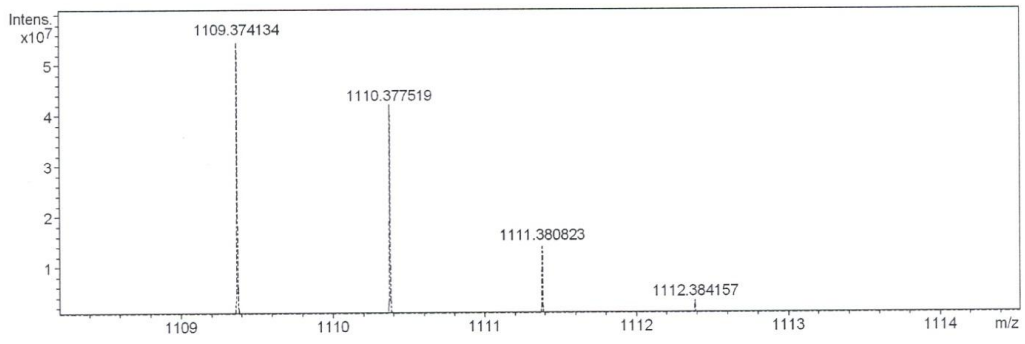
Intens.
x10^7
1109.374134
1110.377519
1111.380823
1112.384157
m/z

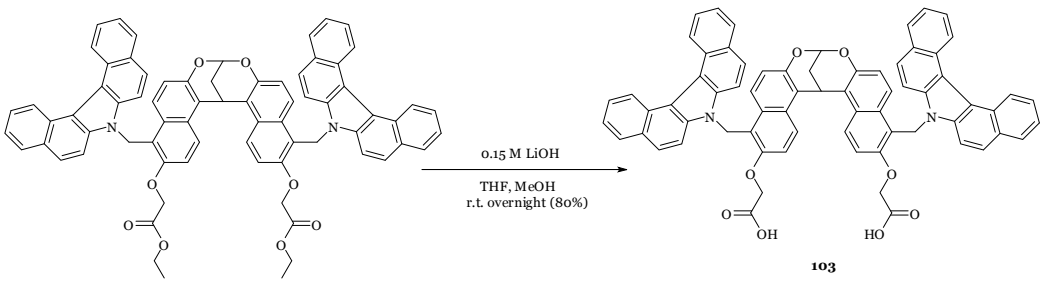

103

Dibenzocarbazole Open-Tube 103: Open-Tube ester (30 mg, 0.05 mmol) was dissolved in THF (8 mL) and MeOH (3 mL), then 0.15 M LiOH (2 mL) was added into the solution. The reaction mixture was stirred at room temperature for 1 hr. 10% HCl was added into the reaction to quench, and then crude product was extracted with DCM (50 mL × 3). The organic layers were dried over Na_2SO_4, and filtered. Solvents were removed *in vacuo*. The residue was dissolved in distilled DCM, and then pentane was slowly added into the solution to give pure white product (42 mg, 0.04 mmol, 80%). m.p.: 250˚C (Dec.); ^{1}H-NMR (500 MHz, DMSO-d_6) δ: 9.03 (d, 4H, *J* = 8.5 Hz, Ar-$\underline{H}_{j, p}$), 8.83 (d, 2H, *J* = 9.5 Hz, Ar-$\underline{H}_b$), 8.06 (d, 4H, *J* = 8.0 Hz, Ar-$\underline{H}_{g, m}$), 8.01 (d, 4H, 8.0 Hz, Ar-$\underline{H}_{e, k}$), 7.85 (d, 4H, 9.0 Hz, Ar-$\underline{H}_{i, o}$), 7.69 (t, 4H, *J* = 7.5 Hz, Ar-$\underline{H}_{h, n}$), 7.53 (t, 8H, *J* = 7.5, Ar-$\underline{H}_{c, d, f, l}$), 6.79 (d, 2H, *J* = 9.0 Hz, Ar-$\underline{H}_a$), 6.19 (s, 1H, -$O_2\underline{CH}CH_2CHAr_2$), 6.05 (q, 4H, *J* = 16.5 Hz, *J* = 14 Hz, -Ar$\underline{CH_2}$N), 5.57 (s, 1H, -$O_2CHCH_2\underline{CH}Ar_2$), 4.94 (q, 4H, *J* = 20.5 Hz, *J* = 16.5 Hz, -O$\underline{CH_2}$CO), 2.26 (s, 2H, -$O_2CH\underline{CH_2}CHAr_2$); ^{13}C-NMR (125 MHz, DMSO-d_6) δ: 171.5, 153.4, 149.0, 138.2, 130.1, 129.9, 129.6, 129.1, 127.6, 127.2, 126.5, 126.3, 125.1, 124.1, 123.7, 120.5, 119.9, 118.7, 116.9, 115.1, 113.1, 91.6, 66.7, 39.3, 26.9, 22.6; IR (KBr, cm^{-1}): 3436, 2921, 2851, 1732, 1597, 1519, 1442, 1397, 1315, 1209, 1098, 1057, 1021; HRMS for M^+ calcd. For $(C_{69}H_{46}N_2O_8)Na^+$ 1053.3146, found 1053.3123

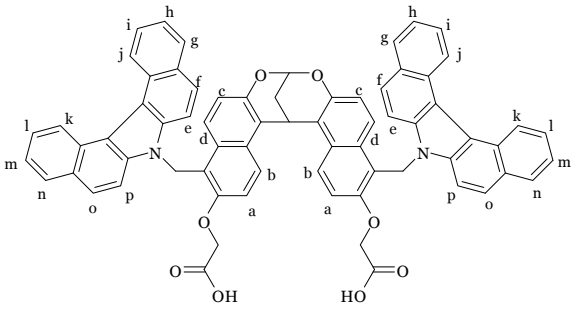
O
O
N
N
O
O
O
O
OH
HO

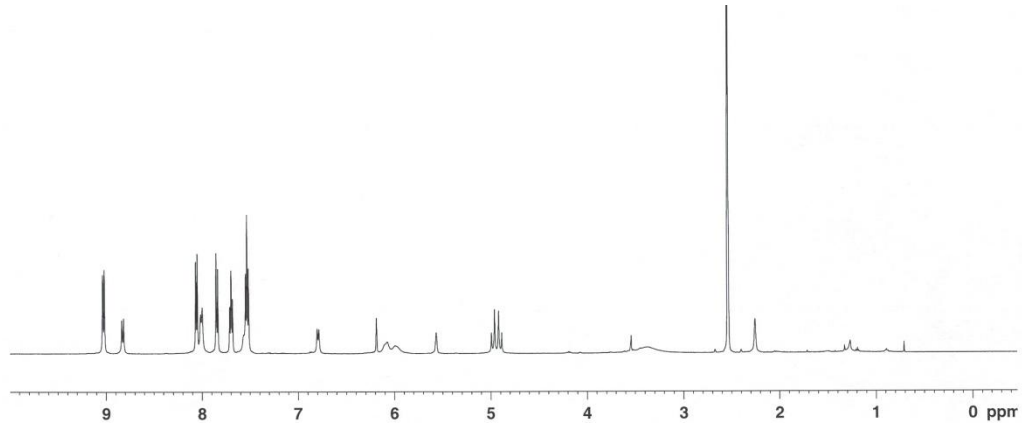
9
8
7
6
5
4
3
2
1
0 ppm

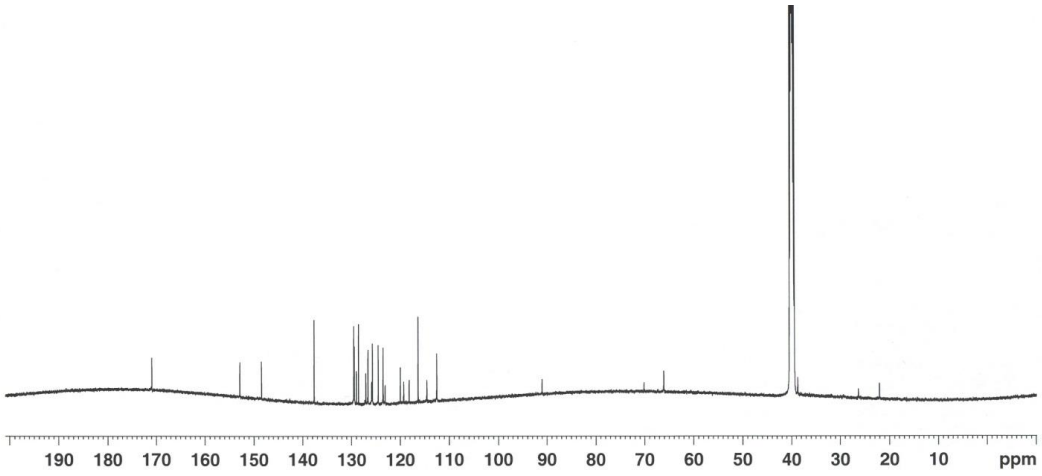
190 180 170 160 150 140 130 120 110 100 90 80 70 60 50 40 30 20 10 ppm

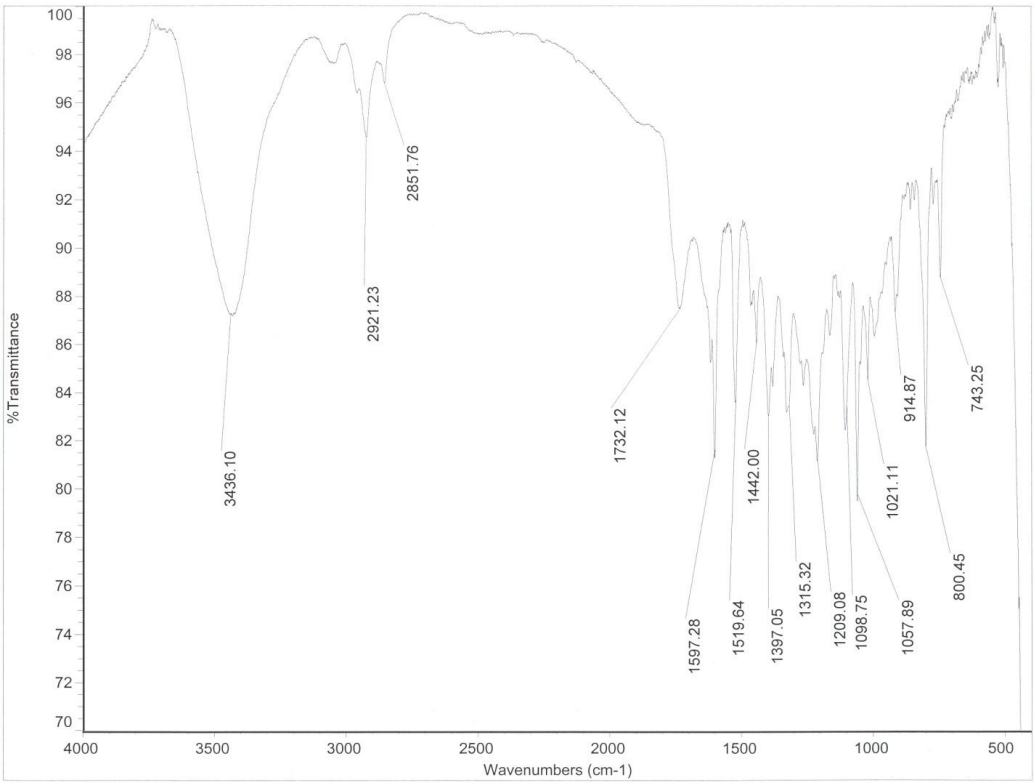
%Transmittance
Wavenumbers (cm-1)
3436.10
2921.23
2851.76
1732.12
1597.28
1519.64
1442.00
1397.05
1315.32
1209.08
1098.75
1057.89
1021.11
914.87
800.45
743.25

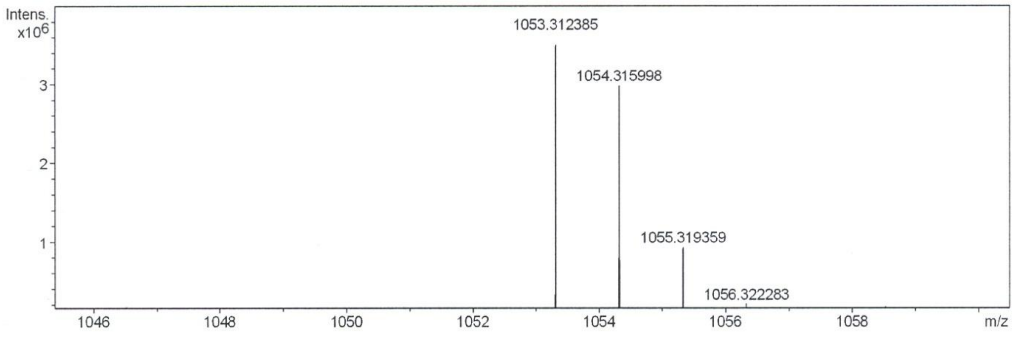
Intens.
x10^6
1053.312385
1054.315998
1055.319359
1056.322283
m/z

REFERENCES

(1) Lehn, J. –M., *Supramolecular Chemistry*; VCH: Winheim 1995.

(2) Gellman, S. H., *Chem. Rev*. **1997**, *97*, 1231-1232.

(3) Buckingham, A. D.; Legon, A. C.; Roberts, S. M., *Principles of Molecular Recognition*; Blackie Academic & Professional: London 1993.

(4) Czarnik, A. W., *Chemistry & Biology* **1995**, *2*, 423-428.

(5) Zhang, J.; Campbell, R. E.; Ting, A. Y.; Tsien, R. Y., *Nature Reviews* **2002**, *3*, 906-918.

(6) Silva, A. P. d.; Gunaratne, H. Q. N.; Gunnlaugsson, T.; Huxley, A. J. M.; McCory, C. P.; Rademacher, J. T.; Rice, T. E., *Chem. Rev*. **1997**, *97*, 1515-1566.

(7) Kyba, E. P.; Helgeson, R. C.; Madan, K.; Gokel, G. W.; Tarnowski, T. L.; Moore, S. S.; Cram, D. J., *J. Am. Chem. Soc*. **1997**, *99*, 2564-2571.

(8) Goke, G., *Crown Ethers & Cryptands*; The Royal Society of Chemistry: Cambridge 1991.

(9) Pederson, C. J., *J. Am. Chem. Soc*. **1967**, *89*, 7017-7036.

(10) Oshima, T.; Nagai, T., *J. Org. Chem*. **1991**, *56*, 673-677.

(11) Schultz, R. A.; Dishong, D. M.; Gokel, G. W., *J. Am. Chem. Soc*. **1982**, *104*, 625-626.

(12) Maye, P. V.; Venanzi, C. A., *J. Compt. Chem*. **1991**, *12*, 994-1007.

(13) Gokel, G. W.; Goli, D. M.; Minganti, C.; Echegoyen, L., *J. Am. Chem. Soc*. **1983**, *105*, 6786-6788.

(14) Martell, A. E.; Hancock, R. D., *Coordination Chemistry, Chapter 20; ACS Symposium Series* **1994**, *565*, 240-254.

(15) Martell, A. E., *Werner Centennial, Chapter 19; Advances in Chemistry* **1967**, *62*, 272-294.

(16) Diehl, H., *Chem. Rev*. **1937**, *21*, 39-111.

(17) Chen, Q.; Cannell, K.; Nicoll, J.; Dearden, D. V., *J. Am. Chem. Soc*. **1996**, *118*, 6335-6344.

(18) Cram, D. J.; Cram, J. M., *Container Molecules & Their Guests*; The Royal Society of Chemistry: Cambridge 1994.

(19) Silwa, W.; Kozlowski, C., *Calixarenes & Resorcinarenes*; Wiley-VCH: Weinheim 2009.

(20) Gutsche, C. D., *Calixarenes*; The Royal Society of Chemistry: Cambridge 2008.

(21) Bakirci, H.; Koner, A. L.; Schwarzlose, T.; Nau, W. M., *Chem. Eur. J.* **2006**, *12*, 4799-4807.

(22) Chen, Q. -Y.; Chen, C. -F., *Tetrahedron Lett.* **2005**, *46*, 165-168.

(23) Fahlbusch, T.; Frank, M.; Schatz, J.; Schmaderer., H. *Eur. J. Org. Chem.* **2006**, 1899-1903.

(24) Poh, B. –L.; Lim, C. S.; Khoo, K. S. *Tetrahedron Lett.* **1989**, *30*, 1005-1008.

(25) Shorthill, B. J.; Granucci, R. G.; Powell, D. R.; Glass, T. E., *J. Org. Chem.* **2002**, *67*, 904-909.

(26) Hooley, R. J.; Rebek Jr. J., *Org. Biomol. Chem.* **2007**, *5*, 3631-3636.

(27) Hof, F.; Trembleau, L.; Ullrich, E. C.; Rebek Jr. J., *Angew. Chem. Int. Ed.* **2003**, *42*, 3150-3153.

(28) Oshovsky, G. V.; Reinhoudt, D. N.; Verboom, W., *Angew. Chem. Int. Ed.* **2007**, *46*, 2366-2393.

(29) Czarnik, A. W., *Fluorescent Chemosensors for Ion and Molecule Recognition, Chapter 1; ACS Symposium Series* **1993**, *538*, 1-9.

(30) Vance, D. H.; Czarnik, A. W., *J. Am. Chem. Soc.* **1994**, *116*, 9397-9398.

(31) Czarnik, A. W., *Interfacial Design & Chemical Sensing, Chapter 27; ACS Symposium Series*, **1994**, *561*, 314-323.

(32) James, T. D.; Samankumara Sandanayake, K. R. A.; Shinkai, S., *Angew. Chem. Int. Ed.* **1994**, *33*, 2207-2209.

(33) Birks, J. B., *Rep. Prog. Phys.* **1975**, *38*, 903-974.

(34) Jung, H. S.; Park, M.; Han, D. Y.; Kim, E.; Lee, C.; Ham, S.; Kim, J. S., *Org. Lett.* **2009**, *11*, 3378-3381.

(35) Kim, S. K.; Lee, S. H.; Lee, J. Y.; Lee, J. Y.; Bartsch, R. A.; Kim, J. S., *J. Am. Chem. Soc.* **2004**, *126*, 16499-16506.

(36) Kim, J. S.; Quang, D. T., *Chem. Rev.* **2007**, *107*, 3780-3799.

(37) Vance, D. E.; Vance, J. E., *Biochemistry of Lipids, Lipoprotein and Membranes; 4th ed.*; Elsevier: Amsterdam 2002.

(38) Reiffel, J. A.; McDonald, A., *Am. J. Cardiol.* **2006**, *98*, 50i-60i.

(39) Honoré, E.; Barhanin, J.; Attali, B.; Lesage, F.; Lazdunski, M., *Proc. Natl. Acad. Sci. USA*, **1994**, *91*, 1937-1944.

(40) Ball, M.; Mann, J., *Lipids and Heart Disease*, *A Guide for the Primary Care Team 2nd ed.*; Oxford University Press: New York 1994.

(41) Moss, G. P. *Pure & appl. Chem*. **1989**, *61*, 1783-1822.

(42) Moss, G. P. *Eur. J. Biochem*. **1989**, *186*, 429-458.

(43) Myant, N. B., *Cholesterol Metabolism, LDL, and the LDL Receptor*; Academic Press: San Diego 1990.

(44) Betteridge, D. J., *Lipids and Vascular Disease*; Martin Dunitz: London 2000.

(45) Wallimann, P.; Marti, T.; Fürer, A.; Diederich, F., *Chem. Rev*. **1997**, *97*, 1567-1608.

(46) Szejtli, J., *Chem. Rev*. **1998**, *98*, 1743-1753.

(47) Breslow, R.; Zhang, B., *J. Am. Chem. Soc*. **1996**, *118*, 8495-8496.

(48) Ferguson, S. B.; Seward, E. M.; Diederich, F.; Sandord, E. M.; Chou, A.; Inocencio-Szweda, P.; Knobler, C. B., *J. Org. Chem*. **1988**, *53*, 5593-5595.

(49) Peterson, B. R.; Wallimann, P.; Carcanague, D. R.; Diederich, F., *Tetrahedron* **1995**, *51*, 401-421.

(50) Hevonoja, T.; Pentikäinen, M. O.; Hyvönen, M. T.; Kovanen, P. T.; Ala-Korpela, M., *Biochim. Biophy. Acta*, **2000**, *1488*, 189-210.

(51) Cromwell, W. C.; Otvos, J. D., *Curr. Atheroscler. Rep*. **2004**, *6*, 381-387.

(52) Berliner, J. A.; Subbanagounder, G.; Leitinger, N.; Watson, A. D.; Vora, D., *Trends Cardiovas. Med*. **2001**, *11*, 142-147.

(53) Leitinger, N., *Curr. Opin. Lipido*. **2003**, *14*, 421-430.

(54) Berliner, J. A.; Watson, A. D., *New Engl. J. Med*. **2005**, *353*, 9-11.

(55) Tsimikas, S.; Brilakis, E. S.; Miller, E. R.; McConnell, J. P.; Lennon, R. J.; Kornman, K. S.; Witztum, J. L.; Berger, P. B., *New Engl. J. Med*. **2005**, *353*, 46-57.

(56) Fruhwirth, G. O.; Loidl, A.; Hermetter, A., *Biochim. Biophys. Acta*, **2007**, *1772*, 718-736.

(57) McIntyre, T. M.; Zimmerman, G. A.; Prescott, S. M., *J. Biol. Chem*. **1999**, *274*, 25189-25192.

(58) Ashraf, M. Z.; Kar, N. S.; Podrez, E. A., *Int. J. Biochem. Cell Biol.* **2009**, *41*, 1241-1244.

(59) Podrez, E. A.; Poliakov, E.; Shen, Z.; Zhang, R.; Deng, Y.; Sun, M.; Finton, P. J.; Shan, L.; Gugiu, B.; Fox, P. L.; Hoff, H. F.; Salomon, R. G.; Hazen, S. L., *J. Biol. Chem.* **2002**, *277*, 38503-38561.

(60) Gibb, C. L. D.; Gibb, B. C., *J. Am. Chem. Soc.* **2006**, *128*, 16498-16499.

(61) Gibb, C. L. D.; Gibb, B. C., *Chem. Commun.* **2007**, 1635-1637.

(62) Chandler, D., *Nature* **2002**, *417*, 491.

(63) Ben-Naim, A., *Hydrophobic Interaction*; Plenum Press: New York 1980.

(64) Schramm, M. P.; Rebek Jr, J., *Chem. Eur. J.* **2006**, *12*, 5924-5933.

(65) Trembleau, L.; Rebek Jr, J., *Science* **2003**, *301*, 1219-1220.

(66) Trembleau, L.; Rebek Jr, J., *Chem. Commun.* **2004**, 58-59.

(67) Hayashida, O.; Shivanyuk, A.; Rebek Jr, J., *Angew. Chem. Int. Ed.* **2002**, *41*, 3423-3426.

(68) Rudkevich, D. M.; Rebek Jr, J., *Eur. J. Org. Chem.* **1999**, 1991-2005.

(69) Heinz, T.; Rudkevich, D. M.; Rebek Jr, J., *Nature* **1998**, *394*, 764-766.

(70) Ajami, D.; Rebek Jr, J., *J. Am. Chem. Soc.* **2006**, *128*, 5314-5315.

(71) Hou, J. –H.; Ajami, D.; Rebek Jr, J., *J. Am. Chem. Soc.* **2008**, *130*, 7810-7811.

(72) Dube, H.; Ams, M. R.; Rebek Jr, J., *J. Am. Chem. Soc.* **2010**, *132*, 9984-9985.

(73) Ajami, D.; Rebek Jr, J., *Angew. Chem. Int. Ed.* **2007**, *46*, 9283-9286.

(74) Shorthill, B. J.; Avetta, C. T.; Glass, T. E., *J. Am. Chem. Soc.* **2004**, *126*, 12732-12733.

(75) Katritzky, A. R.; Wang, Z., *J. Heterocyclic Chem.* **1988**, *25*, 671-675.

(76) Liu, L.; Yang, B.; Katz, T. J.; Poindexter, M. K., *J. Org. Chem.* **1991**, *56*, 3769-3775.

(77) Connors, K. A. *Binding Constants*; John Wiley: New York 1987.

(78) Hargrove, A. E.; Zhong, Z.; Sessler, J. L.; Anslyn, E. V., *New J. Chem.*, **2010**, *34*, 348-354.

Vita, Jae Seung Lee

The author was born in Ilsan, Kyung-gi, S. Korea in 1973. He graduated Jamshil High School in 1992. He attended the Sahmyook University at Seoul, S. Korea and graduated with a Bachelor of Science degree in Chemistry in 1996. In 1996, He enrolled in the graduate program at the Konkuk University at Seoul, S. Korea and graduated with a Master of Science degree in Chemistry in 1998. After he graduate, the author joined SunBio, Inc, Choong-Ang A^+ Institute, and the Korea Institute of Science and Technology (KIST). In 2005, he enrolled in the graduate program at the University of Missouri-Columbia as a Ph.D. candidate in chemistry and accepted a position working for Dr. Timothy E. Glass. Prior to the completion of his Ph.D. degree, the author accepted a post-doctoral appointment with Dr. Hyunsoo Han at the University of Texas at San Antonio.

Publications & Patents

Kim, S. J.; Park, H. B.; **Lee, J. S**.; Jo, N. H.; Yoo, K. H.; Baek, D; Kang, B.-W.; Cho, J.-H.; Oh, C.-H. "Novel 1-β-methylcarbapenems having cyclic sulfonamide moieties: Synthesis and evaluation of *in vitro* antibacterial activity." *Eur. J. Med. Chem.*, **2007**, *42(9)*, 1176-1183.

Hyun, C. M.; Kim, G. S.; Kim, Y. H.; Lee, E. J.; Lee, H. J.; **Lee, J. S**.; Lee, J. H.; Lee, J. W.; Noh, G.; Park, M. G. "Polyethylene glycol hydrogel for bioadhesive." Repub. Korean Kongkae Taeho Kongbo, KR 2002089772 A 20021130, Nov 30, **2002**.

Shin, P. S.; **Lee, J. S**.; An, J. B. "Polyethylene glycol-acrylate and -metacrylate." Repub. Korean Kongkae Taeho Kongbo, KR 2000065551 A 20001115, Nov 15, **2000**.

Shin, P. S.; **Lee, J. S**.; An, J. B. "Polyethylene glycol-amine." Repub. Korean Kongkae Taeho Kongbo, KR 2000065550 A 20001115, Nov 15, **2000**.

Presentations

Lee, J. S.; Glass, T. E. "New Fluorescent Chemosensor for Detecting Lipids" Mar. **2010** American Chemical Society, San Francisco, CA, U.S.A.

Lee, J. S.; Park, S.-U. "Synthesis of pyridazine type ferroelectric liquid crystals" Oct. **1998** Korean Chemical Society, Daegu, S. Korea.